



# PACIFIC EARTHQUAKE ENGINEERING RESEARCH CENTER

## **Shear Strength Models of Exterior Beam-Column Joints without Transverse Reinforcement**

**Sangjoon Park**  
and  
**Khalid M. Mosalam**

University of California, Berkeley

# **Shear Strength Models of Exterior Beam-Column Joints without Transverse Reinforcement**

**Sangjoon Park**

Department of Civil and Environmental Engineering  
University of California, Berkeley

**Khalid M. Mosalam**

Department of Civil and Environmental Engineering  
University of California, Berkeley

PEER Report 2009/106  
Pacific Earthquake Engineering Research Center  
College of Engineering  
University of California, Berkeley

November 2009

## ABSTRACT

This study suggests a semi-empirical model and an analytical model to predict the shear strength of reinforced concrete (RC) exterior beam-column joints without transverse reinforcement (denoted as unreinforced) in the joint region. A large experimental data set of unreinforced exterior beam-column joints from published literature is collected using consistent criteria. From the parametric study of the database, it is proved that the shear strength of unreinforced exterior beam-column joints is significantly influenced by two parameters: (1) the joint aspect ratio, and (2) the beam reinforcement index, which is related to the amount of longitudinal beam reinforcement. Two equations of each parameter are formulated by equilibrium and verified by comparison with the database. A semi-empirical model is developed using the derived equations of the two parameters. The proposed semi-empirical model shows high accuracy for predicting the joint shear strength, compared with other existing models. As another approach, the analytical model is developed based on the two inclined struts mechanism in a parallel system. The fraction of each diagonal strut is assumed based on the bond strength deterioration between the beam reinforcing bars and the surrounding concrete. The proposed analytical model is validated by comparison of its predictions with the test data of unreinforced exterior beam-column joints from published literature. The proposed analytical model is capable of predicting the two main types of joint failure, namely joint shear failure without and with yielding of beam longitudinal reinforcement, without using modification of the diagonal strut width and without the need for the estimation of a ductility factor. Furthermore, demonstration analyses of published tests are successfully performed using a representative rotational spring element for the beam-column joint based on the proposed analytical model. The proposed semi-empirical and analytical shear strength models of unreinforced exterior beam-column joints can be adopted to assess the seismic performance of existing RC buildings with deficient seismic details in the joint region.

## **ACKNOWLEDGMENTS**

The research conducted in this report was supported primarily by the Earthquake Engineering Research Centers Program of the National Science Foundation under award number EEC-0618804 through the Pacific Earthquake Engineering Research Center (PEER). Any opinions, findings, and conclusions or recommendations expressed in this material are those of the authors and do not necessarily reflect those of the National Science Foundation. The authors would like to thank Prof. J.P. Moehle for his instructive suggestions.

# CONTENTS

<b>ABSTRACT</b> .....	<b>iii</b>
<b>ACKNOWLEDGMENTS</b> .....	<b>iv</b>
<b>TABLE OF CONTENTS</b> .....	<b>v</b>
<b>LIST OF FIGURES</b> .....	<b>vii</b>
<b>LIST OF TABLES</b> .....	<b>ix</b>
<b>1 INTRODUCTION</b> .....	<b>1</b>
1.1 Background.....	1
1.2 Objectives and Scope.....	4
1.3 Research Significance.....	4
1.4 Organization of Report .....	5
<b>2 DATABASE AND PARAMETRIC STUDY</b> .....	<b>7</b>
2.1 Database of Unreinforced Exterior Beam-Column Joints.....	7
2.2 Parametric Study.....	12
2.2.1 Effect of Joint Aspect Ratio .....	12
2.2.2 Effect of Beam Reinforcement.....	13
2.2.3 Effect of Column Axial Load.....	16
<b>3 JOINT STRENGTH MODELS AND SIMULATIONS</b> .....	<b>21</b>
3.1 Average Plane Stress and Strain Approach .....	21
3.1.1 Principal Tensile Stress Model.....	21
3.1.2 Pantazopoulou and Bonacci Model.....	22
3.1.3 Tsonos Model.....	24
3.1.4 Wong (Modified Rotating-Angle Softened-Truss) Model.....	26
3.2 Strut and Tie Mechanism.....	30
3.2.1 Hwang and Lee Model .....	30
3.2.2 Ortiz Model .....	33
3.2.3 Vollum Model .....	35
3.3 Single Strut Mechanism.....	37
3.3.1 FEMA 273 Model .....	37
3.3.2 Zhang and Jirsa Model .....	37

3.4	Empirical Models .....	38
3.4.1	Sarsam and Phipps Model.....	38
3.4.2	Taylor Model.....	39
3.4.3	Scott et al. Model .....	40
3.4.4	Bakir and Bodurođlu Model.....	40
3.4.5	Hegger et al. Model.....	41
3.4.6	Vollum Model .....	42
3.5	Shear Strength Degradation.....	42
3.5.1	Modification of Strength Factor.....	42
3.5.2	Modification of Diagonal Strut Width .....	44
3.6	Joint Element Model for RC Frame Simulation.....	44
<b>4</b>	<b>SEMI-EMPIRICAL SHEAR STRENGTH MODEL .....</b>	<b>49</b>
4.1	Development of Semi-Empirical Model.....	49
4.1.1	Joint Aspect Ratio Parameter .....	49
4.1.2	Beam Reinforcement Parameter .....	55
4.1.3	Semi-Empirical Shear Strength Model .....	56
4.2	Evaluation of the Semi-Empirical Model.....	58
<b>5</b>	<b>ANALYTICAL SHEAR STRENGTH MODEL .....</b>	<b>61</b>
5.1	Background.....	61
5.2	Development of Analytical Model .....	62
5.2.1	Assumptions.....	62
5.2.2	Equilibrium .....	66
5.2.3	Fraction Factor .....	67
5.2.4	Definition of Joint Shear Failure.....	70
5.3	Evaluation of Analytical Model .....	71
5.3.1	Evaluation of Test Data for Literature .....	71
5.3.2	Prediction of Joint Shear Failure Modes.....	75
5.4	Simulation of Literature Tests Using Analytical Model .....	75
<b>6</b>	<b>SUMMARY AND CONCLUDING REMARKS.....</b>	<b>81</b>
	<b>REFERENCES.....</b>	<b>83</b>

## LIST OF FIGURES

Fig. 1.1	Collapse of a building by joint shear failure (Sezen et al. 2000).....	3
Fig. 1.2	Examples of tests from literature of exterior beam-column joints.....	3
Fig. 2.1	Beam-column joint types: (a) interior joint, (b) exterior joint with no or one lateral beam (selected in this study), (c) exterior joint with two-sided lateral beams.....	9
Fig. 2.2	Selected anchorage types for exterior beam-column joints. ....	9
Fig. 2.3	Specimen design and test results of Beres et al. (1992).....	9
Fig. 2.4	Effect of joint aspect ratio.....	13
Fig. 2.5	Effect of beam reinforcement.....	16
Fig. 2.6	Complex effect of column axial load ratio.....	18
Fig. 2.7	Change of principal strain due to column axial load ratio. ....	19
Fig. 3.1	Principal tensile stress limits (Priestley 1997). ....	22
Fig. 3.2	Equilibrium of exterior beam-column joint (Tsonos 2007). ....	25
Fig. 3.3	Definition of symbols in MRA-STM (Wong 2005). ....	28
Fig. 3.4	Joint shear resisting mechanisms of SST model (Hwang and Lee 1999).....	31
Fig. 3.5	Ratios of force distribution among mechanisms of SST model (Hwang and Lee 1999).....	32
Fig. 3.6	Free body diagram of joint (Ortiz 1993).....	34
Fig. 3.7	Free body diagram by Vollum (1998).....	35
Fig. 3.8	Calibration of coefficient $k$ (Vollum 1998).....	36
Fig. 3.9	Shear strength degradation by curvature ductility (Park 1997). ....	43
Fig. 3.10	Shear strength degradation by displacement ductility (Hakuto et al. 2000). ....	43
Fig. 3.11	Existing simulation models for beam-column joints (Celik and Elingwood 2008): (a) Alath and Kunnath (1995), (b) Bidida and Ghobara (1999), (c) Youssef and Ghobarah (2001), (d) Lowes and Altoontash (2003), (e) Altoontash and Deierlein (2003), and (f) Shin and LaFave (2004).....	46
Fig. 3.12	Interior joint: (a) Global equilibrium and (b) Joint free body diagram (Celik and Elingwood 2008).....	48
Fig. 3.13	Backbone curves of joint behavior: (a) <i>Pinching4</i> from OpenSees used in Celik and Elingwood (2008), and (b) Proposed by Pampanin et al. (2003).....	48

Fig. 4.1	Single diagonal strut mechanism. ....	50
Fig. 4.2	Comparison of strength reduction factors at C-C-T node (see Table 4.1 for (a)–(j) designation).....	52.
Fig. 4.3	Comparison of proposed joint aspect ratio equation with database.....	54
Fig. 4.4	Global free body diagram of exterior beam-column joint. ....	56
Fig. 4.5	Illustration of proposed semi-empirical model. ....	57
Fig. 4.6	Comparison of evaluation results: (a) Proposed model, (b) Vollum (1998), (c) Hwang and Lee (1999), (d) Bakir and Boduroğlu (2002), (e) Hegger et al. (2003), and (f) Tsonos (2007).....	60
Fig. 5.1	Two inclined struts in unreinforced exterior joints.....	63
Fig. 5.2	Tests of joint with different beam reinforcement anchorage details (Wong 2005). ....	64
Fig. 5.3	Crack patterns of two types of joint failure.....	64
Fig. 5.4	Adopted bond strength model. ....	68
Fig. 5.5	Trilinear curve of fraction factor.....	68
Fig. 5.6	Solution algorithm of proposed analytical joint shear strength model. ....	71
Fig. 5.7	Comparison of evaluation results with existing analytical models.....	72
Fig. 5.8	Illustration of two different shear strengths in same joint.....	72
Fig. 5.9	Relationship of moment versus joint rotation. ....	77
Fig. 5.10	Bond distribution along hooked bar (Lowes and Altoontash 2003). ....	78
Fig. 5.11	Modeling of beam-column joint.....	79
Fig. 5.12	Simulated results by proposed model. ....	79

## LIST OF TABLES

Table 2.1	Experimental database of unreinforced exterior beam-column joints.....	10
Table 3.1	Efficiency factor of transverse reinforcement in (Hegger et al. 2003).....	41
Table 4.1	Strength reduction factor for a C-C-T node.....	52
Table 4.2	Measured joint shear strain and approximation of the principal tensile strain.....	53
Table 5.1	Prediction of joint shear strength and tensile stress of beam reinforcement at joint shear failure. ....	73
Table 5.2	Statistics of evaluation results for investigated values of $l_h$ .....	75

# 1 Introduction

## 1.1 BACKGROUND

Reinforced concrete (RC) buildings designed during the 1960s and 1970s still widely exist in the western U.S. and in other seismically active regions worldwide. Those buildings are mostly assumed to be vulnerable to earthquake loads due to insufficient shear reinforcement, widely spaced column ties, and little or no transverse reinforcement within beam-column joint regions. However, the real risk of older RC buildings is still unknown and under investigation. In particular, beam-column joints play a key role in integrating a whole structural system, and shear failure in beam-column joints may contribute to the collapse of a building as shown Figure 1.1. To assess the performance of RC beam-column joints having no transverse reinforcement (denoted as “unreinforced”), a large number of tests have been conducted with different joint geometries, beam reinforcement ratios and anchorage details, and column axial load ratios, in the U.S., Japan, New Zealand, the United Kingdom, and in other places (Fig. 1.2).

There are some differences in the design of beam-column joints between U.S., Japan and New Zealand codes. The main difference is whether the truss mechanism due to joint hoops and intermediate column bars is taken into account or ignored. Unreinforced beam-column joints are free from this disagreement because a truss mechanism does not take place and joint shear forces are transferred into the column by compression through inclined struts. Therefore, the parameters affecting the joint shear strength in this type of beam-column joint are limited to the following: (1) concrete strength, (2) joint aspect ratio, (3) beam longitudinal reinforcement ratio, (4) column axial load and (5) intermediate column bars. In this study, the effect of intermediate column bars as expressed in an opposing opinion (Hwang et al. 2005) is ignored because this effect is negligible if there are no joint hoops where the inclined strut may not be developed due to its steep angle.

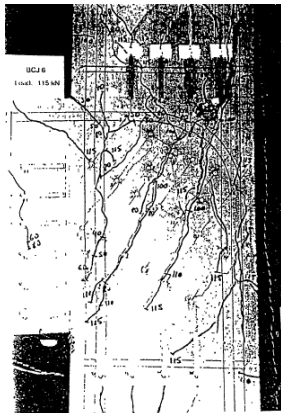
Traditionally, the shear strength of concrete has been expressed in terms of the square root of the concrete standard compressive strength,  $\sqrt{f'_c}$ , in U.S. codes (ACI 318-08, 2008). The shear strength of beam-column joints also follows the same assumption in (ACI 352-02, 2002). However, a different assumption is followed in other codes, e.g., the New Zealand code (NZS 3101, 1995), which specifies that the horizontal shear stress should not exceed  $0.2f'_c$  to avoid the diagonal compression failure by crushing. Some existing empirical models (Scott et al. 1994; Vollum 1998; Bakir and Bodurođlu 2002) use a function of  $\sqrt{f'_c}$ , as ACI 352-02 (2002) suggests, and two other models (Sarsam and Phipps 1985; Hegger et al. 2003) employ a function of  $\sqrt[3]{f'_c}$ . In the present study, it is assumed that the joint shear strength is proportional to  $\sqrt{f'_c}$ . The other three parameters, namely (1) the joint aspect ratio, (2) the beam longitudinal reinforcement ratio, and (3) the column axial load, are investigated from the constructed database of unreinforced exterior beam-column joints.

There has been significant effort to better assess the shear strength of unreinforced concrete beam-column joints. As a result, several empirical and analytical models have been developed based on the test data and mechanistic concepts. However, a robust shear strength model of unreinforced beam-column joints is still lacking. In the case of existing empirical models, inappropriate parameters are used or some parameters are obtained from insufficient data without an attempt to mechanistically address the significance of these parameters. In the case of existing analytical models that are typically developed for reinforced joints and then specialized to unreinforced joints, some conceptual limitations can be directly applied to the unreinforced beam-column joints.

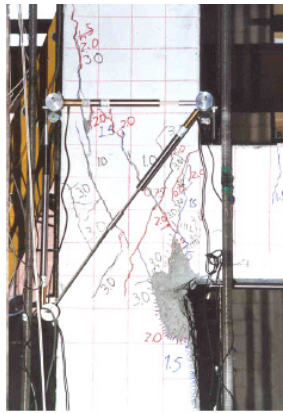
In this study, two shear strength models are proposed by semi-empirical and analytical approaches considering the aforementioned effects. Both shear strength models are validated by comparison of the collected large experimental data set.



**Fig. 1.1 Collapse of a building by joint shear failure (Sezen et al. 2000).**



(a) Ortiz (1993)



(b) Pantelides et al. (2002)



(c) Gohbara and Said (2002)



(d) Wong (2005)



(e) Hwang et al. (2005)



(f) Karayannis et al. (2008)

**Fig. 1.2 Examples of tests from literature of exterior beam-column joints.**

## **1.2 OBJECTIVES AND SCOPE**

The overall objectives of this study are to determine the main parameters affecting the shear strength of unreinforced exterior beam-column joints and to suggest shear strength models of unreinforced exterior joints including these parameters. This study is limited to RC exterior and corner beam-column joints without transverse reinforcement in the joint region and with no lateral beams or a lateral beam on one side only.

The direct objectives of this analytical study are summarized as follows:

1. To obtain the main parameters affecting the shear strength of unreinforced exterior beam-column joints;
2. To propose a semi-empirical model that is expressed as a simple equation but capable of predicting the shear strength with high accuracy;
3. To propose an analytical model to be able to predict two types of joint shear failure modes: joint shear failure without beam reinforcement yielding (J mode) and joint shear failure with beam reinforcement yielding (BJ mode); and
4. To extend the analytical model to the element level of exterior beam-column joint modeling with a rotational spring that can be used in many existing nonlinear structural analysis programs, e.g., OpenSees, to analyze RC frames.

## **1.3 RESEARCH SIGNIFICANCE**

There are several shear strength models for exterior beam-column joints in the literature. Some of these models are developed by statistical regression relying on small size experimental data sets. More sophisticated models, e.g., the softened strut-and-tie (SAT) model by Hwang and Lee (1999) and the modified rotational angle SAT model by Wong (2005), have some conceptual limitations to be directly applied to unreinforced beam-column joints. This study proposes two rational models to predict the shear strength of unreinforced exterior joints by a mechanistic approach. The proposed models are verified by showing better correlation of shear strength prediction with a large database of published tests.

The suggested shear strength models can be adopted to assess the seismic performance of existing old RC buildings with deficient seismic details in the joint region. Furthermore, the analytical model is used to provide the constitutive relationship of a rotational spring to represent the behavior of beam-column joints in structural analysis of frames.

## **1.4 ORGANIZATION OF REPORT**

This paper is organized as follows. A large database of unreinforced exterior beam-column joint tests from published literature is collected and the effect of main parameters on joint shear strength is investigated in Chapter 2, defining main parameters as joint aspect ratio, beam reinforcement, and column axial load ratio. In Chapter 3, existing joint shear strength models are illustrated based on the basic concept of those model and currently available joint elements for frame simulation are reviewed as a background for developing joint shear strength models and elements. A semi-empirical and an analytical model of unreinforced exterior joints are developed in Chapters 4 and 5. In particular, the developed analytical model is extended to the joint element for simulation. Finally, summary and conclusion are given in Chapter 6.

## 2 Database and Parametric Study

A large number of tests of unreinforced beam-column joints have been conducted by researchers in countries located in high seismic areas as well as in low ones. This chapter includes the database of those accessible tests from the 1960s to the present and the parametric studies from this database. The parametric studies provide key information to develop the shear strength models in the subsequent chapters.

### 2.1 DATABASE OF UNREINFORCED EXTERIOR BEAM-COLUMN JOINTS

A large database of unreinforced exterior beam-column joint tests from published literature is collected and analyzed in this chapter. The database includes only tests of corner and exterior beam-column joints without transverse reinforcement. To focus on the joints vulnerable to shear failure, only exterior joints without or with one lateral beam (Fig. 2.1(b)) are included, i.e., interior joints of exterior frames (Fig. 2.1(a)) and exterior joints of internal frames (Fig. 2.1(c)) are excluded. It is reported that crushing along the joint diagonal occurred in the joints with no lateral beams or with a lateral beam on one side only, and that the shear capacity of joints with lateral beams on two sides increased significantly compared with the two other cases in Figure 2.1(b) (Zhang and Jirsa 1982; Ohwada 1976, 1977). The hook anchorage details are also considered as one of the criteria for limiting the database candidates. Several types of hook anchorage detail in the joint region were used in gravity load designed buildings. Figure 2.2 shows the selected anchorage details for collecting database candidates where at least one strut mechanism can develop under lateral loading. Among the shown four types, Type B is most common in older RC gravity load designed buildings, followed by Type A. Types C and D are less common and impractical from a constructability point of view. It is to be noted that the tests designed with a wide beam, i.e., with beam width greater than column width, are not included in the database due to different confinement condition of the joint region.

Tests affected by column or beam shear failure are excluded from the database. For instance, tests conducted by Beres et al. (1992) in Figure 2.3 are excluded because the response of the tested joints appears to be significantly affected by the column shear failure due to the first column hoop located far from the joint region; see the dashed box and arrow in Figure 2.3. It is worth mentioning that most experimental research efforts on beam-column joints have focused on the verification of strength and ductility of reinforced joints, and the retrofit methods of unreinforced joints. Such tests are also not included in the database of this study.

Based on the discussion above, 62 tests for unreinforced beam-column joints satisfying the selection requirements of the database are identified and summarized in Table 2.1. The information of each test is extracted from the published literature and consistent assumptions are made when available data are incomplete. For instance, the joint shear strength specified in the corresponding literature is used in the database, while the joint shear strength is calculated by the constant moment arm assumption if only applied beam or column shear force is reported. In that regard, the constant moment arm is assumed to be  $0.875d_b$  for the joint shear failure without beam reinforcement yielding and  $0.9d_b$  for the joint shear failure with beam reinforcement yielding. Note that  $d_b$  is the effective depth of beam cross section. The effective joint width,  $b_j$ , is taken as  $(b_c+b_b)/2$  which gives a reasonable equivalent strut (Zhang and Jirsa 1982). Note that  $b_c$  and  $b_b$  are the respective widths of the column and beam cross sections. The joint shear strength is normalized by  $\sqrt{f'_c}$ , i.e.,  $\gamma = V_{jh} / b_j h_c \sqrt{f'_c}$ , to be compared with the criteria of the current U.S. code provisions. Note that  $V_{jh}$  is the maximum horizontal shear force in the joint and  $h_c$  is the total height of the column cross section in the loading direction. The specimen failure obtained from tests is categorized into six types: (1) joint shear failure without beam reinforcement yielding (J), (2) joint shear failure with beam reinforcement yielding (BJ), (3) beam flexural failure (BF), (4) column flexural failure (CF), (5) beam reinforcement pull-out failure (P), and (6) anchorage failure (A). From the database, the effects of different parameters on joint shear strength are investigated in the following three subsections.

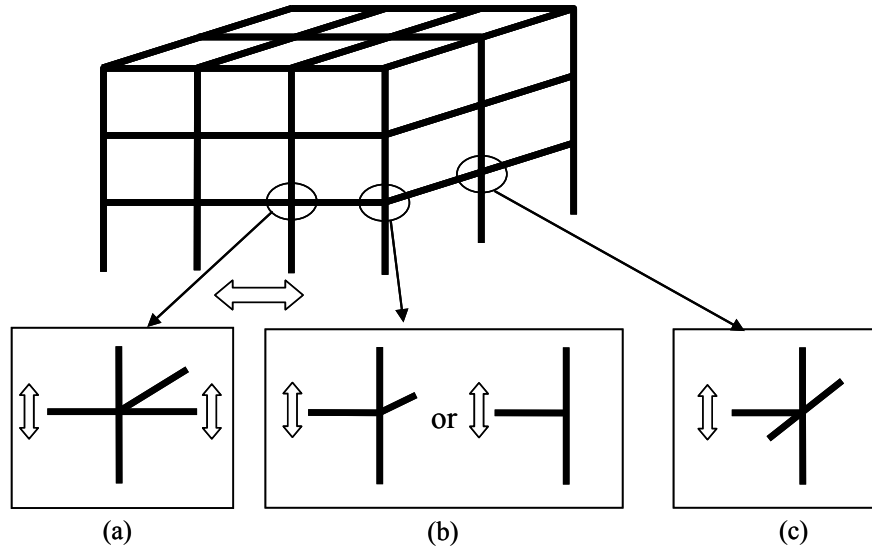


**Fig. 2.1 Beam-column joint types: (a) interior joint, (b) exterior joint with no or one lateral beam (selected in this study), (c) exterior joint with two-sided lateral beams.**

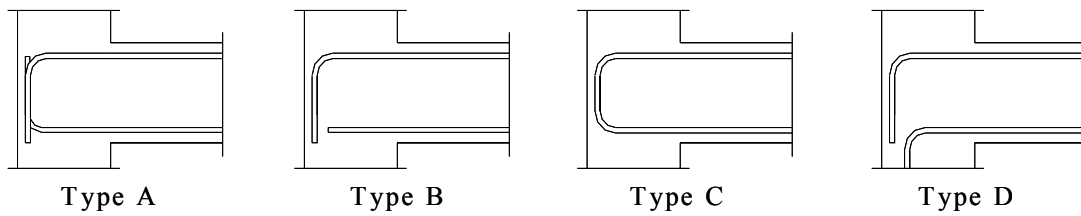
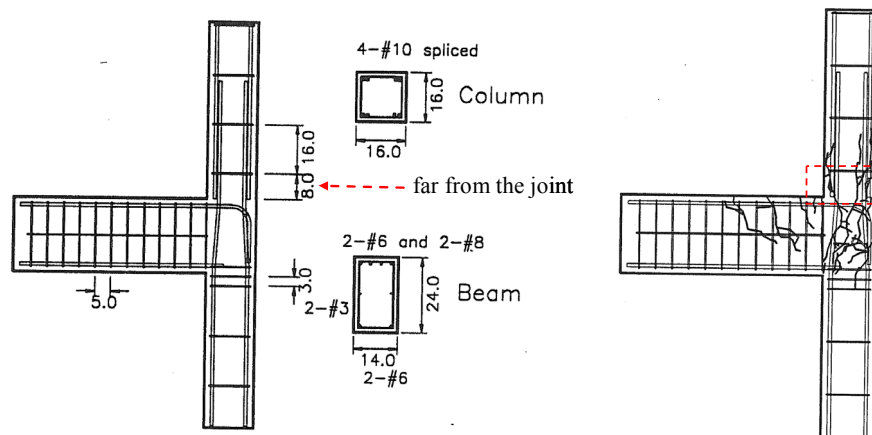


**Fig. 2.2 Selected anchorage types for exterior beam-column joints.**



Note: dimensions are in inches

**Fig. 2.3 Specimen design and test results of Beres et al. (1992).**

**Table 2.1 Experimental database of unreinforced exterior beam-column joints.**

Reference	Specimen	$f'_c$ (ksi)	$f_{y,beam}$ (ksi)	$A_s^{*1}$ (in. <sup>2</sup> )	$b_j$ (in.)	$h_c$ (in.)	$h_b$ (in.)	$P/(b_c h_c f'_c)$	$V_{jh}$ (kip)	$V_{jh}/b_j h_c \sqrt{f'_c}$ (psi <sup>0.5</sup> )	Failure Mode <sup>*2</sup>
Hanson & Connor (1967, 1972)	V	3.30	51.0	4.0	13.5	15.0	20	0.86	138.4	11.9	J
	7	5.70	51.0	4.0	13.5	15.0	20	0.50	189.7	12.4	BJ
Hwang et al. (2005)	OT0	9.76	63.1	3.16	14.6	16.5	17.7	0.02	224.1	9.4	BJ
Uzumeri (1977)	SP1	4.46	50.3	3.0	13.5	15.0	20	0.41	140.9	10.4	BJ
	SP2	4.51	50.6	3.0	13.5	15.0	20	0.41	136.9	10.1	BJ
	SP5	4.63	50.4	3.0	15.0	15.0	20	0.43	136.7	8.9	BJ
Wong (2005)	BS-L	4.48	75.4	1.46	11.0	11.8	17.7	0.15	70.9	8.1	J
	BS-U	4.50	75.4	1.46	11.0	11.8	17.7	0.15	76.7	8.8	J
	BS-L-LS	4.58	75.4	1.46	11.0	11.8	17.7	0.15	77.5	8.8	J
	BS-L-300	4.94	75.4	1.46	11.0	11.8	11.8	0.15	113.5	12.4	BJ
	BS-L-600	5.28	75.4	1.46	11.0	11.8	23.6	0.15	63.8	6.7	J
	BS-L-V2T20	4.73	75.4	1.46	11.0	11.8	17.7	0.15	89.7	10.0	J
	BS-L-V4T10	4.10	75.4	1.46	11.0	11.8	17.7	0.15	90.6	10.9	J
	JA-NN03	6.50	75.4	0.97	11.0	11.8	15.7	0.03	56.0	5.3	BJ
	JA-NN15	6.67	75.4	0.97	11.0	11.8	15.7	0.15	69.9	6.6	BJ
JB-NN03	6.87	75.4	0.97	11.0	11.8	11.8	0.03	70.4	6.5	BJ	
Pantelides et al. (2002)	01	4.79	66.5	4.0	16.0	16.0	16.0	0.10	219.0	10.9	J
	02	4.38	66.5	4.0	16.0	16.0	16.0	0.25	213.5	10.6	J
	03	4.93	66.5	4.0	16.0	16.0	16.0	0.10	207.0	10.2	J
	04	4.58	66.5	4.0	16.0	16.0	16.0	0.25	237.5	11.7	J
	05	4.60	66.5	4.0	16.0	16.0	16.0	0.10	218.1	11.1	J
	06	4.50	66.5	4.0	16.0	16.0	16.0	0.25	221.6	11.3	J
Clyde et al. (2000)	02	6.70	65.9	4.0	12.0	18.0	16.0	0.10	237.2	12.1	J
	06	5.94	65.9	4.0	12.0	18.0	16.0	0.10	229.9	12.7	J
	04	5.37	65.9	4.0	12.0	18.0	16.0	0.25	240.8	13.2	J
	05	5.82	65.9	4.0	12.0	18.0	16.0	0.25	220.8	13.4	J
Ortiz (1993)	BCJ1	4.93	104.4	1.24	7.9	11.8	15.7	0	68.8	10.5	J
	BCJ3	4.79	104.4	1.24	7.9	11.8	15.7	0	72.4	11.3	J
	BCJ5	5.51	104.4	1.24	7.9	11.8	15.7	0.08	70.6	10.2	J
	BCJ6	5.08	104.4	1.24	7.9	11.8	15.7	0.09	70.8	10.7	J

**Table 2.1—continued.**

Scott & Hamil (1998)	C4ALN0	6.15	75.7	0.62	5.1	5.9	8.3	0.05	24.8	10.5	P
	C4ALH0	15.08	75.7	0.62	5.1	5.9	8.3	0.02	42.3	11.4	P
	C6LN0	7.40	75.7	0.62	5.1	5.9	8.3	0.04	23.4	9.0	J
	C6LH0	14.65	75.7	0.62	5.1	5.9	8.3	0.02	35.4	9.7	J
Paker & Bullman (1997)	4a	5.66	82.7	1.52	10.8	11.8	19.7	0	43.0	4.5	CF
	4b	5.66	82.7	1.52	10.8	11.8	19.7	0.09	50.3	5.2	J
	4c	5.66	82.7	1.52	10.8	11.8	19.7	0.16	62.0	6.4	J
	4d	5.66	82.7	1.52	10.8	11.8	19.7	0	54.7	5.7	J
	4e	5.66	82.7	1.52	10.8	11.8	19.7	0.09	58.4	6.1	J
	4f	5.66	82.7	1.52	10.8	11.8	19.7	0.17	66.7	6.9	J
Kananda et al. (1984)	U40L	3.52	56.1	1.76	11.0	11.8	15.0	0	57.7	7.5	J
	U20L	3.87	56.1	0.88	11.0	11.8	15.0	0	42.4	5.2	A
	B101	4.63	56.8	1.76	11.0	11.8	15.0	0	78.3	8.8	J
Ghobarah & Said (2001)	T-1	4.47	61.6	1.85	9.8	15.7	15.7	0.19	124.5	12.0	BJ
	T-2	4.47	61.6	1.85	9.8	15.7	15.7	0.10	117.0	11.3	BJ
Sarsam & Phipps (1985)	EX-2	7.61	75.4	0.88	6.1	10.7	12.0	0.13	39.6	7.0	BJ
Wilson (1998)	J1	4.64	75.4	1.04	6.1	11.8	11.8	0.30	57.1	11.7	J
Woo (2003)	Model 5	3.84	55.8	0.44	6.6	6.6	7.9	0	16.8	6.3	BJ
Liu (2006)	RC-1	2.81	46.9	0.66	8.5	9.1	13.0	0	22.8	7.2	BJ
Engindeniz (2008)	SP1-NS	3.74	45.7	2.64	13.0	14.0	20	0.02	81.4	7.3	J
	SP1-EW	3.74	45.7	2.64	13.0	14.0	20	0.02	90.4	8.1	J
	SP2-NS	5.02	45.7	2.64	13.0	14.0	20	0.02	91.7	7.1	J
	SP2-EW	5.02	45.7	2.64	13.0	14.0	20	0.02	96.9	7.5	J
Karayannis et al. (2008)	A0	4.58	84.1	0.22	7.9	7.9	11.8	0.05	18.2	9.9	BJ
	B0	4.58	84.1	0.66	7.9	11.8	11.8	0.05	44.4	7.1	BJ
	C0	4.58	84.1	0.70	7.9	11.8	11.8	0.05	45.9	7.3	BJ
Gencoğlu & Eren (2002)	RCNH1	4.35	76.1	0.22	4.9	7.9	11.8	0.13	10.9	4.3	BF
El-Amoury & Ghobara (2002)	T0	4.44	61.6	1.95	9.8	15.7	15.7	0.20	91.3	8.8	BJ
Antonopoulos & Triantafillou (2003)	C-1	2.83	84.8	0.72	7.9	7.9	11.8	0.06	24.4	7.4	J
	C-2	3.44	84.8	0.72	7.9	7.9	11.8	0.05	24.2	6.7	J
	T-C	3.57	84.8	0.72	7.9	7.9	11.8	0.05	28.1	7.6	J
Sagbas (2007)	ED1	4.51	50.6	3.0	13.5	15	20	0	134.1	9.9	BJ

\*1  $A_s$  is total area of beam reinforcement in tension

\*2 Failure mode: J = joint shear failure without beam reinforcement yielding, BJ = joint shear failure with beam reinforcement yielding, BF = beam flexural failure, CF = column flexural failure, P = pull-out failure, A = anchorage failure

Note: 1 ksi = 6.90 MPa; 1 kip = 4.45 kN; 1 in. = 25.38 mm

## 2.2 PARAMETRIC STUDY

In this section, three main parameters, namely (1) joint aspect ratio, (2) beam reinforcement, and (3) column axial load, are investigated from the database. These three parameters are selected because of their importance in the behavior of unreinforced exterior and corner beam-column joints.

### 2.2.1 Effect of Joint Aspect Ratio

The effect of the joint aspect ratio has been investigated experimentally. For the case of a reinforced joint, Kim and LaFave (2007) reported that the joint aspect ratio in terms of the total beam cross-section height,  $h_b$ , to the total column cross-section height,  $h_c$ , i.e.,  $h_b/h_c$ , from 1.0 to 1.6 for exterior joints, had little influence on the joint shear stresses and strains for the case of joint failure following beam yielding. Moreover, Kim and LaFave (2007) stated that the increase of the joint aspect ratio slightly reduced the joint shear strength for the case of joint shear failure without beam reinforcement yielding. Wong (2005) tested unreinforced exterior joints having the three joint aspect ratios 1.0, 1.5, and 2.0. These test results showed that the joint strength,  $\gamma\sqrt{f'_c}b_f h_c$  (lb and inch units), is inversely proportional to the joint aspect ratio, where  $\gamma = 6.7 \text{ psi}^{0.5}$  ( $0.56 \text{ MPa}^{0.5}$ ) for the high aspect ratio  $h_b/h_c=2.0$ ,  $\gamma = 8.6 \text{ psi}^{0.5}$  ( $0.71 \text{ MPa}^{0.5}$ ) for the intermediate aspect ratio  $h_b/h_c=1.5$ , and  $\gamma = 12.4 \text{ psi}^{0.5}$  ( $1.03 \text{ MPa}^{0.5}$ ) for the low aspect ratio  $h_b/h_c=1.0$ . Bakir and Bouroğlu (2002) and Vollum (1998) made the same observations using large data sets of previous test results. Each of these studies developed a separate joint strength model including the adverse effect of the joint aspect ratio.

In the SAT approach, a steeper diagonal strut is developed in the high aspect ratio of a joint region if there is no transverse reinforcement in this region because there is no truss mechanism. Consequently, the steeper diagonal strut results in less effective shear resistance to equilibrate the horizontal joint shear force. Hence, the shear strength of unreinforced exterior joints is inversely proportional to its aspect ratio. This trend is supported by the joint database presented in this study as shown in Figure 2.4 where the effect of the joint aspect ratio is more apparent by selecting the cases of J failure mode. Furthermore, the joint shear strengths by other

failure modes do not exceed that by J failure mode except for the pull-out failure and high column axial load specimens.

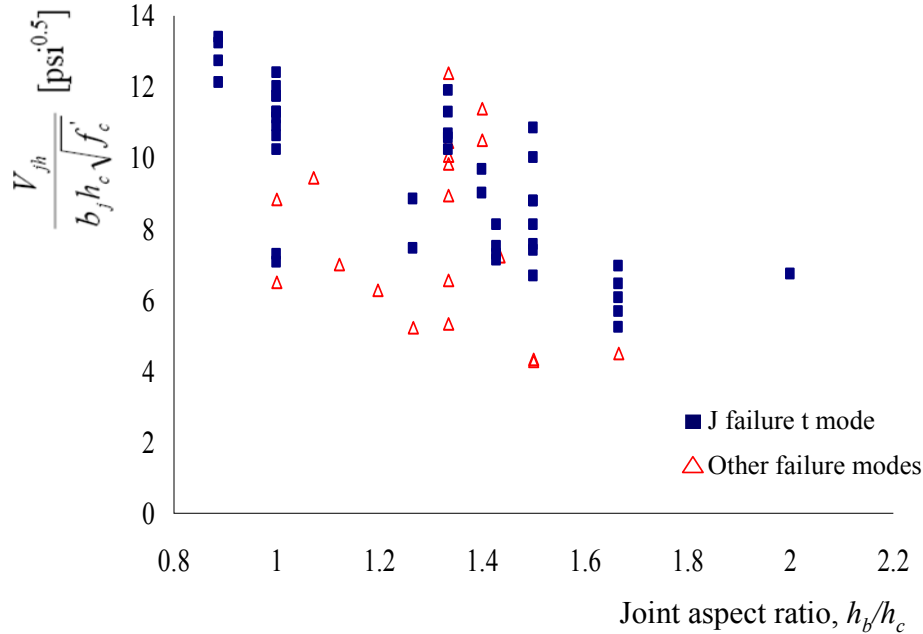


**Fig. 2.4 Effect of joint aspect ratio.**

### 2.2.2 Effect of Beam Reinforcement

According to the ACI Code provisions for beam-column joints (ACI-ASCE 352R-02, 2002), joint shear capacity can be determined by the joint types, dimensions, and concrete strength if joint details meet the minimum requirements of confinement. However, tests on interior beam-column joints without joint transverse reinforcement (Walker 2001; and Alire 2002) showed that joints failed in shear at different levels of shear stress demand: from 10.9 to 15.7  $\sqrt{f'_c} b_j h_c$  (lb) by Walker (2001) and from 8.5 to 25.0  $\sqrt{f'_c} b_j h_c$  (lb) by Alire (2002), although all specimens had the same geometrical dimensions and column axial load. From these observations, Anderson et al. (2008) claimed that joint strength and failure mode depend on joint shear stress demand or the amount of beam reinforcement rather than joint shear capacity. A similar observation was made in exterior beam-column joint tests by Wong (2005). Two different reinforcement ratios were considered in the beam cross section. The test results showed that the specimens having high reinforcement ratio experienced joint shear failure without beam reinforcement yielding, while

the specimens having low reinforcement ratio experienced ductile behavior followed by joint shear failure. Bakir and Bouroğlu (2002) arrived at the conclusion that the normalized joint strength is related to the beam reinforcement ratio after investigating the tests by Scott (1992) which had three different beam reinforcement ratios. Similarly, the shear strength equation of RC beams without stirrups, proposed by Bažant and Yu (2005), includes the reinforcement ratio parameter as follows:

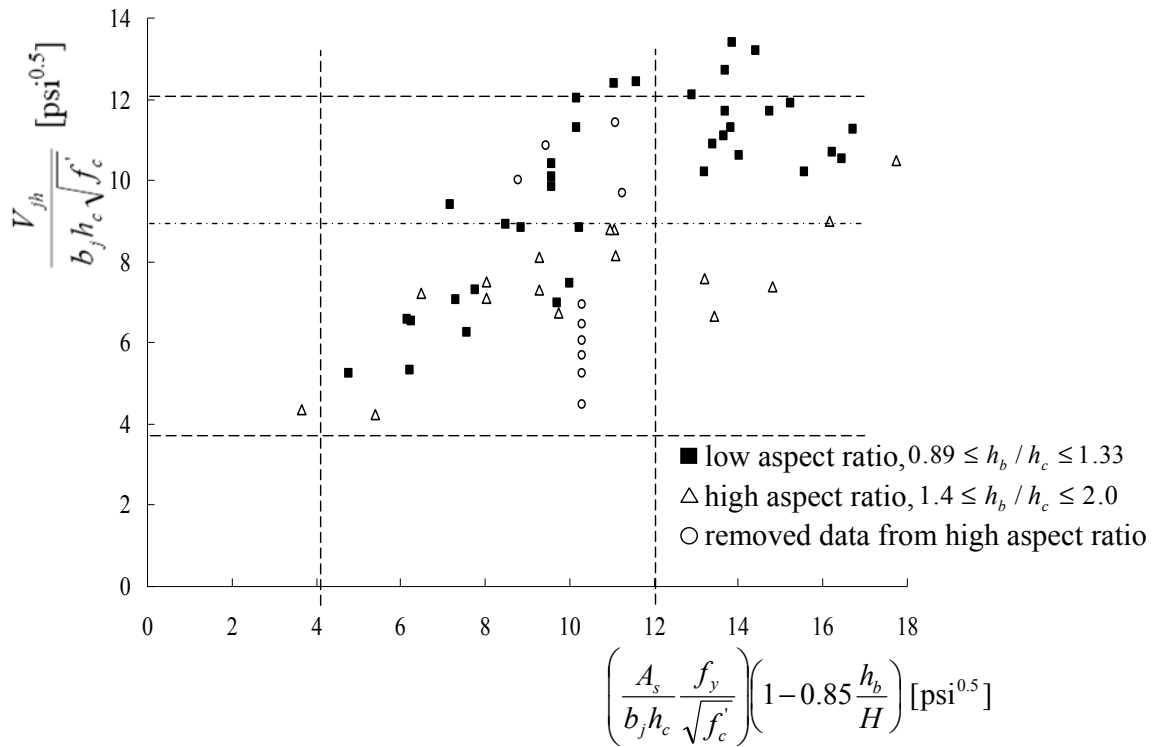
$$v_c = \mu \rho_w^{3/8} \left( 1 + \frac{d_b}{a} \right) \sqrt{\frac{f_c'}{1 + d_b/d_o}} \quad (2.1)$$

where  $\mu$  is a constant defined by regression,  $\rho_w$  is the beam longitudinal reinforcement ratio,  $a$  is the shear span, and  $d_o$  is the size effect parameter.

In unreinforced joints, the improvement of joint shear strength due to increasing the beam reinforcement ratio can be explained as follows: an increase of the beam reinforcement ratio must cause an increase in the compression force in the diagonal strut with less loss of bond resistance because there is no truss mechanism to transmit horizontal joint shear. This more stable bond resistance induces an inclined strut which can carry horizontal joint shear stress. This inclined strut will be utilized when developing the analytical model in Chapter 5. From the analysis of the database, it is shown that the joint shear strength is approximately linearly proportional to the amount of beam reinforcement if beam reinforcement yield strength,  $f_y$ , and geometry are identical; see Figure 2.5. For better understanding, the data of low joint aspect ratio ( $0.89 \leq h_b/h_c \leq 1.33$ ) and high joint aspect ratio ( $1.4 \leq h_b/h_c \leq 2.0$ ) are plotted with different symbols in Figure 2.5. It is noted that the following test data marked with open circles in Figure 2.5 can be excluded from the high joint aspect ratio: (1) six tests by Parker and Bullman (1997) whose test results are questionable due to low joint shear strength as discussed by Vollum (1998), (2) two tests (C4ALH0 and C6LH0) by Scott and Hamil (1998) due to high joint shear strength by using high strength concrete, and (3) two tests (BS-L-V2T10 and BS-L-V4T10) by Wong (2005) due to high joint shear strength by using unusual intermediate column bars. Considering the data of low joint aspect ratio, the increase of joint shear strength (y-axis) due to beam reinforcement (x-axis) is valid within an approximate range of 4 to 12 of the x-axis in Figure 2.5. This range corresponds to where the cases of joint shear failure with beam reinforcement yielding (BJ mode) are located. Beyond the value of 12, the joint shear strength does not increase. Considering the data of the high joint aspect ratio case, fewer experimental data points are

available to analyze compared with those of the low joint aspect ratio case. From these limited data points, the joint shear strengths for the same aspect ratio,  $h_b / h_c = 1.5$ , are compared. The minimum joint shear strength is  $4.3\sqrt{f'_c}b_jh_c$  for the beam reinforcement index of 3.6 and 5.4 for specimen A0 (Karayannis et al. 2007) and specimen RCNH1 (Gencoğlu and Eren 2002), respectively. It is noted that specimen RCNH1 (Gencoğlu and Eren 2002) failed due to the widening of beam flexural cracks. The maximum joint shear strength is  $8.6\sqrt{f'_c}b_jh_c$  for the beam reinforcement index of 11.0 for specimens BS-L, BS-U, and BS-L-LS from (Wong 2005), where beam reinforcements did not yield. Therefore, the maximum joint shear strength for high aspect ratio can be assumed to be bounded by the value of 9. Moreover, a similar assumption can be made for the high aspect ratio joints as that of the low aspect ratio joints for the range of 4 to 9 for both the x- and y-axes in Figure 2.5. This assumption will be experimentally investigated in future phases of the presented research.

The non-dimensional parameter reflecting the effect of the amount of beam reinforcement is selected as  $\frac{A_s}{b_jh_c} \frac{f_y}{\sqrt{f'_c}} \left(1 - 0.85 \frac{h_b}{H}\right)$  based on the global equilibrium and the joint strength normalization, as discussed in the subsequent section. This parameter reflects the joint shear demand at the onset of beam reinforcement yielding and beyond yielding if the beam reinforcement is assumed elastic-perfectly-plastic (EPP) material. From Figure 2.5, it can be stated that joint shear strength is close to joint shear demand within the aforementioned range. This observation is similar to that for unreinforced interior beam-column joints (Anderson et al. 2008). The three approximate values, 12, 9, and 4, shown in Figure 2.5, are explained as follows: (1) the value of 12 and 9 are close to the maximum normalized joint shear strength having joint aspect ratio, 1.0 and 1.5, respectively, as shown in Figure 2.4, and (2) the value of 4 is coincident with the minimum joint shear strength of unreinforced exterior joints suggested by Moehle (2008) based on the tests of Hakuto et al. (2000).



Note: 1 ksi = 6.90 MPa; 1 kip = 4.45 kN

**Fig. 2.5 Effect of beam reinforcement.**

### 2.2.3 Effect of Column Axial Load

The effect of column axial load on beam-column joint strength is not completely known. Some researchers, e.g. (Jirsa and Meinheit, 1977; Kurose et al., 1988; Kitayama et al., 1991; Pantazopoulou and Bonacci, 1992; Vollum, 1998) conclude that joint strength is influenced little by column axial load. On the other hand, some experimental reports, e.g. (Beres et al., 1992; Clyde et al., 2000; Pantelides et al., 2002) claim that high axial load on columns increases joint strength. In the case of weak column–strong beam design, it is obvious that increasing the column axial load up to the balanced point improves the joint shear strength because the column moment capacity is positively affected by the axial load. On the other hand, in the case of strong column–weak beam design, which is the case of most tests, there have been reports that column axial load gives joint shear strength both beneficial and detrimental effects. In summary, for column axial load less than  $0.2f'_c A_g$ , little and unclear influence on the joint shear strength is observed as shown in Figure 2.6. Note that  $A_g = h_c b_c$  is the gross area of the column cross section.

In the case of higher column axial load, more test data are needed. The positive and negative effects are explained briefly in the following paragraphs.

#### *Positive Effects*

From the aspect of the diagonal strut mechanism in the joint region, a compressive diagonal strut width is determined by the compression block depth of the column and the beam. The column compression block depth is obviously increasing with the increase of the column axial load. Thus increasing the column axial load has a positive effect on improving joint strength. Applying principal tensile stress as the failure criterion, it is also concluded that high column axial load decreases this principal tensile stress and, accordingly, increases joint shear strength. As another positive effect, high column axial load improves bond strength between the beam reinforcing bars and the surrounding concrete. This leads to increasing joint shear strength because the horizontal shear force is transferred into the joint by bond and anchorage of the beam reinforcement.

#### *Negative Effects*

Most joint shear failures take place after cracking in the joint panel. The crack width is usually transformed into an average principal tensile strain for use in softening a concrete constitutive model, such as the Modified Compression Field Theory (MCFT) (Vecchio and Collins 1986). Therefore, the crack propagation is accelerated due to the Poisson's effect as the column axial load increases and consequently the joint has less shear strength. Minami and Nishimura (1985) reported a similar observation, where the anchorage strength of the hooked bar in the joint region increased with column axial load but rapidly deteriorated under high axial load. Considering the equilibrium at the strut node, the failure of the diagonal strut can be triggered by the high column axial load. P-delta effects and buckling of the column reinforcement lead to further negative effects of the column axial load on the joint shear strength.

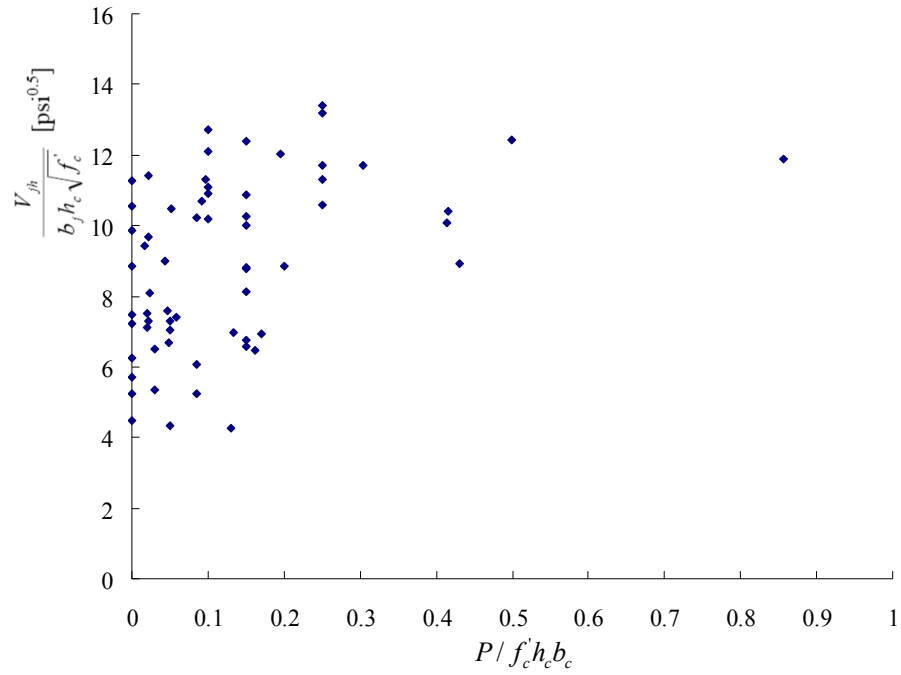


**Fig. 2.6 Complex effect of column axial load ratio.**

The principal tensile strain in Equation (2.2), derived by Pantazopoulou and Bonacci (1992) has been used to explain the detrimental effect of high column axial load by other researchers.

$$\varepsilon_1 = \frac{\varepsilon_x - \varepsilon_y \tan^2 \beta}{1 - \tan^2 \beta} \quad (2.2)$$

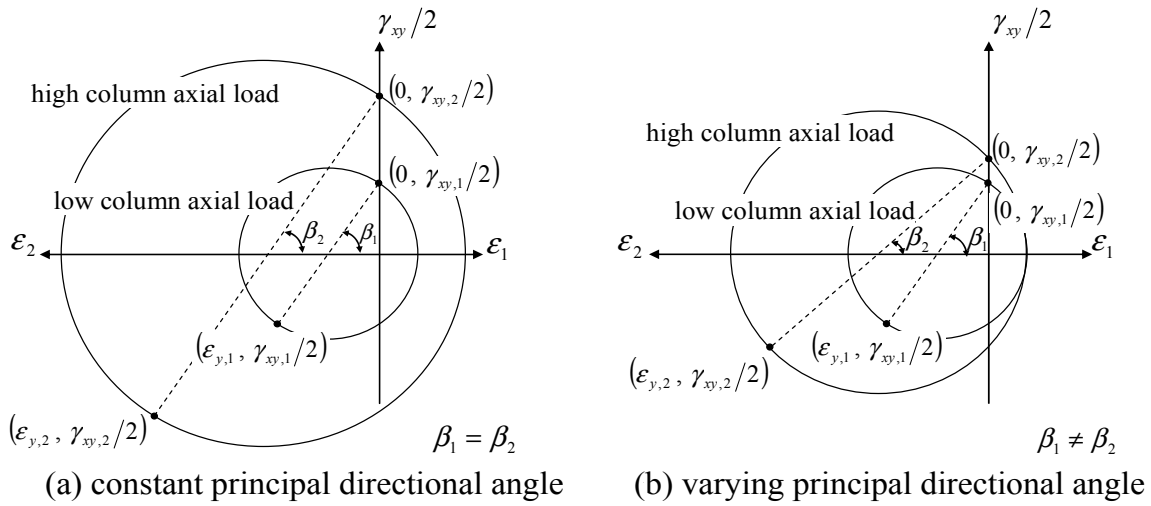
where  $\varepsilon_x$  and  $\varepsilon_y$  are the average joint transverse (horizontal) and longitudinal (vertical) strains, respectively, and  $\beta$  is the angle of inclination (from the horizontal axis) of the principal tensile joint strain. Note that the positive sign represents the tensile strain in this study. Pantazopoulou and Bonacci (1992) concluded that the principal tensile strain,  $\varepsilon_1$ , increases as the average compressive longitudinal strain,  $\varepsilon_y$ , increases due to increase of the column axial load. This conclusion is based on the assumption that the principal tensile strain direction, i.e., the angle  $\beta$ , is fixed while the column axial load increases. However, the shear strain has to significantly increase to keep the principal tensile strain direction fixed, which is unacceptable (Fig. 2.7(a)). The principal tensile strain seems to change little as the average compressive (negative) longitudinal strain,  $\varepsilon_y$ , increases if the shear strain increase is not significant considering

Equation (2.3a). This is more apparent if the average transverse strain,  $\epsilon_x$ , is assumed to be zero, as shown in Equation (2.3b); see Figure 2.7(b).

$$\epsilon_1 = \frac{\epsilon_x + \epsilon_y}{2} + \frac{1}{2} \sqrt{(\epsilon_x - \epsilon_y)^2 + \gamma_{xy}^2} \quad (2.3a)$$

Let  $\epsilon_x = 0$

$$\epsilon_1 = \frac{\epsilon_y}{2} + \frac{1}{2} \sqrt{\epsilon_y^2 + \gamma_{xy}^2} \quad (2.3b)$$



Note:  $\epsilon_x$  is assumed to be zero because of negligible axial load in the beam.

**Fig. 2.7 Change of principal strain due to column axial load ratio.**

## 3 Joint Strength Models and Simulations

Several existing shear strength models are categorized with respect to the type of underlying basic concept. Some of these models are selected to perform predictions of tests from the database and the given discussion explains the reasons of good and poor predictions. Lastly, existing beam-column joint element models for simulation are introduced. In the single spring model, it is shown that the relationship of shear stress versus shear strain can be transformed into that of moment versus rotation to represent the constitutive behavior of this rotational spring.

### 3.1 AVERAGE PLANE STRESS AND STRAIN APPROACH

#### 3.1.1 Principal Tensile Stress Model

One approach to assess the shear strength of beam-column joints without joint reinforcement is to compare the average principal tensile stress of the joint panel with some critical values representing diagonal cracking and shear failure. This approach has been traditionally used by many researchers to estimate the concrete shear strength of columns with different limits of principal tensile stress. Under the assumption of no axial force in the beam, the principal tensile stress is calculated as follows:

$$\sigma_1 = -\frac{1}{2}\left(\frac{P}{A_g}\right) + \sqrt{\frac{1}{4}\left(\frac{P}{A_g}\right)^2 + \left(\frac{V_{jh}}{A_g}\right)^2} \quad (3.1)$$

where  $P$  is the column axial load (positive for compression),  $V_{jh}$  is the horizontal joint shear stress, and  $A_g$  is the gross area of the column cross section, i.e.,  $A_g = b_c h_c$ .

As shown in Figure 3.1, Priestley (1997) suggested the limit of  $\sigma_1 = 3.5\sqrt{f'_c}$  psi ( $0.29\sqrt{f'_c}$  MPa) for onset of joint shear cracking, and  $\sigma_1 = 5.0\sqrt{f'_c}$  psi ( $0.42\sqrt{f'_c}$  MPa) for maximum shear strength of an unreinforced joint. The joint shear strength degradation is also considered in terms of joint rotation. Kim and LaFave (2007) collected a large number of test

data and observed that the principal tensile stresses of the joint panel are close to  $\sigma_1 = 4.0\sqrt{f'_c}$  psi ( $0.33\sqrt{f'_c}$  MPa) at the initiation of diagonal shear cracking. However, the principal tensile stress approach may be too conservative because more joint shear can be carried by the diagonal compression strut mechanism (Hakuto et al. 2000). Moreover, a high column axial load on the joint improves the joint shear strength based on Equation (3.1), which is not true, since the column axial load also has a negative effect on the joint shear strength as discussed in Section 2.2.3.

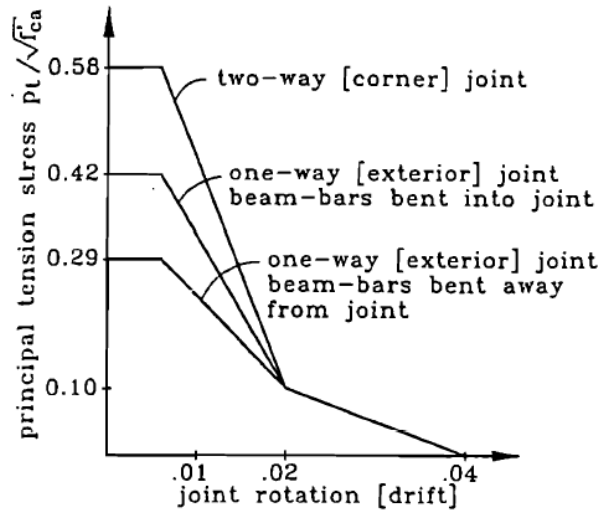


Fig. 3.1 Principal tensile stress limits (Priestley 1997).

### 3.1.2 Pantazopoulou and Bonacci Model

Pantazopoulou and Bonacci (1992) developed a shear strength model of interior beam-column joints based on mechanical considerations, i.e., kinetics, equilibrium, and material constitutive relationships, under the assumption that the joint is well confined such that average stress and strain values can be used. The average stresses in the transverse direction ( $x$ ) and longitudinal direction ( $y$ ) satisfy the following relationships,

$$\sigma_x = -\rho_s f_x^s - \rho_b f_x^b - \frac{P_x}{b_c h_b} \Rightarrow \sigma_x = -\rho_x f_x - \frac{P_x}{b_c h_b}, \quad \rho_x = \rho_s + \beta \rho_b, \quad f_x = f_x^s, \quad \beta = f_x^b / f_x^s \quad (3.2)$$

$$\sigma_y = -\rho_y f_y - \frac{P}{b_c h_c} \quad (3.3)$$

where  $\rho_s, \rho_b, \rho_y$  are the area ratio of transverse reinforcement, beam reinforcement, and column reinforcement, respectively;  $f_x^s, f_x^b, f_y$  are the average stress of transverse reinforcement, beam reinforcement, and column reinforcement, respectively;  $P_x$  is the axial load in the beam; and  $\beta$  is zero for perfect bond, while  $\beta$  is 1 for complete loss of bond resistance. Assuming that the concrete tensile strength  $\sigma_1$  is negligible, the following relationship can be derived using Mohr's circle.

$$\sigma_2 = \sigma_x + \sigma_y = -v_{jh} \left( \tan \theta + \frac{1}{\tan \theta} \right) \quad (3.4)$$

where  $\sigma_2$  is the principal compressive stress and  $\theta$  is the angle of inclination of  $\sigma_2$  from the horizontal axis ( $x$ ). Furthermore, assuming that the direction of principal strain is identical to that of principal stress, the stress-strain relationship can be derived from the kinetic relationship,

$$\tan^2 \theta = \frac{\varepsilon_2 - \varepsilon_y}{\varepsilon_2 - \varepsilon_x} = \left( \frac{\sigma_2 - f_y}{E_c(\varepsilon)} - \frac{f_y}{E_s} \right) \left( \frac{\sigma_2 - f_x}{E_c(\varepsilon)} - \frac{f_x}{E_s} \right)^{-1} \quad (3.5)$$

where  $\varepsilon_2$  is the principal compressive strain,  $\varepsilon_x$  and  $\varepsilon_y$  are the average transverse and longitudinal strain, respectively,  $E_c(\varepsilon)$  is the secant modulus of concrete as a function of the current strain,  $\varepsilon$ , and  $E_s$  is the elastic modulus of reinforcement. Using Equations (3.2)–(3.4)

and  $v_{jh} = -\frac{\sigma_x}{\tan \theta} = \left( \rho_x f_x + \frac{P_x}{b_c h_b} \right) / \tan \theta$ , Equation (3.5) can be rewritten as a function of  $\tan \theta$  as follows:

$$\left[ \frac{1 + 1/(\zeta \rho_x) - r / (\zeta \rho_x (\zeta \rho_x + r))}{1 + 1/(\zeta \rho_y)} \right] \tan^4 \theta + \left[ \frac{e_y / \varepsilon_x}{(1 + \zeta \rho_y)(r + \zeta \rho_x)} \right] \tan^2 \theta - 1 = 0 \quad (3.6)$$

where  $\zeta = \zeta(\varepsilon) = E_s / E_c(\varepsilon)$ ,  $r = e_x / \varepsilon_x$ ,  $e_x = \frac{P_x}{E_c(\varepsilon) b_c h_b}$ , and  $e_y = \frac{P}{E_c(\varepsilon) b_c h_c}$ . If the transverse reinforcement in the joint is prior to yielding, the average state of strain is obtained as follows:

$$\varepsilon_x = \frac{1}{\rho_x E_s} \left( v_{jh} \tan \theta - \frac{P_x}{b_c h_b} \right), \quad \varepsilon_y = \frac{1}{\rho_y E_s} \left( \frac{v_{jh}}{\tan \theta} - \frac{P}{b_c h_c} \right) \quad (3.7)$$

$$\varepsilon_1 = \frac{\varepsilon_x - \varepsilon_y \tan^2 \theta}{1 - \tan^2 \theta} = \frac{1}{E_s (1 - \tan^2 \theta)} \left( v_{jh} \tan \theta \frac{\rho_y - \rho_x}{\rho_y \rho_x} - \frac{P_x}{b_c h_b \rho_x} + \frac{P \tan^2 \theta}{b_c h_c \rho_y} \right) \quad (3.8)$$

$$\frac{\gamma}{2} = \frac{\varepsilon_1 - \varepsilon_x}{\tan \theta} = \frac{1}{E_s(1 - \tan^2 \theta)} \left\{ \frac{v_{jh}}{\rho_y \rho_x} (\rho_y \tan^2 \theta - \rho_x) - \left( \frac{P_x}{b_c h_b \rho_x} - \frac{P}{b_c h_c \rho_y} \right) \tan \theta \right\} \quad (3.9)$$

Pantazopoulou and Bonacci (1992) formulated the relationship between average joint shear stress and strain before joint reinforcement yielding. They concluded that the principal tensile strain increases with increasing column axial load as well as shear stress based on Equation (2.2), which leads to decreasing the compressive strength of the diagonal strut. This conclusion has been referred to as evidence of the detrimental effect of column axial load on the joint shear strength. However, this conclusion is drawn by the unrealistic assumption that the principal direction is not changed regardless of column axial load, as discussed in 2.2.3.

Pantazopoulou and Bonacci (1992) defined two types of failure without yielding of joint reinforcement: (a) column reinforcement yielding and (b) concrete crushing in the principal compressive stress direction.

Case (a): column reinforcement yielding

$$v_{jh} = \sqrt{\left( \rho_x f_y + \frac{P_x}{b_c h_b} \right) \left( \rho_y f_y + \frac{P}{b_c h_c} \right)} \quad (3.10)$$

where the yield strength of both joint reinforcement and column reinforcement is assumed to be  $f_y$ .

Case (b): concrete crushing in the principal compressive stress direction

$$v_{jh} = \sqrt{\left( |f_{\max}^c| - \rho_x f_y - \frac{N_x}{b_c h_b} \right) \left( \rho_x f_y + \frac{N_x}{b_c h_b} \right)} \quad (3.11)$$

where  $|f_c^{\max}| = \lambda f_c'$  and  $\lambda = \frac{1 + \rho_s |f_y / f_c'|}{0.8 - 0.34 \varepsilon_1 / \varepsilon_0}$ , and  $\varepsilon_0$  is the concrete compressive (negative) strain at the peak compressive stress.

### 3.1.3 Tsonos Model

Tsonos (2007) proposed a new formulation to predict beam-column joint ultimate shear strength based on the strut-and-tie mechanism. The main difference of this model from the previous is to assume the biaxial concrete strength curve as a fifth-degree polynomial and solve this fifth-order polynomial equation. It is assumed that the summation of vertical and horizontal forces equals the vertical and horizontal joint shear force as follows:

$$D_{cy} + (T_1 + T_2 + \dots) = D_{cy} + D_{sy} = V_{jv} \quad (3.12)$$

$$D_{cx} + (D_{1x} + D_{2x} + \dots) = D_{cx} + D_{sx} = V_{jh} \quad (3.13)$$

where  $D_{cx}$  and  $D_{cy}$  are, respectively, the transverse and the longitudinal components of the compression force induced by diagonal strut mechanism,  $T_i$  are the tension forces acting on the longitudinal column bars in the side faces of the column, and  $D_{ix}$  are the transverse component of compression force induced by truss mechanism; see Figure 3.2.

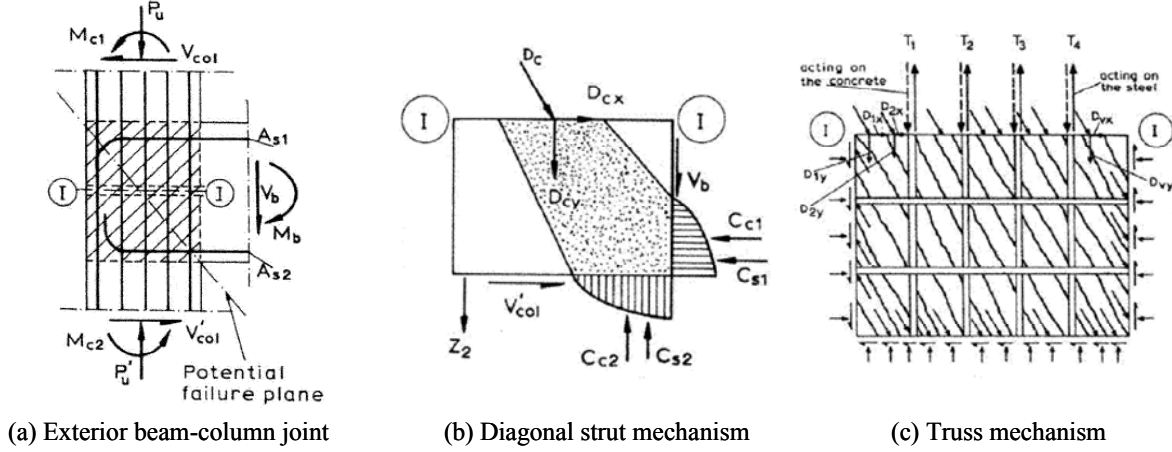


**Fig. 3.2 Equilibrium of exterior beam-column joint (Tsonos 2007).**

The vertical normal compressive stress  $\sigma$  and the shear stress  $v_{jh}$  uniformly distributed over the horizontal joint mid-section are given by

$$\sigma = \frac{D_{cy} + D_{sy}}{b_c h_c} = \frac{V_{jv}}{b_c h_c} \quad (3.14a)$$

$$v_{jh} = \frac{V_{jh}}{b_c h_c} \quad (3.14b)$$

The relationship between the average normal compressive stress and the average shear stress is defined as follows:

$$\sigma = \frac{V_{jv}}{V_{jh}} v_{jh} = \frac{h_b}{h_c} v_{jh} \quad (3.15)$$

where  $h_b$  is total beam cross-section height, and  $h_c$  is total column cross-section height. The principal compressive and tensile stresses are calculated by

$$\sigma_{1,2} = \frac{\sigma}{2} \pm \frac{\sigma}{2} \sqrt{1 + 4 \left( \frac{\tau}{\sigma} \right)^2} \quad (3.16)$$

Equation (3.17) is adopted for the representation of the concrete biaxial strength curve as follows:

$$-10\frac{\sigma_1}{f_c} + \left(\frac{\sigma_2}{f_c}\right)^5 = 1 \quad (3.17)$$

where  $f_c$  is the increased joint concrete compressive strength due to confinement by transverse reinforcement, which is given by the model of Scott et al. (1982) as follows:

$$f_c = K \times f'_c, \quad K = 1 + \frac{\rho_s \times f_{yh}}{f'_c} \quad (3.18)$$

Let  $\tau = \gamma\sqrt{f_c}$  and using the above equations, one obtains

$$\left[\frac{\alpha\gamma}{2\sqrt{f_c}}\left(1 + \sqrt{1 + \frac{4}{\alpha^2}}\right)\right]^5 + 5\frac{\alpha\gamma}{\sqrt{f_c}}\left(\sqrt{1 + \frac{4}{\alpha^2}} - 1\right) = 1 \quad (3.19)$$

where  $\alpha = h_b / h_c$ . Assuming  $x = \frac{\alpha\gamma}{2\sqrt{f'_c}}$  and  $\psi = \frac{\alpha\gamma}{2\sqrt{f'_c}}\sqrt{1 + \frac{4}{\alpha^2}}$ , Equation (3.19) becomes

$$(x + \psi)^5 + 10\psi - 10x = 1 \quad (3.20)$$

Two terms,  $x$  and  $\psi$ , can be expressed by the single variable  $\gamma$  given the aspect ratio  $\alpha = h_b / h_c$ . Therefore, the normalized joint shear strength  $\gamma$  is determined by solving Equation (3.20) explicitly.

### 3.1.4 Wong Model

Wong (2005) developed an exterior joint shear strength model, named “Modified Rotating-Angle Softened-Truss Model (MRA-STM)”, based on the compatibility equation proposed by him modifying three existing softened concrete models, namely (1) modified concrete field theory (MCFT), (2) rotating-angle softened truss-model (RA-STM), and (3) fixed-angle softened truss model (FA-STM). The effect of aspect ratio is considered by accounting for the effect of the shear span to depth ratio as in deep beams. This model is extended to consider the joint shear strength degradation in terms of displacement ductility by reducing the effective stress in the joint region.

### Equilibrium

The total average stress consists of concrete stress and reinforcement stress. The stress states of concrete in the joint are expressed by using Mohr's circle as follows:

$$f_{cx} = f_{c1} - v_{cxy} \cot \theta, \quad f_{cy} = f_{c1} - v_{cxy} \tan \theta, \quad v_{cxy} = \frac{f_{c1} - f_{c2}}{2} \sin 2\theta \quad (3.21)$$

where  $f_{cx}$  and  $f_{cy}$  are the average concrete stress in the transverse and the longitudinal directions, respectively,  $f_{c1}$  and  $f_{c2}$  are the average principal stresses of concrete,  $v_{cxy}$  is the average shear stress of concrete, and  $\theta$  is the inclination angle of principal compressive stress with respect to the transverse direction.

The constitutive models of the concrete in the directions of principal compressive stress and principal tensile stress are defined using the softening concrete model proposed by Belarbi and Hsu (1995). For the compression, the stress-strain relationship is defined as follows:

$$f_{c2} = \zeta f'_c \left\{ 2 \left( \frac{\epsilon_{c2}}{\zeta \epsilon_0} \right) - \left( \frac{\epsilon_{c2}}{\zeta \epsilon_0} \right)^2 \right\} \quad \text{for } \frac{\epsilon_{c2}}{\zeta \epsilon_0} \leq 1 \quad (3.22a)$$

$$f_{c2} = \zeta f'_c \left\{ 1 - \left( \frac{\epsilon_{c2}/\zeta \epsilon_0 - 1}{4/\zeta - 1} \right)^2 \right\} \quad \text{for } \frac{\epsilon_{c2}}{\zeta \epsilon_0} > 1 \quad (3.22b)$$

where  $\zeta = \frac{5.8}{\sqrt{f'_c}} \frac{1}{\sqrt{1+400\epsilon_{c1}}} \leq \frac{0.9}{\sqrt{1+400\epsilon_{c1}}}$ ,  $\epsilon_{c2}$  is the principal compressive (negative) strain, and

$\epsilon_0$  is the concrete strain at maximum compressive stress defined as

$\epsilon_0 = -0.002 - 0.001 \left( \frac{f'_c - 20}{80} \right)$  for  $20 \leq f'_c \leq 100$  (MPa). There is no mention of the cases in

which concrete strength is less than 20 MPa and greater than 100 MPa. For the tension, the stress-strain relationship is defined as follows:

$$f_{c1} = E_c \epsilon_{c1} \quad \text{for } \epsilon_{c1} \leq \epsilon_{cr} \quad (3.23)$$

$$f_{c1} = f_{cr} \left( \frac{0.00008}{\epsilon_{c1}} \right)^{0.4} \quad \text{for } \epsilon_{c1} > \epsilon_{cr} \quad (3.24)$$

where  $E_c = 3875 \sqrt{f'_c}$  MPa,  $\epsilon_{cr} = 0.00008$ , and  $f_{cr} = 0.31 \sqrt{f'_c}$  MPa.

Horizontal and vertical effective stresses are defined based on the empirical results of shear span to depth ratio in deep beams as follows:

$$p_1 = \frac{2V_{jh}}{bH_c} \quad \text{for } \frac{L_v}{H_c} \leq 0.5 \text{ (i.e. low aspect ratio)} \quad (3.25a)$$

$$= \frac{V_{jh}}{bH_c} \left( \frac{4}{3} - \frac{2L_v}{3H_c} \right) \quad \text{for } 0.5 \leq \frac{L_v}{H_c} \leq 2.0 \text{ (i.e. high aspect ratio)} \quad (3.25b)$$

$$p_2 = \frac{2V_{jv}}{bH_b} \quad \text{for } \frac{L_h}{H_b} \leq 0.5 \text{ (i.e. high aspect ratio)} \quad (3.26a)$$

$$= \frac{V_{jv}}{bH_b} \left( \frac{4}{3} - \frac{2L_h}{3H_b} \right) \quad \text{for } 0.5 \leq \frac{L_h}{H_b} \leq 2.0 \text{ (i.e. low aspect ratio)} \quad (3.26b)$$

where  $L_v$  is the span between the horizontal forces, and  $L_h$  is the span between the vertical forces as shown in Figure 3.3.

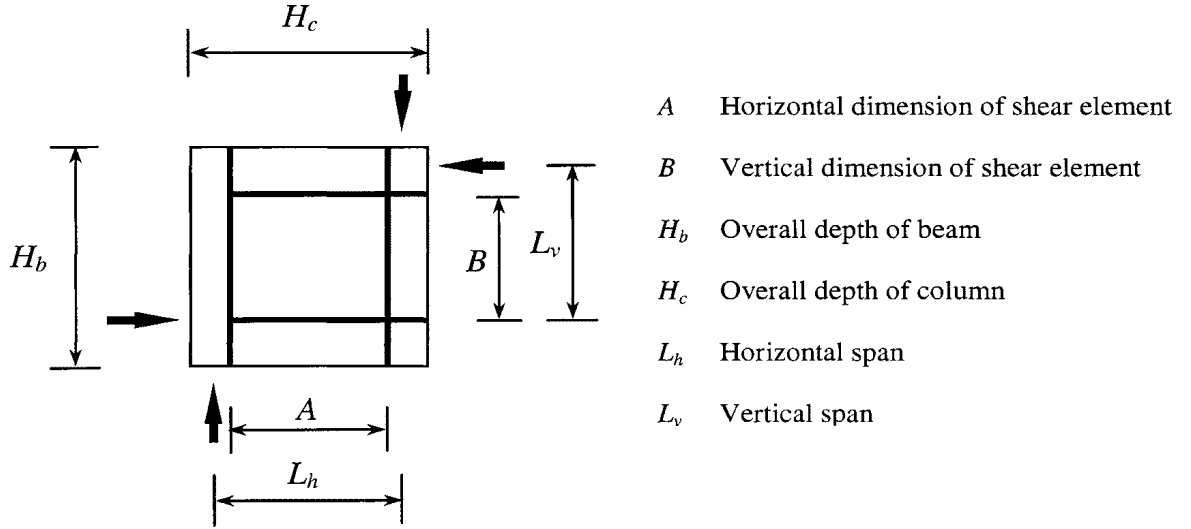


**Fig. 3.3 Definition of symbols in MRA-STM (Wong 2005).**

To reduce the joint shear strength with increasing ductility, the effective stresses are multiplied by a reduction factor as follows:

$$p_{ir} = R(\mu) p_i, \quad R(\mu) = \begin{cases} \frac{6-\mu}{5} & \text{without joint hoop} \\ \frac{6}{5} \left( \frac{1}{\mu} - \frac{1}{6} \right) & \text{with joint hoop} \end{cases} \quad (3.27)$$

where  $p_{ir}$  is the reduced effective stress of the  $i$ -th ( $i=1,2$ ) component  $p_i$ , and  $\mu$  is the displacement ductility factor.

Final equilibrium equations are set up for both the horizontal and vertical directions as follows:

$$f_{cx} + \rho_{sx} f_{sx} + p_{1r} = 0 \quad (3.28)$$

$$f_{cy} + \rho_{sy} f_{sy} + p_{2r} = 0 \quad (3.29)$$

where  $\rho_{sx}$  and  $\rho_{sy}$  are the area ratio of reinforcement in the x and y directions, respectively, and  $f_{sx}$  and  $f_{sy}$  are the stress of reinforcement in the x and y directions, respectively.

### Compatibility

The strain state of concrete in the joint is described by the Mohr's circle as follows:

$$\varepsilon_{cx} = \frac{\varepsilon_{c1} - \varepsilon_{c2}}{2} (1 - \cos 2\theta) + \varepsilon_{c2} \quad (3.30)$$

$$\varepsilon_{cy} = \varepsilon_{cx} + (\varepsilon_{c1} - \varepsilon_{c2}) \cos 2\theta \quad (3.31)$$

$$\gamma_{cxy} = 2(\varepsilon_{cy} - \varepsilon_{c2}) \tan \theta = 2(\varepsilon_{c1} - \varepsilon_{cx}) \tan \theta \quad (3.32)$$

where  $\varepsilon_{cx}$  and  $\varepsilon_{cy}$  are the average concrete strain in the x and y directions, respectively,  $\varepsilon_{c1}$  and  $\varepsilon_{c2}$  are the average principal strains of the concrete, and  $\gamma_{cxy}$  is the average shear strain of the concrete.

The principal direction of strain is continuously updated once the principal tensile strain exceeds the concrete strain at cracking onset, while the principal direction of stress is retained. After cracking, the local strains at the cracks are calculated and added to the global average strain following the procedure below,

$$w = s_{\chi} \varepsilon_{cn} \quad \text{and} \quad \Delta = s_{\chi} \gamma_{cmn} \quad (3.33)$$

$$\varepsilon_{cn} = \varepsilon_{c2} \sin^2 \beta + \varepsilon_{c1} \cos^2 \beta \quad (3.34)$$

$$\gamma_{cmn} = (\varepsilon_{c1} - \varepsilon_{c2}) \sin 2\beta \quad (3.35)$$

$$s_{\chi} = \frac{1}{\frac{\cos \chi}{s_{mx}} + \frac{\sin \chi}{s_{my}}} \quad (3.36)$$

$$\varepsilon_{xw} = \frac{w}{s_{\chi}} \cos^2 \chi, \quad \varepsilon_{yw} = \frac{w}{s_{\chi}} \sin^2 \chi, \quad \gamma_{xyw} = \frac{w}{s_{\chi}} \sin 2\chi \quad (3.37)$$

$$\varepsilon_{x\Delta} = -\frac{\Delta}{2s_{\chi}} \sin 2\chi, \quad \varepsilon_{y\Delta} = \frac{\Delta}{2s_{\chi}} \sin 2\chi, \quad \gamma_{xy\Delta} = \frac{\Delta}{s_{\chi}} \cos 2\chi \quad (3.38)$$

where  $s_{mx}$  and  $s_{my}$  are the mean crack spacing in the x and y directions, respectively,  $\beta = \alpha - \theta$

where  $\alpha$  is the angle between the crack and the x direction, and  $\chi = 90^\circ - \alpha$ .

Ultimately, the updated strains including local components by cracking are presented as follows:

$$\varepsilon_x = \varepsilon_{cx} + \varepsilon_{xw} + \varepsilon_{x\Delta} \quad (3.39)$$

$$\varepsilon_y = \varepsilon_{cy} + \varepsilon_{yw} + \varepsilon_{y\Delta} \quad (3.40)$$

$$\gamma_{xy} = \gamma_{cxy} + \gamma_{xyw} + \gamma_{xy\Delta} \quad (3.41)$$

From the updated strains, maximum stresses in the transverse and the longitudinal directions are determined following the assumed softening concrete constitutive model and two equilibrium equations, Equations (3.28) and (3.29), are checked. If both equilibriums are not satisfied, all procedures are repeated by changing the principal directional angle,  $\theta$ . Therefore, an extensive numerical iteration is required to obtain joint shear strength by this model. The horizontal and vertical effective stresses from the analogy of shear span to depth ratio in a deep beam are introduced in the equilibrium equation, but it is to be noted that the boundary condition of the exterior joints is completely different from that of a deep beam.

## 3.2 STRUT AND TIE MECHANISM

### 3.2.1 Hwang and Lee Model

Hwang and Lee (1999) developed a joint shear strength model named ‘‘Softened Strut-and-Tie (SST) model’’ to satisfy equilibrium, compatibility, and constitutive laws of cracked reinforced concrete. The authors claimed that the SST model showed good agreement with available experimental data. The SST model assumes that the joint shear resisting mechanisms are composed of these three mechanisms: (1) the diagonal strut mechanism, (2) the horizontal mechanism, and (3) the vertical mechanism, as shown in Figure 3.4.

#### *Equilibrium*

$$V_{jh} = D \cos \theta + F_h + F_v \cot \theta \quad (3.42)$$

where  $D$  is the compression force in the diagonal strut,  $F_h$  is the tension force in the horizontal tie, and  $F_v$  is the tension force in the vertical tie, and diagonal angle  $\theta = \tan^{-1} \left( \frac{h_b''}{h_c''} \right)$  where  $h_b''$  is the distance between the top and bottom beam reinforcement and  $h_c''$  is the distance between the tail

of the beam reinforcement hook anchorage and the inner side of column reinforcement as shown in Figure 3.4.

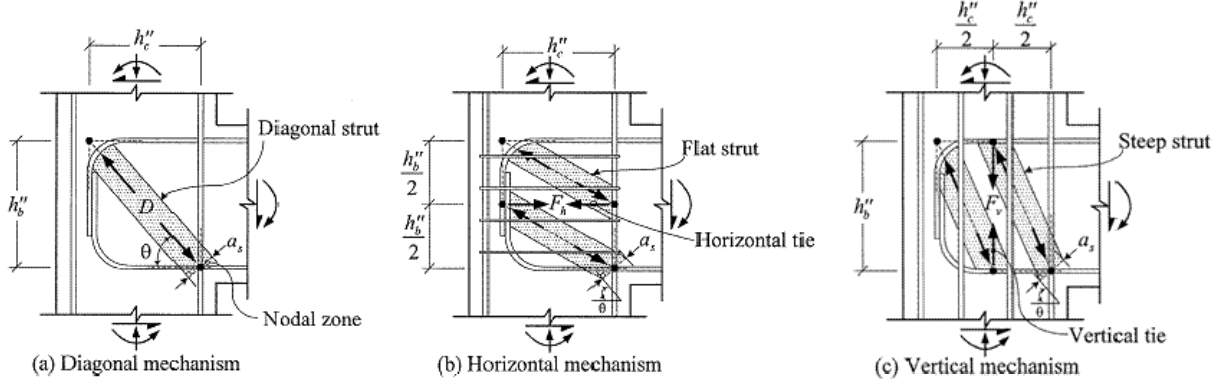


**Fig. 3.4 Joint shear resisting mechanisms of SST model (Hwang and Lee 1999).**

The ratios of the horizontal shear  $V_{jh}$  assigned among the three mechanisms are directly defined by the diagonal strut angle as follows:

$$D \cos \theta = \frac{(1-\gamma_h)(1-\gamma_v)}{1-\gamma_h\gamma_v} \times V_{jh} \quad (3.43)$$

$$F_h = \frac{\gamma_h(1-\gamma_v)}{1-\gamma_h\gamma_v} \times V_{jh} \quad (3.44)$$

$$F_v \cot \theta = \frac{(1-\gamma_h)\gamma_v}{1-\gamma_h\gamma_v} \times V_{jh} \quad (3.45)$$

where  $\gamma_h = \frac{2 \tan \theta - 1}{3}$  and  $\gamma_v = \frac{2 \cot \theta - 1}{3}$ . The strut angle is limited by  $\frac{1}{2} \leq \tan \theta \leq 2$ . The

fraction of each mechanism depending on the diagonal strut angle is shown in Figure 3.5. The maximum compressive stress acting on the nodal zone of the diagonal strut is formulated as follows:

$$\sigma_{d,\max} = \frac{1}{A_{str}} \left\{ D + \frac{\cos \left( \theta - \tan^{-1} \left( \frac{h_b}{2h_c} \right) \right)}{\cos \left( \tan^{-1} \left( \frac{h_b}{2h_c} \right) \right)} F_h + \frac{\cos \left( \theta \tan^{-1} \left( \frac{2h_b}{h_c} \right) - \theta \right)}{\sin \left( \tan^{-1} \left( \frac{2h_b}{h_c} \right) \right)} F_v \right\} \quad (3.46)$$

where  $A_{str}$  is the effective area of the diagonal strut,  $A_{str} = h_s b_j$ , and

$$h_s = \left( 0.25 + 0.85 \frac{P}{A_g f'_c} \right) h_c \quad (3.47)$$

and  $b_j$  is defined following ACI 318-95 (1995).

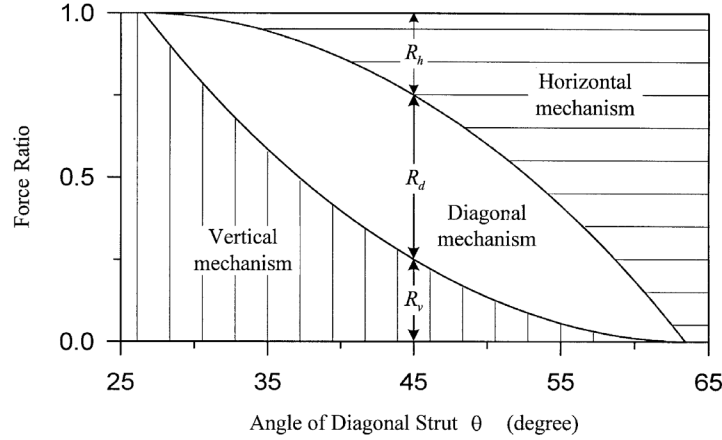


**Fig. 3.5 Ratios of force distribution among mechanisms of SST model (Hwang and Lee 1999).**

#### Constitutive Laws

The concrete strength in the diagonal strut follows the softening concrete model by Belarbi and Hsu (1995) as follows:

$$\sigma_d = \zeta f'_c \left[ 2 \left( \frac{\varepsilon_2}{\zeta \varepsilon_0} \right) - \left( \frac{\varepsilon_2}{\zeta \varepsilon_0} \right)^2 \right] \quad \text{for} \quad \frac{\varepsilon_2}{\zeta \varepsilon_0} \leq 1 \quad (3.48)$$

where  $\zeta = \frac{5.8}{\sqrt{f'_c}} \frac{1}{\sqrt{1+400\varepsilon_1}} \leq \frac{0.9}{\sqrt{1+400\varepsilon_1}}$  and  $\varepsilon_0 = -0.002 - 0.001 \left( \frac{f'_c - 20}{80} \right)$  for  $20 \leq f'_c \leq 100$

(MPa). The SST model defines the joint shear strength as the joint shear at the point where the compressive stress and strain of the diagonal strut reach their peaks as follows:

$$\sigma_d = \zeta f'_c \quad \text{and} \quad \varepsilon_d = \zeta \varepsilon_0 \quad (3.49)$$

The behavior of the reinforcing steel is assumed to be elastic-perfectly-plastic. Therefore,

$$f_s = E_s \varepsilon_s \quad \text{for} \quad \varepsilon_s < \varepsilon_y \quad (3.50)$$

$$f_s = f_y \quad \text{for} \quad \varepsilon_s \geq \varepsilon_y \quad (3.51)$$

From the above constitutive relationships, the horizontal and vertical tension tie force is determined by

$$F_h = A_{th} E_s \varepsilon_h \leq F_{yh} \quad \text{and} \quad F_{yh} = A_{th} f_y \quad (3.52)$$

$$F_v = A_{tv} E_s \varepsilon_v \leq F_{yv} \quad \text{and} \quad F_{yv} = A_{tv} f_y \quad (3.53)$$

where  $A_{th}$  and  $A_{tv}$  are the areas of reinforcement in the horizontal and vertical directions, respectively, and  $\varepsilon_h$  and  $\varepsilon_v$  are the average strains in the horizontal and vertical directions, respectively.

### *Compatibility*

The two-dimensional compatibility condition is constructed considering the average strains in the joint panel as follows:

$$\varepsilon_1 = \varepsilon_h + (\varepsilon_h - \varepsilon_2)^2 \cot^2 \theta \quad (3.54)$$

$$\varepsilon_1 = \varepsilon_v + (\varepsilon_v - \varepsilon_2)^2 \tan^2 \theta \quad (3.55)$$

An iterative solver is needed to calculate the joint shear strength using the SST model. The iterative solver controls a softening coefficient such that this coefficient satisfies both equilibrium and compatibility, while other parameters, i.e., joint geometry (actually diagonal strut angle), concrete strength, diagonal strut depth, Young's modulus of reinforcing steel, and horizontal and vertical reinforcement ratios, are given as user input values. For unreinforced joints, the strain of the beam reinforcement is considered as the horizontal strain  $\varepsilon_h$  in Equation (3.54). Similarly, the strain of the column reinforcement in tension is taken as the vertical strain  $\varepsilon_v$  in Equation (3.55) if there is no intermediate column bar in the joint. Given the assumptions of horizontal and vertical strain in unreinforced joints, this model is not able to predict the joint shear failure without beam reinforcement yielding.

The shear strength of the joint is defined when the compressive stress and strain of the concrete diagonal strut reach Equation (3.49). These stress and strain values are dependent on each other. Therefore, an iterative procedure is needed to calculate the joint shear strength.

### **3.2.2 Ortiz Model**

Ortiz (1993) used the strut-and-tie (SAT) concept to predict the shear strength of exterior beam-column joints with and without transverse reinforcement. The concrete strength of the diagonal

strut is taken as the design strength for cracked concrete proposed by the CEB Model Code (1990). The formulation is as follows:

$$D \sin \theta = F_{ve}, \quad D \cos \theta = V_j \quad (3.56)$$

$$F_{ve} = P + T_{c,i} + T_{c,e}, \quad V_{jh} = T_b - V_c \quad (3.57)$$

$$D / (w_i b_c) = \sigma_d = 0.6 f'_c (1 - f'_c / 250) \quad (3.58)$$

where  $P$  is the column axial load,  $T_{c,i}$  is the tension of the interior column reinforcing bars,  $T_{c,e}$  is the tension of the exterior column reinforcing bars, and  $T_b$  is the tension of the top beam reinforcement (Fig. 3.6). A strut depth is simply assumed to be

$$w_i = 0.45W \quad (3.59)$$

where  $W = h_c \sin \theta + s \cos \theta$ ,  $\theta = \tan^{-1} \left( \frac{F_{ve}}{V_{jh}} \right)$ , and  $s$  is the depth to the neutral axis of the beam

from the extreme compression fiber at the intersection with the column. To determine the joint shear strength,  $V_{jh}$ , an iterative solution procedure is needed because  $W$  is dependent on both  $s$  and  $\theta$  which are dependent on the applied loading.

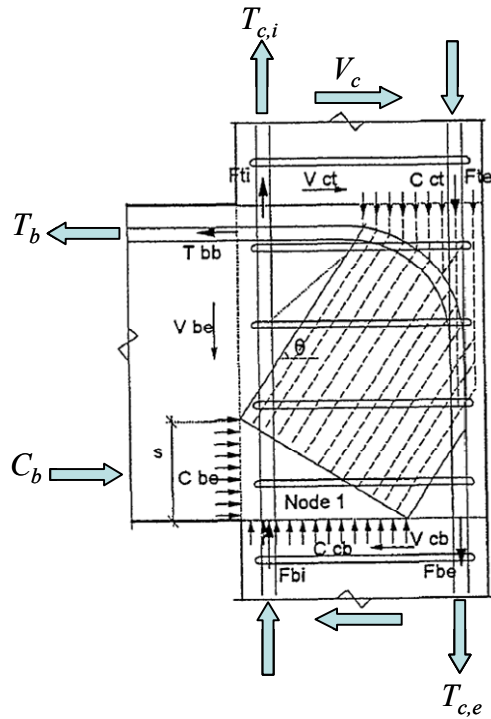


Fig. 3.6 Free body diagram of joint (Ortiz 1993).

### 3.2.3 Vollum Model

Vollum (1998) constructed a SAT model for exterior beam-column joints with and without transverse reinforcement (Fig. 3.7). The geometry of the top and bottom nodes is defined by the section analysis of beam and column under the Bernoulli assumption of a plane section remaining plane after bending. From the stress state and experimental observation, this model defines the joint shear failure when the maximum diagonal stress at the top node reaches the cracked concrete strength. The maximum stress and tensile strain are determined by

$$\sigma_d = \lambda f'_c \left[ 2 \left( \frac{\varepsilon_2}{\varepsilon_o} \right) - \left( \frac{\varepsilon_2}{\varepsilon_o} \right)^2 \right], \quad \lambda = \frac{1}{0.8 - 0.34 \frac{\varepsilon_1}{\varepsilon_o}} \quad (3.60)$$

$$\varepsilon_1 = \varepsilon_h + (\varepsilon_h - \varepsilon_o) \cot^2 \theta \quad (3.61)$$

where  $\varepsilon_1$  and  $\varepsilon_2$  are principal tensile and compressive strain, respectively,  $\varepsilon_o$  is the maximum compressive (negative) strain in the diagonal strut and assumed to be -0.002, and  $\varepsilon_h$  is tensile strain in the transverse direction.

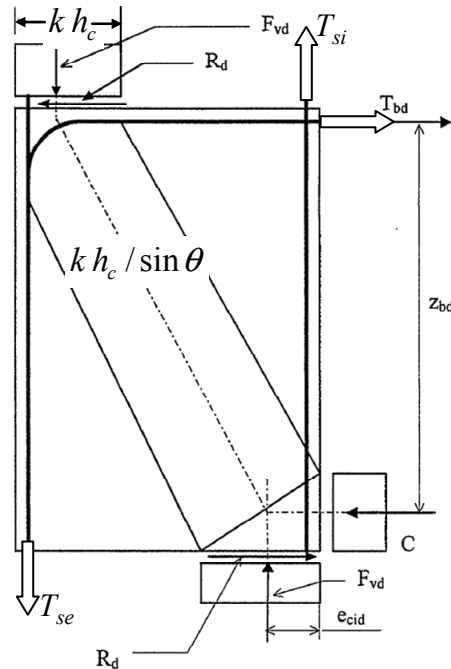


**Fig. 3.7 Free body diagram by Vollum (1998).**

Vollum (1998) investigated a coefficient  $k$  (Fig. 3.7) under different levels of column axial load using one of the Oritz (1993) test results that failed in joint shear. The value of  $k$  is

calibrated to be 0.4 under zero axial load as shown in Figure 3.8. Then, two approaches are made to simplify the analytical model by:

**Approach A**

Two assumptions are made: (1) the column axial load is zero, which means ignoring the column load effect and (2) the strut width is taken as  $0.4h_c / \sin \theta$  where  $\theta$  can be determined by the aspect ratio or the horizontal and vertical shear force ratio. Under these two assumptions, this approach finds  $T_{si}$  required to satisfy the specified strut width of  $0.4h_c / \sin \theta$  by an iterative procedure.

**Approach B**

All of the forces in the column and beam reinforcements are calculated with increasing column axial load by conventional section analysis. This approach adjusts  $T_{si}$  until the minimum strut width is obtained, but it should be kept equal to or greater than  $0.4h_c / \sin \theta$ .

Vollum (1998) indicated that approach B underestimates the joint shear strength at low to medium column loads because the resulting strut width is less than required to maintain constant joint shear strength. Therefore, approach A is selected due to its simplicity and accuracy for estimating the joint failure load.

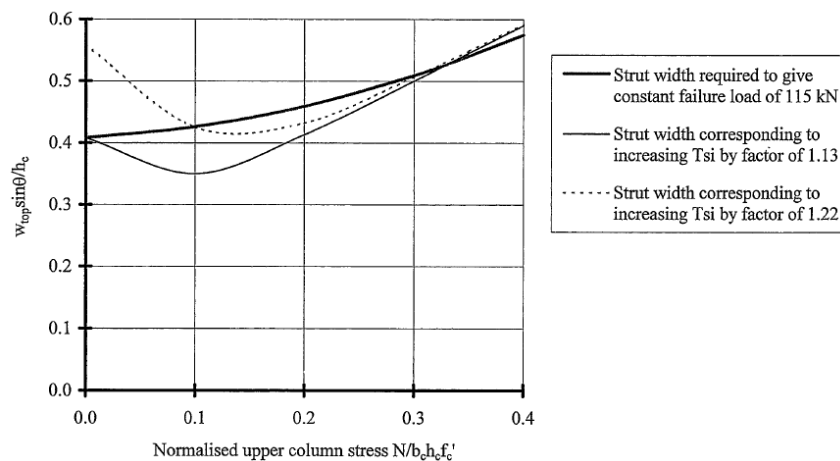


**Fig. 3.8 Calibration of coefficient  $k$  (Vollum 1998).**

### 3.3 SINGLE STRUT MECHANISM

#### 3.3.1 FEMA 273 Model

The FEMA 273 (1997) suggests a joint shear stress-strain response envelope with a backbone curve. The maximum shear capacity,  $Q_{CE}$ , is defined as follows:

$$Q_{CE} = \lambda_{FEMA} \Gamma \sqrt{f'_c} A_j \quad (3.62)$$

where  $\lambda_{FEMA} = 0.75$  for lightweight concrete and 1.0 for normal weight concrete.

$\Gamma = 6$  (psi<sup>0.5</sup>) for exterior joints with  $\rho_j < 0.003$ .

$\rho_j$  is the volumetric ratio of the transverse reinforcement in the joint region.

$A_j$  is the joint area defined by a joint depth equal to the column dimension in the direction of framing and a joint width equal to the smallest of (1) the column width, (2) the beam width plus the joint depth, and (3) twice the smaller perpendicular distance from the longitudinal axis of the beam to the column side.

#### 3.3.2 Zhang and Jirsa Model

Zhang and Jirsa (1982) developed an approach to determine the shear strength and behavior of beam-column joints under monotonic and cyclic loading from a large number of published test data. This model assumes that the joint shear strength is determined by the failure of a single diagonal strut that is affected by several parameters including: the concrete strength, the hinge mechanism, the column axial load, the transverse reinforcement ratio, the joint aspect ratio, and the existence of lateral beams. The effects of these parameters were derived by a statistical approach. The joint strength equation for monotonic loading is given depending on forming plastic hinges due to beam reinforcement yielding in the beams adjacent to the joint as follows:

$$Q_m = K \zeta \gamma f'_c b_c \sqrt{a_c^2 + a_b^2} \cos \theta \quad \text{for joints without beam hinge} \quad (3.63a)$$

$$= K \zeta \gamma f'_c b_c a_c \cos \theta \quad \text{for joints with beam hinge} \quad (3.63b)$$

where  $K$  represents the effect of concrete strength such that  $K = 1.20 - 0.1f'_c$ ,  $f'_c$  in (ksi),  $\zeta$  represents the effect of the volumetric transverse reinforcement ratio,  $\rho_s$ , as follows:

$$\zeta = 0.95 + 4.5\rho_s \leq 1.20, \quad 0.01 \leq \rho_s \leq 0.06 \quad (3.64)$$

$\gamma$  represents the effect of the lateral beams as follows:

$$\gamma = 0.85 + 0.30 \frac{W_L}{h_c}, \quad 0.5 \leq \frac{W_L}{h_c} \leq 1.0 \quad (3.65)$$

where  $W_L$  is the width of the lateral beam.  $a_c$  and  $a_b$  are the depth of the compression zone in column and beam, respectively, which are determined considering the effect of column axial load.  $\theta$  represents the angle of inclined of the strut as follows:

$$\theta = \tan^{-1} \left( \frac{h_b - \frac{2}{3} a_b}{h_c - \frac{2}{3} a_c} \right) \quad \text{for joints without beam hinge} \quad (3.66a)$$

$$\theta = \tan^{-1} \left( \frac{h_b}{h_c - \frac{2}{3} a_c} \right) \quad \text{for joints with beam hinge} \quad (3.66b)$$

The joint strength under cyclic loading was modified from the monotonic loading case by adding one parameter  $\eta$  as follows:

$$Q_c = \eta Q_m, \quad \eta = \begin{cases} 1.0 - 4.0R & \text{as an average value} \\ 0.83 - 4.0R & \text{for design purpose} \end{cases} \quad (3.67)$$

where  $R$  is defined as rotation index,  $R = \frac{\Delta}{L}$ ,  $\Delta$  is total beam end deflection, and  $L$  is the length from the beam inflection point to the column face. The average value is determined by a statistical analysis of literature test data and the design value is the lower limit of those data.

### 3.4 EMPIRICAL MODELS

Several empirical models for the strength of beam-column joints have been suggested by researchers in Europe. They extracted some parameters to affect the joint shear strength from their tests or from literature and used statistical regression analysis under the assumption that each parameter is independent (uncorrelated) from other parameters.

#### 3.4.1 Sarsam and Phipps Model

Sarsam and Phipps (1985) proposed the following equation for the design of exterior beam-column joints under monotonic loading,

$$V_{cd} = 5.08(f_{cu}\rho_c)^{0.33}\left(\frac{d_c}{d_b}\right)^{1.33} b_c d_c \sqrt{1 + 0.29\frac{N}{A_g}} \quad (3.68)$$

$$V_{sd} = 0.87 A_{js} f_{yv} \quad (3.69)$$

$$V_{ud} = V_{cd} + V_{sd} \quad (3.70)$$

where  $f_{cu}$  is the concrete cube strength (MPa) and  $\rho_c$  is the column longitudinal reinforcement ratio,  $\rho_c = \frac{A_{so}}{b_c d_c}$ , where  $A_{so}$  is the area of the layer of steel farthest from the maximum compression face in a column ( $\text{mm}^2$ ),  $N$  is the axial column load (N),  $A_{js}$  is the total area of the transverse reinforcement ( $\text{mm}^2$ ) crossing the diagonal plane from corner to corner of the joint between the beam compression and tension reinforcement, and  $f_{yv}$  is the tensile strength of the transverse reinforcement (MPa).

### 3.4.2 Taylor Model

Taylor (1974) employed the deep beam analogy to predict the joint shear strength. The effective depth ratio of beam to column in a joint is considered analogous to the shear span to depth ratio in a deep beam. The ultimate joint shear strength,  $v_u$ , is compared with the nominal shear strength of a column without stirrups,  $v_c$ , given in the British Code of Practice CP 110 (1972) by using the effective depth ratios in the joints and the following design equation is proposed,

$$\frac{v_u}{v_c} = 3 + 2 \frac{d_c}{z_b} \quad (3.71)$$

where  $v_u$  is the ultimate joint shear strength,  $v_c$  is the nominal shear stress,  $d_c$  is the effective depth of column, and  $z_b$  is the distance between tension and compression resultant in the beam cross section at the column face. The ratio  $\frac{d_c}{z_b}$  is analogous to the ratio of shear span to beam depth in a deep beam.

Taylor (1974) also assumed that the column shear is negligible because it is very small compared to the joint shear force provided by the beam reinforcement, and finally the total design joint shear force is  $0.87A_{js}f_y$ . From this assumption, the above equation can be rewritten as follows:

$$\frac{0.87 A_s f_y}{b_c d_c} \leq \left( 3 + 2 \frac{d_c}{z_b} \right) v_c \quad (3.72)$$

### 3.4.3 Scott et al. Model

Scott et al. (1994) proposed a model to predict the shear strength of exterior beam-column joints based on a single diagonal strut without either horizontal or vertical mechanisms.

$$v_{crsh} = 2\sqrt{f_{cu}} / (z_{col} / z_{bm} + z_{bm} / z_{col}) \quad (3.73)$$

$$V_{crsh} = v_{crsh} b_c d_c \quad (3.74)$$

where  $f_{cu}$  is the concrete characteristic strength,  $z_{bm} / z_{col}$  is  $\tan \theta$  where  $\theta$  is the angle between the diagonal strut and the horizontal axis. They determined  $z_{bm}$  from a section analysis of a beam and defined  $z_{col}$  as the distance between the centers of two outer column bars. Note that the subscript *crsh* implies crushing of the diagonal strut with  $45^\circ$ .

### 3.4.4 Bakir and Bodurođlu Model

Bakir and Bodurođlu (2002) developed an empirical model based on SI units by regression of published test data. Remarkably, this model includes the parameters of the beam reinforcement ratio,  $100A_s / b_b d_b$ , and the joint aspect ratio,  $h_b / h_c$ . The total joint shear strength is the sum of: (1) concrete contribution using Equation (3.75) and (2) steel contribution using Equation (3.76).

$$V_c = \frac{0.71 \beta \gamma \left( \frac{100 A_{sb}}{b_b d} \right)^{0.4289}}{\left( \frac{h_b}{h_c} \right)^{0.61}} \left( \frac{b_c + b_b}{2} \right) h_c \sqrt{f'_c} \quad \text{for joints without transverse reinforcement} \quad (3.75)$$

$$V_s = \alpha A_{sje} f_y \quad (3.76)$$

where  $\beta$  represents the effect of anchorage detail:  $\beta = 1.0$  for anchorage type A (Fig. 2.2)

$= 0.85$  for anchorage type C (Fig. 2.2)

$\gamma = 1.37$  for inclined bars in the joint and  $\gamma = 1.0$  for others

$\alpha = 0.664$  for joints with low amount of transverse reinforcement

$= 0.6$  for joints with medium amount of transverse reinforcement

= 0.37 for joints with high amount of transverse reinforcement

$A_{sb}$  is the total area of beam reinforcement in tension.

$A_{sje}$  is the total area of the transverse reinforcement in the joint.

### 3.4.5 Hegger et al. Model

Hegger et al. (2003) developed the empirical model in SI units including the parameters of column reinforcement ratio and joint aspect ratio. The model is formulated as follows:

$$V_j = V_c + V_s \quad (3.77)$$

$$V_c = \alpha_1 A B C b_j h_c \quad (3.78)$$

$$V_s = \alpha_2 A_{sj,eff} f_y \quad (3.79)$$

where  $\alpha_1$  represents the effect of anchorage detail:  $\alpha_1 = 0.95$  for anchorage type A

= 0.85 for anchorage type C

$A$  represents the effect of aspect ratio:  $A = 1.2 - 0.3h_b / h_c$ ,  $0.75 \leq h_b / h_c \leq 2$ .

$B$  represents the effect of column reinforcement ratio:  $B = 1.0 + \frac{\rho_{col} - 0.5}{7.5}$ .

$\rho_{col}$  is the ratio of column longitudinal reinforcement in tension.

$C$  represents the effect of concrete strength:  $C = 2 \sqrt[3]{f'_c}$ ,  $20 \leq f'_c \leq 100$  MPa.

$\alpha_2$  represents the efficiency of transverse reinforcement according to Table 3.1.

$A_{sj,eff}$  is the effective cross section area of transverse reinforcement within the joint located outside the compression zone of beam with yield strength  $f_y$ .

**Table 3.1 Efficiency factor of transverse reinforcement in Hegger et al. (2003).**

Anchorage type*	Hairpins	Closed stirrups
Type A	0.7	0.6
Type C	0.6	0.5

\*Anchorage types are designated in Figure 2.2

### 3.4.6 Vollum Model

Vollum (1998) developed an empirical strength model based on SI units for exterior beam-column joints with and without transverse reinforcement. Vollum and Newman (1999) insisted that it is not feasible to develop a realistic strut and tie model due to its complexity. The difficulties are to define node dimensions and equivalent strut width as well as to calculate column bar forces. The following equation is derived and calibrated by published test data,

$$V_c = 0.642 \beta [1 + 0.552(2 - h_b/h_c)] b_e h_c \sqrt{f'_c} \quad \text{for joints without transverse reinforcement} \quad (3.80)$$

$$V_j = \max \left[ \left( V_c - \alpha b_e h_c \sqrt{f'_c} \right) + A_{sj} f_y, V_c \right] \leq 0.97 b_e h_c \sqrt{f'_c} [1 + 0.552(2 - h_b/h_c)] \\ \leq 1.33 b_e h_c \sqrt{f'_c}$$

for joints with transverse reinforcement (3.81)

where  $\beta$  represents the effect of anchorage detail:  $\beta = 1.0$  for anchorage type A (Fig. 2.2)

$= 0.9$  for anchorage type C (Fig. 2.2)

$\alpha$  represents the effect of column axial load and concrete strength taken as  $\alpha = 0.2$ .

$A_{sj}$  is the cross-sectional area of the joint stirrups within the top two thirds of the beam depth below the main beam reinforcement.

## 3.5 SHEAR STRENGTH DEGRADATION

Joint shear failure modes are mainly divided into two types: (1) joint shear failure without beam reinforcement yielding (J) and (2) joint shear failure with beam reinforcement yielding (BJ) as discussed in Chapter 2. The joint shear strength of the BJ failure mode is less than that of the J failure mode due to lower beam reinforcement ratio. To obtain the reduced shear strength of the BJ failure mode, three modification methods are adopted in the existing models.

### 3.5.1 Modification of Strength Factor

Park (1997) proposed the simple linear degradation model of joint shear strength normalized by  $\sqrt{f'_c}$  in terms of curvature ductility in the beam plastic hinges at the faces of the column (Fig. 3.9).

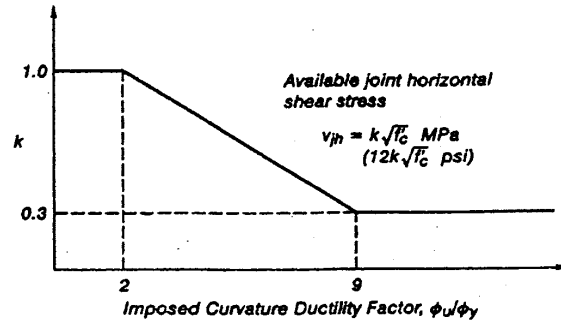


**Fig. 3.9 Shear strength degradation by curvature ductility (Park 1997).**

Hakuto et al. (2000) suggested the degradation curve of joint shear strength in terms of the displacement ductility for joints without transverse reinforcement in which only a diagonal strut mechanism exists. The maximum horizontal joint shear stress ratio,  $v_{jh} / f'_c$ , is 0.17 at a displacement ductility factor  $\mu$  of 1 and the minimum horizontal shear stress ratio is 0.05 at  $\mu$  of 8 (Fig. 3.10). The joints having shear demand less than the minimum value do not experience shear failure, and beam flexural hinges are developed.

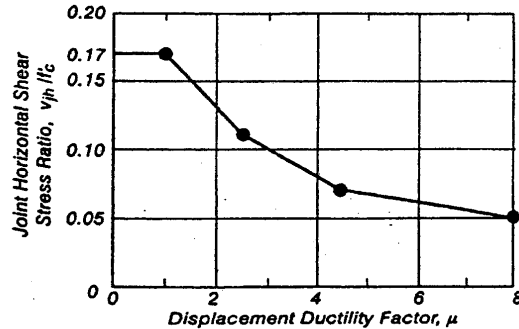


**Fig. 3.10 Shear strength degradation by displacement ductility (Hakuto et al. 2000).**

Wong (2005) used a similar approach in the MRA-STM that he developed. The effective horizontal stresses in equilibrium equations, Eqs. (3.28) and (3.29), are reduced by the reduction factor  $R$  which depends on the ductility level as shown Equation (3.27).

### 3.5.2 Modification of Diagonal Strut Width

Zhang and Jirsa (1982) used two different diagonal strut width equations, Equation (3.63a) and (3.63b), depending on the occurrence of a beam hinge mechanism. The diagonal strut width of the joint with a beam hinge mechanism is less than that of a joint without one and thus the joint shear strength of the former is also less than that of the latter. However, it is not simple to define the occurrence of a beam hinge mechanism. and this approach does not consider the ductility as a variable parameter.

Hwang (2001) modified his SST model to add a ductility parameter in the equation to determine the strut width,  $a_s$ , as follows:

$$a_s = \sqrt{a_b^2 + a_c^2} - \left( \sqrt{a_b^2 + a_c^2} - a_c \right) \times \sqrt{\frac{\mu - 1}{3}} \quad (3.82)$$

where  $a_b$  is the compression block in the beam section at the column joint face, assuming  $a_b = 0.2h_b$ ,  $a_c$  is the compression block in the column section at the beam joint face, assuming  $a_c = \left( 0.25 + 0.85 \frac{P}{f_c' A_g} \right) h_c$ , and  $\mu$  is the displacement ductility factor. As the ductility increases, the width of diagonal strut decreases and the joint shear strength also decreases.

## 3.6 JOINT ELEMENT MODEL FOR RC FRAME SIMULATION

There have been several attempts to simulate RC frames by including the deformation of beam-column joints. Due to the inherent complex behavior of RC beam-column joints, rotational spring elements have been used to simply represent the shear deformation of the joint panel combined with the rotation due to bar slip. Theiss (2005), and Celik and Ellingwood (2008) summarized the published analytical models (Fig. 3.11).

*Alath and Kunnath (1995), Figure 3.11(a)*

- Zero length rotational spring and rigid links to represent joint panel geometry
- Flexibility of rotational spring is determined by empirical joint shear stress-strain relationship
- Including hysterical degradation

*Biddah and Ghobarah (1999), Figure 3.11(b)*

- Zero length rotational springs to consider separately joint shear deformation and bond-slip deformations
- In an interior joint, two rotational springs for bond-slip deformation and one spring for joint shear deformation. In an exterior joint, one rotational spring for bond-slip deformation and the other for joint shear deformation.
- Shear stress-strain relationship of a joint is defined as a trilinear idealization based on the softening truss model (Hsu 1988).
- The cyclic behavior included hysteretic degradation without pinching effect.
- The bond-slip relationship was idealized with a bilinear model and cyclic pinching effect.

*Youssef and Ghobarah (2001), Figure 3.11(c)*

- Twelve translational zero length springs located at all four side interfaces between joint panel and beam or column to simulate inelastic behaviors (e.g., bond slip and concrete crushing)
- Two elastic diagonal springs to simulate joint shear deformation

*Lowes and Altoontash (2003) and Mitra and Lowes (2007), Figure 3.11(d)*

- In each side, two 1D-springs for bar slip and one spring for shear at the interface, totaling twelve springs between external nodes and internal nodes in the interior joint
- One rotational spring for joint shear distortion

Thirteen springs are needed for an internal joint, while ten springs are needed for an external joint.

- Lowes and Altoontash (2003) model used the modified compression field theory (MCFT) (Vecchio and Collins 1986) to derive the constitutive relationship of the joint panel.
- Mitra and Lowes (2007) model derived empirically diagonal concrete strut strength with the concept of confinement effect of transverse hoop suggested by Mander et al. (1988).
- “*beamColumnJoint*” element object in OpenSees represents the model by Mitra and Lowes (2007).

*Altoontash and Deierlein (2003), Figure 3.11(e)*

- Simplification of the model by Lowes and Altoontash (2003): one rotational spring for beam end rotation due to bar slip per each side
- One rotational spring for joint panel distortion
- Constitutive relationship of joint panel is still using MCFT (Vecchio and Collins 1986).
- “*Joint2D*” element object in OpenSees

*Shin and LaFave (2004), Figure 3.11(f)*

- Assemble four rigid elements by hinge to represent the joint panel, and one rotational spring is located on one of four hinges.
- Two rotational springs (in series) are located between the beam and the joint to represent beam end rotations due to bar slip and plastic hinge rotation.

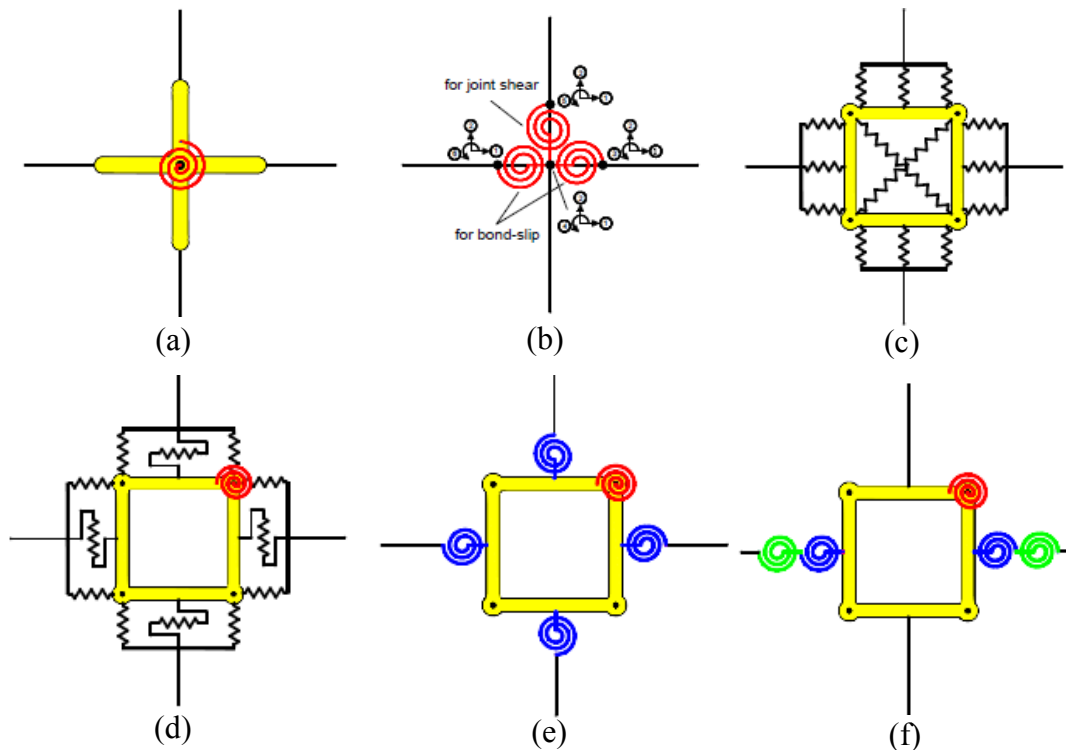


**Fig. 3.11 Existing simulation models for beam-column joints (Celik and Elingwood 2008): (a) Alath and Kunnath (1995), (b) Bidda and Ghobara (1999), (c) Youssef and Ghobarah (2001), (d) Lowes and Altoontash (2003), (e) Altoontash and Deierlein (2003), and (f) Shin and LaFave (2004).**

Multi-spring models in the above, except for Alath and Kunnath (1995), are intended to simulate more realistic behavior of beam-column joints but need significant calibration per each spring based on test data. Even though the springs are calibrated from some test data, they do not ensure the accuracy of the analysis for other test results. Multi-spring models also have a high possibility of causing numerical divergence during frame analysis. Thus, a single rotational spring with a rigid panel to represent the joint geometry is adopted by Celik and Elingwood (2008), Theiss (2005), and Pampanin et al. (2003). Hertanto (2005) used the same concept but split one spring into two springs with identical properties, half of the joint strength and stiffness. In the single spring models, a bar slip element can be added separately to the column face.

The moment-rotation backbone relationship of the rotational springs is calculated from the backbone shear stress-strain relationship of the joints once the dimensions of frame and joint are known, Figure 3.12.

$$M_j = \tau_{jh} A_j / \lambda, \quad \lambda = (1 - h_c / L_b) / jd - \alpha / L_c \quad (3.83)$$

$$\theta_j = \gamma_j \quad (3.84)$$

where  $M_j$  is the moment,  $\tau_{jh}$  is the shear stress,  $A_j$  is the joint area, i.e.,  $A_j = h_c \times b_j$ ,  $b_j$  is the width of the joint panel, i.e.,  $b_j = 0.5(b_b + b_c)$ ,  $L_b$  is the total length of the left and right beams,  $L_c$  is the total length of the top and bottom columns,  $jd$  is the distance between the top and bottom reinforcements of the beam,  $\alpha$  is a constant which is equal to 2 for the top floor joints and 1 for the others,  $\theta_j$  is the joint rotation, and  $\gamma_j$  is the shear strain of the joint.

To define the backbone curve for the shear stress-strain relationship of the joints, Celik and Elingwood (2008) adopted the *Pinching4* material object available in OpenSees (Fig. 3.13(a)). They defined the key points of the envelope based on the available test data. Hertanto (2005) used the hysteresis model with pinching behavior proposed by Pampanin et al. (2003) (Fig. 3.13(b)). The yielding point of the envelope is determined by the principal tensile stress limit proposed by Priestley (1997). For practicality, a single spring model is planned for analyzing the prototype buildings in this study.

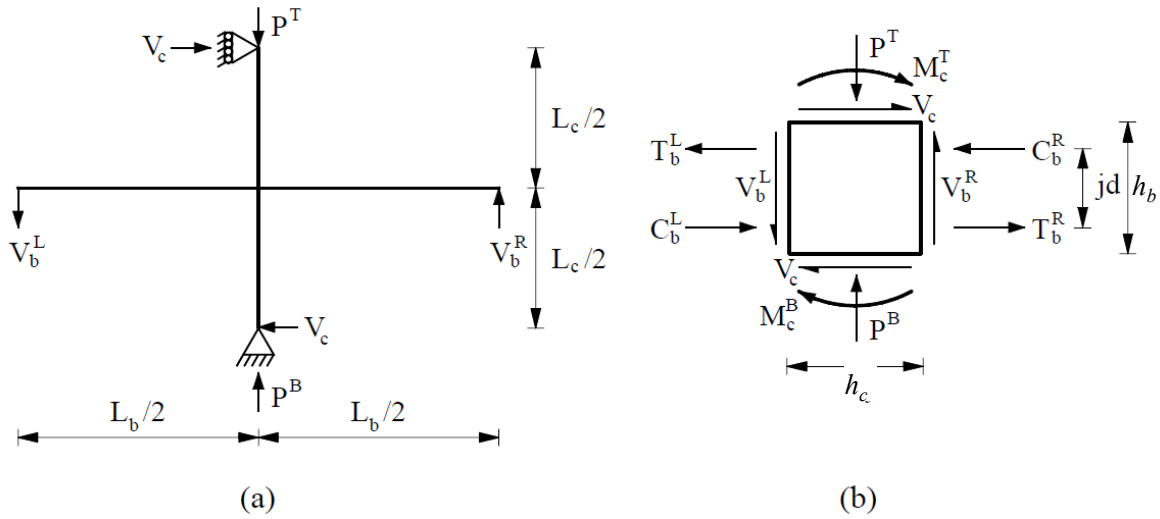


Fig. 3.12 Interior joint: (a) Global equilibrium and (b) Joint free body diagram (Celik and Elingwood 2008).

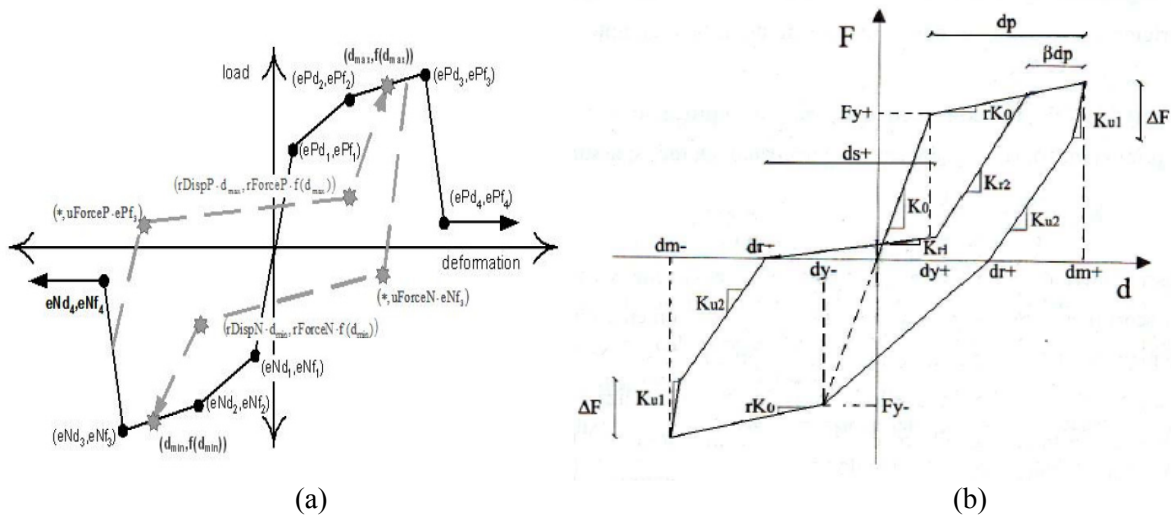


Fig. 3.13 Backbone curves of joint behavior: (a) *Pinching4* from OpenSees used in Celik and Elingwood (2008), and (b) Proposed by Pampanin et al. (2003).

## 4 Semi-Empirical Shear Strength Model

### 4.1 DEVELOPMENT OF SEMI-EMPIRICAL MODEL

In this section, the shear strength model is developed by mechanistic and statistical approaches. Two parameters, the joint aspect ratio and the beam reinforcement index, are selected to derive the shear strength equation, while the effect of column axial load is ignored due to the reasons mentioned in the previous section. The joint shear strength is assumed to be proportional to the square root of the concrete standard compressive strength.

#### 4.1.1 Joint Aspect Ratio Parameter

Assuming that a single diagonal strut (FEMA 273, 1997; Zhang and Jirsa 1982) resists all the horizontal shear force in the joint panel (Fig. 4.1), the equilibrium equation is derived as follows:

$$V_{jh} = c_0 D \cos \theta, \quad \theta = \tan^{-1}(h_b / h_c) \quad \text{and} \quad D = \sigma_d b_j h_s \quad (4.1)$$

where  $c_0$  is a constant to be determined from experimental data, and  $D$  is the compressive force in the diagonal strut with  $\sigma_d$  as its average compressive stress and  $h_s$  is its width (Fig. 4.1). To express the joint shear strength in terms of  $\sqrt{f'_c}$ , the softening concrete model suggested by Vollum (1998) is adopted to develop a relevant model for the concrete panel of unreinforced joints. Vollum (1998) modified the strain-softening concrete model of Collins et al. (1996) as

$$\sigma_d = \frac{a_1 \sqrt{f'_c}}{0.8 + 170 \varepsilon_1} \quad (4.2)$$

where  $a_1$  is a constant with values of 71.3 (psi units) and 5.92 (MPa units).

To determine  $\varepsilon_1$ , the strain compatibility equations in an average sense have been adopted in most of the existing analytical models. More simply, the direction of  $\varepsilon_1$  is

approximated as orthogonal to the assumed diagonal strut (Vollum 1998, Hwang and Lee 1999) and the principal tensile strain is accordingly calculated as follows:

$$\varepsilon_1 = \varepsilon_x + (\varepsilon_x - \varepsilon_d) \cot^2 \theta \quad (4.3a)$$

$$\varepsilon_1 = \varepsilon_y + (\varepsilon_y - \varepsilon_d) \tan^2 \theta \quad (4.3b)$$

where  $\varepsilon_x$  is the horizontal tensile (positive) strain,  $\varepsilon_y$  is the vertical tensile (positive) strain, and  $\varepsilon_d$  is the compressive (negative) strain in the diagonal strut.

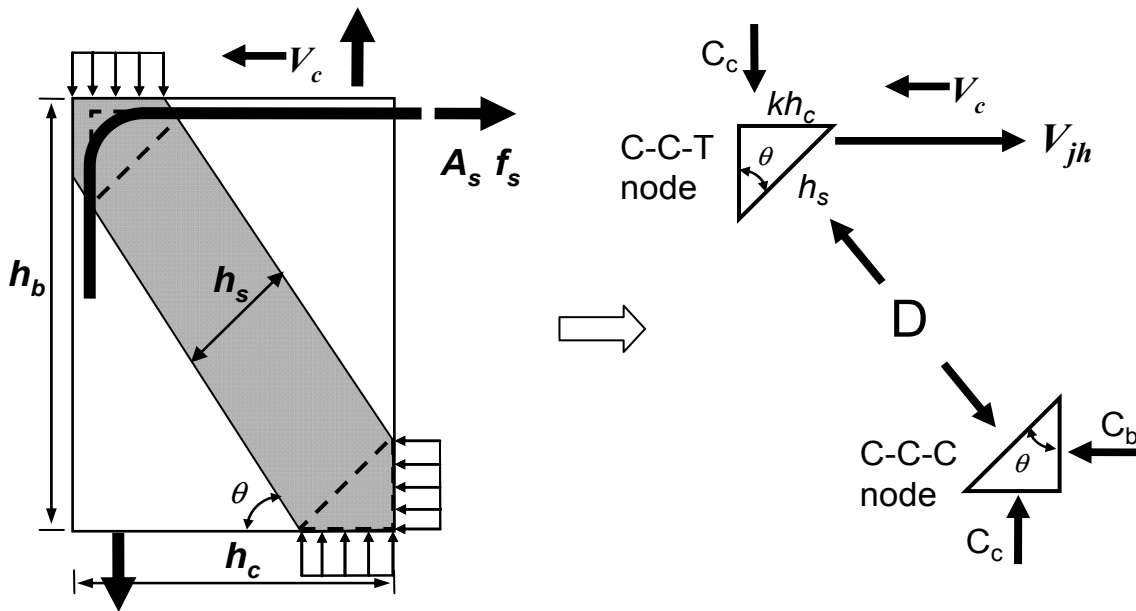


**Fig. 4.1 Single diagonal strut mechanism.**

The above compatibility equations are derived from the continuum element and extended to the membrane element having longitudinal and transverse reinforcement. In the membrane element, the angle  $\theta$  is determined from the strains of the longitudinal and transverse reinforcement and thus the principal tensile strain is the same from these two equations. However, these strain compatibility equations are not applicable in the same way to unreinforced beam-column joints for two reasons: (1) there is no longitudinal and transverse reinforcement and (2) the angle,  $\theta$ , is defined by the given joint geometry. Furthermore, Equation (4.3a) gives smaller principal tensile strain, i.e., larger joint strength, as the joint aspect ratio,  $\theta = \tan^{-1}(h_b / h_c)$ , increases, which is opposite to the observation from the database (Fig. 2.4).

The softening SAT model by Hwang and Lee (1999) takes the vertical strain as the tensile yield strain of column reinforcement to calculate the principal tensile strain by Equation (4.3b). Contrarily, this strain is compressive in the nodal zones of the diagonal strut as shown in Figure 4.1. Moreover, the assumed yield strain is not realistic if the reinforcement does not yield. Therefore, one concludes that Equations (4.3a) and (4.3b) are not suitable for calculating the principal tensile strain of unreinforced beam-column joints.

In this study, the principal tensile strain at the joint shear failure is determined by comparing the concrete strength calculated by Equation (4.2) with that of the nodal zone suggested by previous researchers and current codes. From the observations of published experiments, the joint shear failure in most of the tests was initiated adjacent to the top node when the beam top reinforcement was in tension (Vollum 1998), C-C-T node in Figure 4.1. This behavior is confirmed by the test observation that the transverse reinforcement at the 90° hook is effective in increasing the anchorage strength of beam reinforcement (Minami and Nishimura 1985), which results in increasing the strength of the C-C-T node. It is noted that the top node is considered as a node anchoring only one tie, i.e. C-C-T node. The strength reduction factors for a C-C-T node in the literature and codes are compared in Table 4.1, where code safety factors are excluded for proper comparison. Figure 4.2 shows that the principal tensile strain can be considered to have a reasonable value of 0.0035 using Equation (4.2) in comparison with different strength reduction factors in Table 4.1 for concrete strength ranging from 3 ksi to 7 ksi (20.7 MPa to 48.3 MPa). As shown in Table 4.2, this selected principal tensile strain at joint shear failure is justified using the experimental data (mean value plus about one-half standard deviation) and based on Equation (2.3b) with  $\epsilon_y = 0$ .

**Table 4.1 Strength reduction factor for a C-C-T node.**

	Reference	$\eta$ where $f_{c,node} = \eta f'_c$
(a)	Collins and Mitchell (1986)	0.75
(b)	Schlaich and Schäfer (1991)	0.68
(c)	MacGregor (1997)	$0.85\eta_1, \eta_1 = 0.55 + \eta_2 / \sqrt{f'_c}$ * <sup>1</sup>
(d)	Jirsa et al. (1991)	0.80
(e)	ACI-318-08 Appendix A (2008)	0.68
(f)	AASHTO (1996)	0.75
(g)	CEB-FIP 1990 (1993)	$0.60(1 - f'_c/\eta_3)$ * <sup>2</sup>
(h)	DD ENV 1992-1-1 (1992)	0.70
(i)	CAN A23.3M94 (1994)	0.75
(j)	NZS 3101: Part 2 (1995)	0.55

\*<sup>1</sup>  $\eta_2 = 15$  for  $\sqrt{f'_c}$  psi<sup>0.5</sup>, = 1.25 for  $\sqrt{f'_c}$  MPa<sup>0.5</sup>

\*<sup>2</sup>  $\eta_3 = 36250$  for  $f'_c$  psi, = 250 for  $f'_c$  MPa.

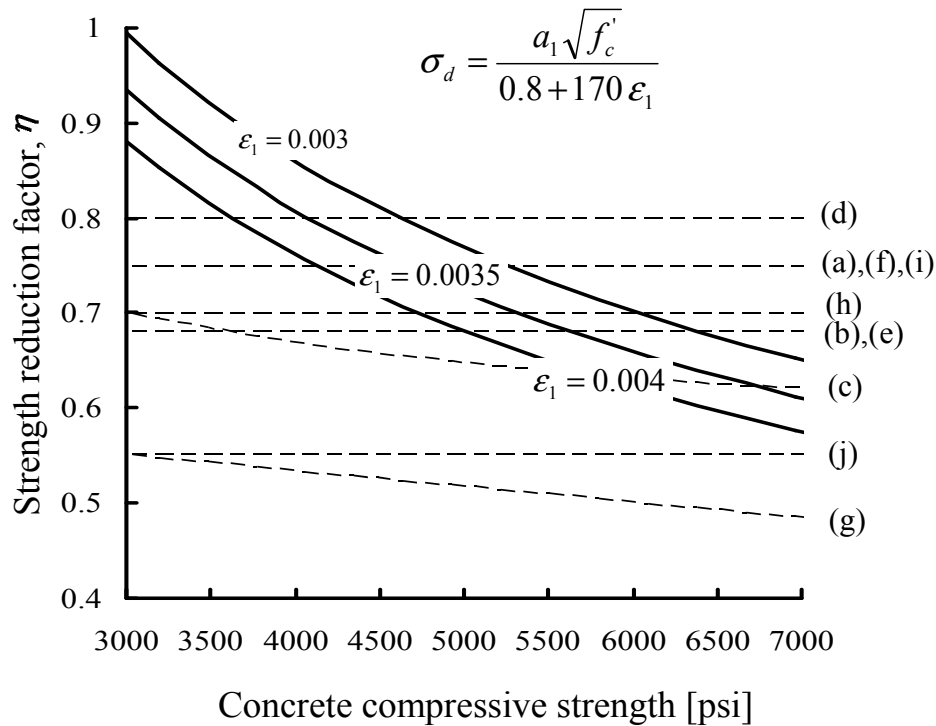


**Fig. 4.2 Comparison of strength reduction factors at C-C-T node (see Table 4.1 for (a)–(j) designation).**

**Table 4.2 Measured joint shear strain and approximation of principal tensile strain.**

Specimen	$h_b/h_c$	$P/A_g f'_c$	Shear strain, $\gamma_{xy}$	$\varepsilon_1 \approx 2\gamma_{xy}$
Clyde <sup>*1</sup> -#2	0.89	0.1	$7.18 \times 10^{-3}$	$3.59 \times 10^{-3}$
Clyde <sup>*1</sup> -#6	0.89	0.1	$4.81 \times 10^{-3}$	$2.41 \times 10^{-3}$
Clyde <sup>*1</sup> -#4	0.89	0.25	$8.45 \times 10^{-3}$	$4.23 \times 10^{-3}$
Clyde <sup>*1</sup> -#5	0.89	0.25	$4.84 \times 10^{-3}$	$2.42 \times 10^{-3}$
Pantelides <sup>*2</sup> -#3	1.0	0.1	$8.08 \times 10^{-3}$	$4.04 \times 10^{-3}$
Pantelides <sup>*2</sup> -#4	1.0	0.25	$4.73 \times 10^{-3}$	$2.37 \times 10^{-3}$
Pantelides <sup>*2</sup> -#5	1.0	0.1	$6.10 \times 10^{-3}$	$3.05 \times 10^{-3}$
Pantelides <sup>*2</sup> -#6	1.0	0.25	$6.54 \times 10^{-3}$	$3.27 \times 10^{-3}$
Mean				$3.17 \times 10^{-3}$
Standard Deviation				$0.69 \times 10^{-3}$

<sup>\*1</sup> from Clyde et al. (2000)

<sup>\*2</sup> from Pantelides et al. (2002)

The horizontal length of the C-C-T node (Fig. 4.1) is expressed using the constant  $k$  as follows:

$$h_s \sin \theta = kh_c, \quad \sin \theta = \frac{1}{\sqrt{1 + (h_c/h_b)^2}} \propto \frac{h_b}{h_c} \quad (4.4)$$

Substituting Equations (4.2) and (4.4) into Equation (4.1) and normalizing, the equilibrium equation becomes

$$\frac{V_{jh}}{b_j h_c \sqrt{f'_c}} = c_1 \left\{ \frac{a_1}{(0.8 + 170\varepsilon_1) \sin \theta} \right\} \cos \theta \quad (4.5)$$

where  $c_1 = c_0 k$  is a constant to be determined from the experimental data. The terms in the brace reflect the strength of the C-C-T nodal zone, and  $\sin \theta$  in the denominator provides the adverse effect of the joint aspect ratio; see Equation (4.4). It is worth mentioning that  $\sin \theta$  remains in the brace separated from  $\cos \theta$  because  $\sin \theta$  is related to the size of nodal zone, while  $\cos \theta$  is related to the equilibrium in the joint.

For simplicity, it is assumed that the adverse effect of the joint aspect ratio in the nodal zone is included by increasing the average principal tensile strain linearly with the joint aspect ratio without changing the nodal zone size. Therefore, one obtains the following approximation:

$$(0.8+170 \varepsilon_1) \sin \theta \approx 0.8+170 \left\{ 0.0035+0.0005 \left( \frac{h_b}{h_c} -1 \right) \right\} \quad (4.6)$$

Substituting Equation (4.6) into Equation (4.5) and combining the two constants  $a_1$  and  $c_1$ , Equation (4.5) becomes

$$\frac{V_{jh}}{b_j h_c \sqrt{f'_c}} = a_2 \frac{\cos \theta}{1.31+0.085 \frac{h_b}{h_c}} \quad (4.7)$$

where  $a_2$  is determined from the database.  $a_2 \approx 23$  (psi units) or 1.91 (MPa units) for the upper limit from (Pantelides et al. 2002),  $\gamma = 11.7$ , and  $a_2 \approx 10$  (psi units) or 0.83 (MPa units) for the lower limit from the database,  $\gamma = 5.0$  at the joint aspect ratio of 1.0, i.e.  $\theta = \pi/4$ . The values of 23 and 10 are obtained by rounding off 23.1 and 9.9, respectively. Equation (4.7) is compared with the database for  $0.8 \leq h_b/h_c \leq 2.2$  in Figure 4.3, where it is shown that Equation (4.7) accurately represents the trend for the effect of the aspect ratio from the database.

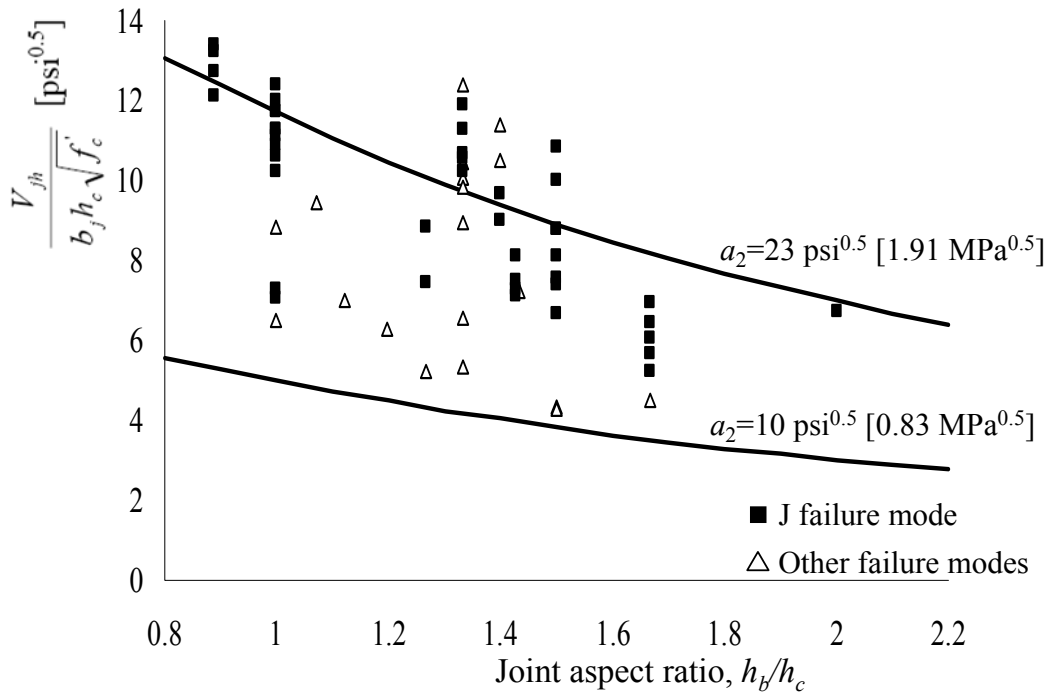


**Fig. 4.3 Comparison of proposed joint aspect ratio equation with database.**

#### 4.1.2 Beam Reinforcement Ratio Parameter

From Figure 4.4, the global equilibrium equation is presented as follows

$$M_b = V_b \times L = A_s f_s \times jd_b \quad (4.8)$$

$$V_c = \frac{L + h_c / 2}{H} V_b \quad (4.9)$$

where  $V_b$  and  $V_c$  are the beam and column shear forces, respectively,  $L$  is the length from the beam inflection point to the column face,  $H$  is the height between upper and lower column inflection points,  $A_s$  and  $f_s$  are the area and stress of the beam reinforcement in tension, respectively,  $d_b$  is the effective depth of the beam, and  $jd_b$  indicates the internal moment arm of the beam cross section at the column face. Accordingly, the horizontal shear force of the joint panel is calculated as follows:

$$V_{jh} = A_s f_s - V_c = A_s f_s \left( 1 - \frac{L + h_c / 2}{H} \frac{jd_b}{L} \right) \quad (4.10)$$

It is assumed that the beam reinforcement ratio affects the joint shear strength only in the case of joint shear failure with beam reinforcement yielding. This assumption is based on the fact that the joint shear strength does not increase with increasing the amount of beam reinforcement once the joint shear demand exceeds the maximum joint strength as mentioned in the preceding section (Fig. 2.5). Therefore,  $f_s = f_y$  can be used in Equation (4.10) assuming that the material of the beam reinforcement is elastic-perfectly-plastic (EPP). Dividing Equation (4.10) by  $b_j h_c \sqrt{f'_c}$ , the following equation is obtained,

$$\frac{V_{jh}}{b_j h_c \sqrt{f'_c}} = \left( \frac{A_s f_y}{b_j h_c \sqrt{f'_c}} \right) \left( 1 - \frac{L + h_c / 2}{H} \frac{jd_b}{L} \right) \quad (4.11)$$

Approximation can be made as follows:

$$jd_b = 0.8h_b \quad (4.12a)$$

$$\frac{L + h_c / 2}{H} \frac{jd_b}{L} = \frac{L + h_c / 2}{L} \frac{0.8h_b}{H} \approx 0.85 \frac{h_b}{H} \quad (4.12b)$$

Finally, Equation (4.11) can be simply rewritten as

$$\frac{V_{jh}}{b_j h_c \sqrt{f'_c}} \approx \left( \frac{A_s f_y}{b_j h_c \sqrt{f'_c}} \right) \left( 1 - 0.85 \frac{h_b}{H} \right) \quad (4.13)$$

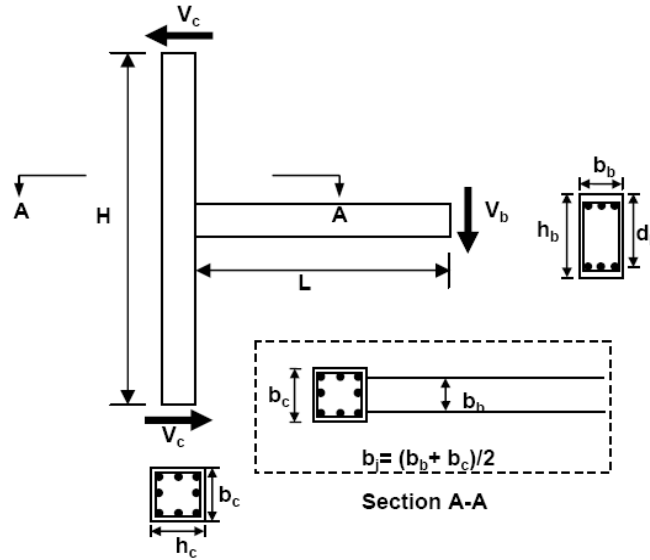


**Fig. 4.4 Global free body diagram of exterior beam-column joint.**

Based on the above equation, a non-dimensional parameter, referred to as the beam reinforcement index, is defined as  $\frac{A_s f_y}{b_j h_c \sqrt{f'_c}} \left(1 - 0.85 \frac{h_b}{H}\right)$  in this study. This parameter directly represents the joint shear demand at the onset of beam reinforcement yielding.

### 4.1.3 Semi-Empirical Shear Strength Model

To develop a semi-empirical model, two basic concepts are assumed as follows: (1) maximum and minimum joint shear strengths are affected by the joint aspect ratio without regard to the beam reinforcement index and (2) joint shear strength is linearly proportional to the beam reinforcement index between maximum and minimum joint shear strengths. In the first assumption, the maximum and minimum joint shear strengths' dependency on the joint aspect ratio is justified by the plots of Equation (4.7) on Figure 4.3. The second assumption is based on the observation of low joint aspect ratio data from the database in Figure 2.5. For the case of high joint aspect ratio, the same assumption is also made in this study based on the discussion in Chapter 2 related to Figure 2.5 and utilizing the observation that the joint aspect ratio affects the equilibrium and nodal zone strength as discussed in the preceding section.

When the beam reinforcement index causes the joint strength to be between the maximum and minimum strengths determined based on the given joint geometry, concrete

strength and joint aspect ratio, the joint shear strength is equal to the beam reinforcement index multiplied by an over-strength factor  $\Phi \geq 1.0$ . This factor considers the fact that the tensile stress of the beam reinforcement in the BJ failure mode is greater than the yield strength, i.e.  $f_s > f_y$ , due to strain hardening of the beam reinforcement. The overstrength factor is larger for smaller beam reinforcement index due to the expected larger plastic strain. For simplicity,  $\Phi$  is assumed to be 1.25, i.e.  $f_s = 1.25 f_y$ , at the minimum joint shear strength and decreases linearly to  $\Phi = 1.0$ , i.e.  $f_s = f_y$  at the maximum joint shear strength, Figure 4.5. Finally, the shear strength equation is proposed as

$$\frac{V_{jh}}{b_j h_c \sqrt{f'_c}} = \Phi \left[ \left( \frac{A_s f_y}{b_j h_c \sqrt{f'_c}} \right) \left( 1 - 0.85 \frac{h_b}{H} \right) \right] \geq a_{\min} \frac{\cos \theta}{1.31 + 0.085 \left( \frac{h_b}{h_c} \right)} \quad (4.14a)$$

$$\leq a_{\max} \frac{\cos \theta}{1.31 + 0.085 \left( \frac{h_b}{h_c} \right)} \quad (4.14b)$$

where  $a_{\min}$  is 10 in (lb and in. units) and 0.83 in (N and mm units) and  $a_{\max}$  is 23 in (lb and in. units) and 1.91 in (N and mm units).

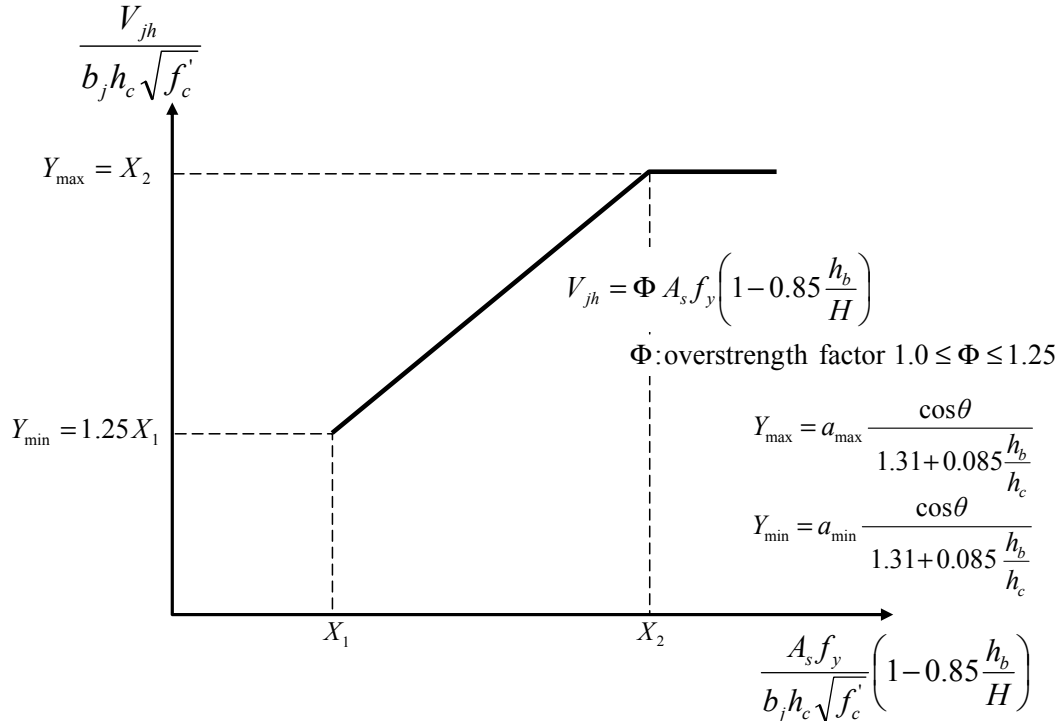


**Fig. 4.5 Illustration of proposed semi-empirical model.**

The procedure to predict the joint shear strength using the proposed model is summarized as follows:

1. Input the joint geometry, concrete strength, and joint aspect ratio.
2. Determine the minimum ( $Y_{\min}$ ) and maximum ( $Y_{\max}$ ) joint shear strengths as shown in Figure 4.5.
3. Calculate the beam reinforcement index by Equation (4.13)
4. Check if the calculated beam reinforcement index is located between  $X_1$  and  $X_2$ . If so, interpolate the corresponding overstrength as shown in Figure 4.5.
5. Calculate the joint shear strength by Equation (4.14a) and (4.14b)

## 4.2 EVALUATION OF THE SEMI-EMPIRICAL MODEL

To verify the proposed shear strength model, the shear strength of exterior joints from the database is evaluated. The accuracy of the proposed model is compared with that of five existing strength models proposed by Vollum (1998), Hwang and Lee (1999), Bakir and Bodurođlu (2002), Hegger et al. (2003), and Tsonos (2007) in Figure 4.6. The proposed model predicts the joint shear strengths of the database with a mean value of 0.97 for the ratio between the test results and model predictions and a corresponding coefficient of variation (COV) of 16% as shown in Figure 4.6(a). When the six tests by Parker and Bullman (1997) are excluded, the accuracy of the proposed model is improved to a mean value of 0.99 for this ratio and a corresponding COV of 14%.

The model by Vollum (1998) includes the detrimental effect of the joint aspect ratio but this model does not consider the change of the joint shear strength with the variation of beam reinforcement. Due to the lack of the effect of beam reinforcement, this model overestimates the joint shear strength of specimens showing the BJ failure mode, while it shows accurate predictions of specimens with joint shear strength for the J failure mode where the joint shear strength is little influenced by the beam reinforcement. The evaluation results using this model are shown in Figure 4.6(b).

In the model by Hwang and Lee (1999), the following formula is used to determine the width of the diagonal strut,

$$h_s \approx \left( 0.25 + 0.85 \frac{P}{f_c A_g} \right) h_c \quad (4.15)$$

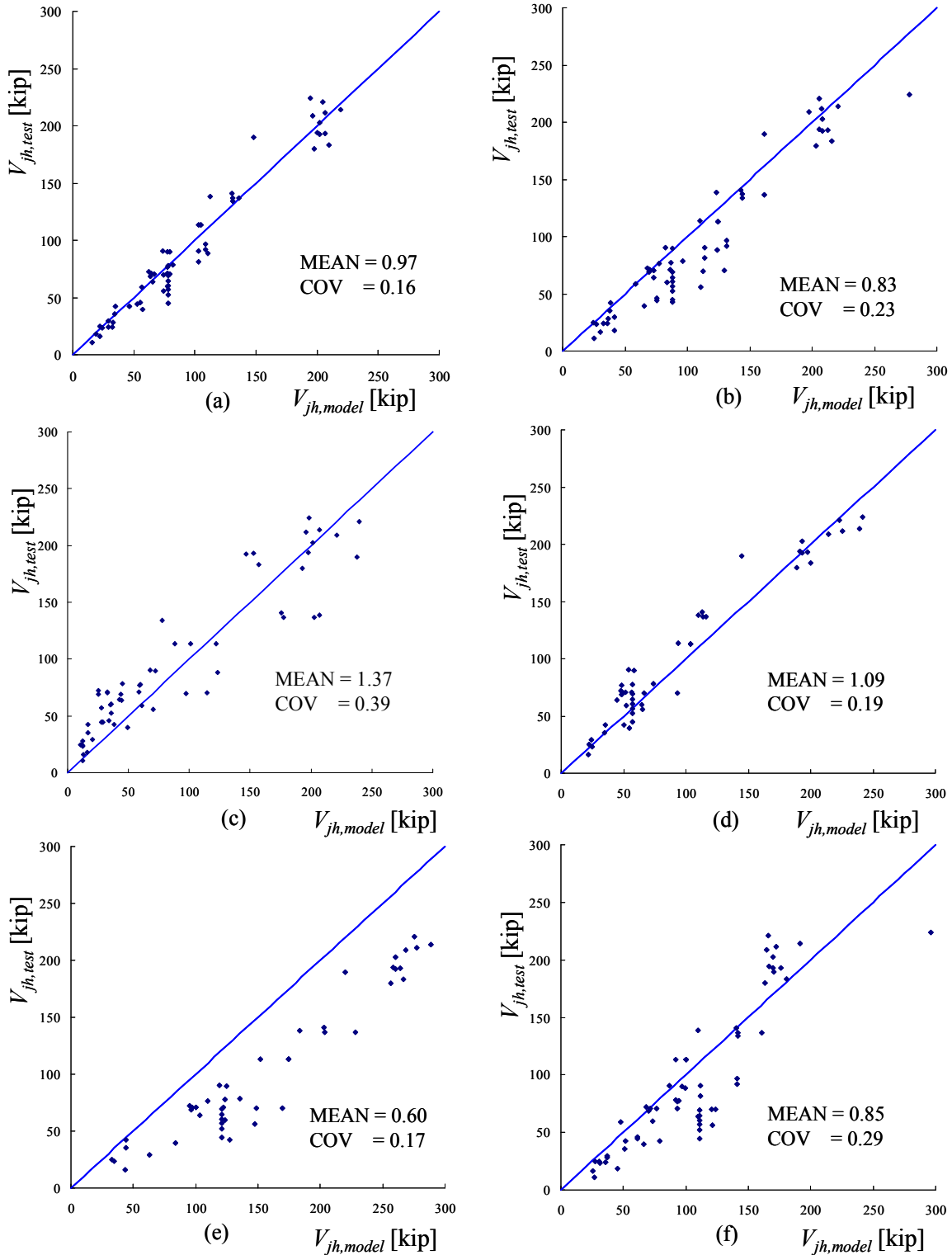
Hwang and Lee (1999) originally developed their model for reinforced joints and assumed its extension to unreinforced joints. However, this model is not applicable to unreinforced joints for the following reasons: (1) the average strain compatibility equations do not reflect the real deformation as previously discussed; (2) intermediate column bars may not develop the inclined strut due to its steep angle; (3) it is assumed that the beam and the column reinforcements are yielding regardless of the joint shear failure mode; (4) only beneficial effects of column axial load on joint shear strength are included; and (5) this model highly depends on the estimate of the diagonal strut width (Hwang and Lee, 2002). The evaluation results using this model are shown in Figure 4.6(c).

Bakir and Boduroğlu (2002) developed an empirical model by regression of published test data. The model includes the parameters of the beam reinforcement ratio,  $100A_s / b_b d_b$ , and the joint aspect ratio,  $h_b / h_c$ . The evaluation results (Fig. 4.6(d)) show good correlation with test data due to the inclusion of the beam reinforcement ratio. However, the defect of this model is that the exponential parameter including the beam reinforcement ratio in the model is obtained with its exponent value of 0.4289, which is less than 1.0, by a statistical approach with a relatively small data set.

Hegger et al. (2003) developed an empirical model including the parameters of column reinforcement ratio and joint aspect ratio. The evaluation results (Fig. 4.6(e)) show consistent overestimation of the joint shear strength. From the overestimation of joint shear strength by this model, it is concluded that the column reinforcement ratio may not be an influencing parameter to predict the shear strength of unreinforced joints as assumed in the presented semi-empirical model.

The model by Tsonos (2007) overestimates the unreinforced joint shear strength and this overestimation results from the use of the overly simplified average stress equilibrium equation and the increase of joint shear strength with increasing joint aspect ratio, which is in contradiction with the observation from the database. The evaluation results using this model are shown in Figure 4.6(f).

From the above validation, the proposed semi-empirical model is shown to be accurate and consistent compared with existing models and using a large experimental data set. This model can be easily implemented in many existing nonlinear structural analysis programs to evaluate the seismic response of non-ductile RC frames with unreinforced beam-column joints.



Note: Mean and COV = Coefficient of Variation for  $V_{jh,test}/V_{jh,model}$ , 1 kip = 4.45 kN

**Fig. 4.6 Comparison of evaluation results: (a) Proposed model, (b) Vollum (1998), (c) Hwang and Lee (1999), (d) Bakir and Boduroglu (2002), (e) Hegger et al. (2003), and (f) Tsonos (2007).**

# 5 Analytical Shear Strength Model

## 5.1 BACKGROUND

There have been many analytical studies to better assess the shear strength of unreinforced concrete beam-column joints. As a result, several analytical models have been developed based on the average stress assumption or the strut-and-tie (SAT) approach with the average strain compatibility. As discussed in chapter 3, Priestley (1997) proposed a limit for the average principal tensile stress in the joint panel to predict the joint shear failure, and Tsonos (2007) used a fifth-order polynomial for the concrete failure surface with the average principal compressive and tensile stresses to calculate the joint shear strength. Hwang and Lee (1999) and Vollum (1998) developed shear strength models based on the SAT approach. Wong (2005) developed an exterior joint shear strength model with the modified rotating-angle softened-truss model accounting for the effect of shear span to depth ratio as in deep beams.

The average principal stresses and strain compatibility equation using beam and column longitudinal reinforcement strains are not able to reflect the realistic behavior of unreinforced exterior beam-column joints where the joint shear failure is localized. In other words, the tensile strains of beam and column reinforcements cannot represent the strain within the joint panel. Moreover, the SAT approach faces the critical issue of estimating the diagonal strut area because the joint shear strength is very sensitive to this estimated area (Hwang and Lee 2002).

From the literature review, the analytical joint strength model developed in this study is motivated by the following observations. First, it is reported that the unreinforced exterior joints having the same concrete strength and geometry fail in shear at different levels of joint shear stress demand with changing beam reinforcement ratio. This is an interesting observation considering that the unreinforced exterior joint resembles an unconfined concrete rectangular cuboid with seemingly unique strength. Second, to obtain the reduced shear strength of unreinforced exterior joints for joint shear failure following beam reinforcement yielding, three

modification methods are adopted in the existing models: (1) directly reducing the joint shear strength by a ductility factor (Park 1997; Hakuto et al. 2000), (2) reducing the area of diagonal strut by a ductility factor (Hwang et al. 2001), and (3) reducing the applied joint shear force in the average joint stress equilibrium equation by a ductility factor (Wong 2005). The relationship between the reduction of joint shear strength and the ductility factor are proposed empirically in each model. The ductility factor can be defined in different ways and it includes the deformation of other members in addition to the joint distortion. Therefore, the empirically proposed relationships are not possible to generalize to other cases. Moreover, all three modification methods require monitoring the ductility factor during the analysis of the specimen or the frame, which means that it is impossible to predict the joint shear strength before analyzing the whole frame.

The newly proposed analytical approach to predict the joint shear strength in this paper is intended to fulfill the following objectives:

1. Two types of joint shear failure, which are joint shear failure without beam reinforcement yielding (J mode) and with beam reinforcement yielding (BJ mode), are considered. A consistent procedure is followed for both failure modes without including a ductility factor.
2. Two parameters affecting the shear strength of unreinforced beam-column joints are included: the joint aspect ratio and the beam reinforcement ratio. The second parameter is related to the bond distribution of beam reinforcement in the joint and the failure mode type, i.e., J or BJ.
3. The new approach does not require the estimation of the diagonal strut area,  $A_{str}$ .
4. The new approach can establish the envelope of the shear stress-strain relationship that can be transformed to the moment-rotation relationship of a rotational spring representing the joint region. This objective is essential to simulate the joints in structural analysis of frames.

## **5.2 DEVELOPMENT OF ANALYTICAL MODEL**

### **5.2.1 Assumptions**

In the proposed model, two inclined struts are first assumed to resist the horizontal joint shear in a parallel system (Fig. 5.1). The major diagonal strut (ST1) is developed by the 90° hook of beam

reinforcement, while the minor inclined strut (ST2) is developed by the bond resistance of the concrete surrounding the beam reinforcement. In unreinforced joints, ST2 has generally been ignored. However, tests by Wong (2005) having the detail of beam reinforcement bent outside the joint region show that ST2 has a considerable contribution to resisting the joint shear force compared to those with bent inside the joint region; see Figure 5.2. This contribution is also inferred from the crack patterns of the joint panels, e.g., the contribution of strut ST2 appears to be significant in the case of the J failure mode due to the high beam reinforcement ratio leading to distribution of cracks over the whole joint panel. Crack patterns for two types of failure modes are illustrated in Figure 5.3. Presumably, the fraction of each strut can be determined by the level of beam reinforcement tensile stress which is related to the bond resistance, as discussed later in this paper.

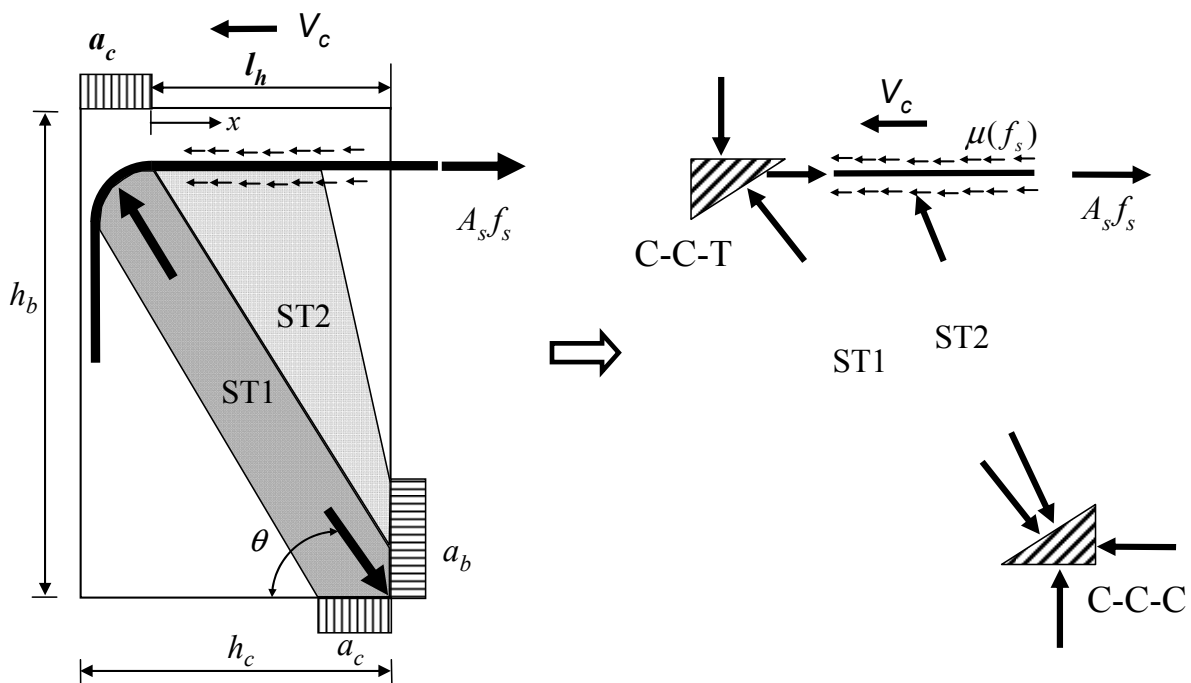
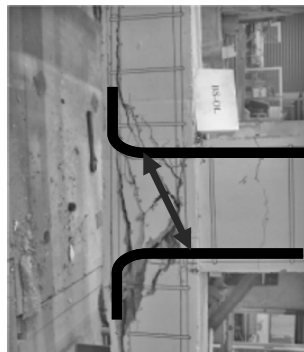
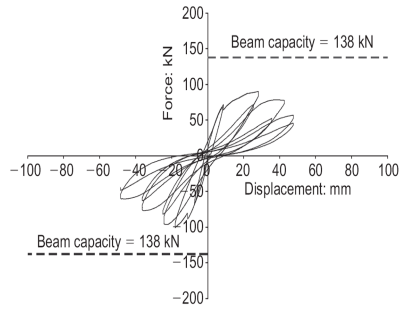


**Fig. 5.1 Two inclined struts in unreinforced exterior joints.**



(a) Beam reinforcement bent inside the joint



(b) Beam reinforcement bent outside the joint

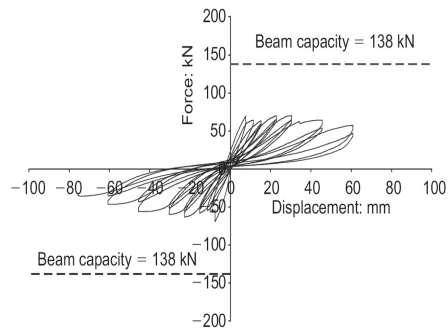
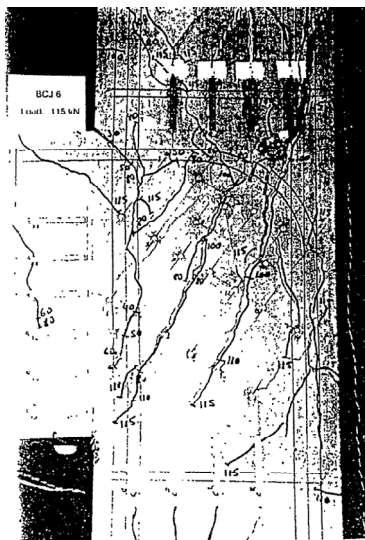
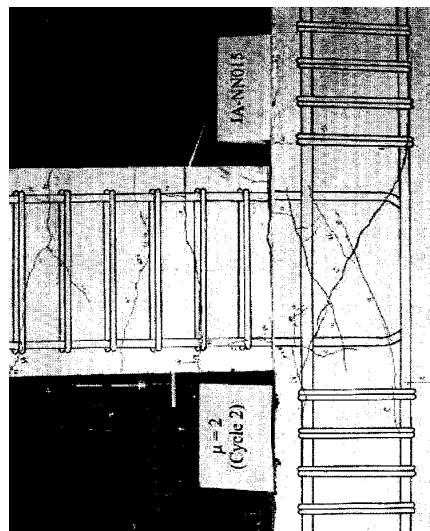


**Fig. 5.2 Tests of joint with different beam reinforcement anchorage details (Wong 2005).**



(a) J failure [Ortiz, 1993]



(b) BJ failure [Wong, 2005]

**Fig. 5.3 Crack patterns of two types of joint failure.**

The second assumption is that the joint shear failures are initiated adjacent to the top node of ST1 under the loading condition of top beam longitudinal reinforcement in tension (Vollum 1998). This assumption is made for two reasons: (1) the top node is considered as a node anchoring one tie, i.e., C-C-T node and (2) the crack width is greatest at the top node. This assumption is justified by the test results that the beam bar anchorage strength is increased by the transverse reinforcement at the bent portion (Minami and Nishimura 1985). Hence, the joint shear failure is defined when the concrete stress of the C-C-T node in ST1 reaches its peak in a softening concrete constitutive model.

The third assumption is that the proposed model uses the softening concrete model suggested by Vollum (1998) but the principal tensile strain at the point of joint shear failure is not determined by the average strain compatibility equation. Instead, the following principal tensile strain equation proposed in Chapter 4 is adopted for developing this analytical model.

$$\varepsilon_1 = 0.0035 + 0.0005 \left( \frac{h_b}{h_c} - 1 \right) \quad (5.1)$$

where  $h_b$  is the height of the beam cross section, and  $h_c$  is the height of the column cross section in the loading direction. Furthermore, the shear strain  $\gamma_{xy}$  can be determined from the pre-defined principal tensile strain by

$$\varepsilon_1 = \frac{\varepsilon_y}{2} + \frac{1}{2} \sqrt{\varepsilon_y^2 + \gamma_{xy}^2} \quad (5.2)$$

where  $\varepsilon_y$  is the compressive (negative) strain from the column in the vertical,  $y$ , direction. Equation (5.2) indicates that the shear strain increases with increasing the compressive strain in the column, i.e., the shear strain in the high column axial load is greater than that in the low column axial load, under the assumption that the principal tensile strain is fixed. However, the increase of joint shear strain with increasing column axial load is not significant compared to that of compressive strain, as discussed in Section 2.2.3. In most tests, the compressive strain  $\varepsilon_y$  is negligible because the applied column axial load ratio is low, i.e.,  $P / f'_c h_c b_c \leq 0.2$  where  $P$  is the column axial load and  $b_c$  is the width of the column cross section. Therefore, test data with high column axial load are needed to justify the increase of the principal tensile strain with increasing column axial load. These types of tests are pursued in a future experimental phase of this study.

## 5.2.2 Equilibrium

The horizontal joint shear force is estimated from the global equilibrium of a joint panel in Equation (4.14). For clarity, it is re-written here as follows:

$$V_{jh} = A_s f_s - V_c \approx A_s f_s \left( 1 - 0.85 \frac{h_b}{H} \right) \quad (5.3)$$

where  $A_s$  and  $f_s$  are the area and the stress of the beam longitudinal reinforcement in tension, respectively,  $V_c$  is the column shear force, and  $H$  is the height between the upper and lower inflection points of the column. This equilibrium equation is decomposed as follows:

$$V_{jh} = V_{jh,ST1} + V_{jh,ST2} \quad (5.4)$$

$$V_{jh,ST1} = A_s f_s - n \pi \phi_b \int_0^{l_h} \mu(f_s) dx \quad (5.5)$$

$$V_{jh,ST2} = n \pi \phi_b \int_0^{l_h} \mu(f_s) dx - V_c \quad (5.6)$$

where  $n$  is the number of beam longitudinal bars in tension with diameter  $\phi_b$ , and  $V_c$  is the shear force in the column. Note that  $\mu(f_s)$  is the bond stress distribution along the beam bar (Fig. 5.1) as a function of the tensile stress of the bar,  $f_s$ , which varies with the distance  $x$ , i.e.,  $f_s = f_s(x)$ . The  $x$ -axis and  $l_h$  are depicted in Figure 5.1(a). Vollum (1998) and Hwang and Lee (1999) approximated the horizontal projection of the width of the diagonal strut ST1 using Equation (5.7a) and (5.7b), respectively.

$$a_c = 0.4 h_c \quad (5.7a)$$

$$a_c = \left( 0.25 + 0.85 \frac{P}{f_c h_c b_c} \right) h_c \quad (5.7b)$$

Therefore, the horizontal projection of the inclined strut ST2 can be obtained as follows:

$$l_h = h_c - a_c \quad (5.8)$$

Equation (5.7a) is selected from the best fit of the Ortiz (1993) test data, and Equation (5.7b) is employed from the depth of the flexural compression zone of the elastic column suggested by Paulay and Priestley (1992). In this study, the horizontal width  $l_h$  is investigated in this section from 0.6,  $h_c$  corresponding to Equation (5.7a), to 0.75,  $h_c$  corresponding to Equation (5.7b) with  $P=0$ .

The column shear force is excluded in the equilibrium of the diagonal strut ST1, Equation (5.5), and included in the equilibrium of the inclined strut ST2, Equation (5.6), because most of the column shear force is concentrated in the middle of the column cross section due to the shear flow distribution in a cracked rectangular cross section of the column due to cyclic loading. This decomposition of the total horizontal joint shear force is similar to the truss model of Paulay et al. (1978) in which they assumed that the joint shear force is resisted by the combination of the diagonal strut action and the panel truss action.

### 5.2.3 Fraction Factor

The shear forces of struts ST1 and ST2 can be expressed using a fraction factor  $\alpha$  as follows:

$$V_{jh,ST1} = \alpha V_{jh} \quad (5.9)$$

$$V_{jh,ST2} = (1 - \alpha) V_{jh} \quad (5.10)$$

This fraction factor is expressed as a function of the tensile stress of the beam reinforcement because it is related to the bond deterioration of this reinforcement. Obviously, the fraction factor increases as the bond strength deteriorates because the ST1 strut contribution dominates after bond failure occurs (Fenwick 1994). In this model, the bi-uniform bond strength model proposed by Lehman and Moehle (2000) is extended to be tri-uniform and adopted to represent the trilinear behavior of the reinforcing steel. The bond strength in the elastic beam tensile reinforcement,  $\mu_E$ , is  $12\sqrt{f'_c}$  psi<sup>0.5</sup> ( $1.0\sqrt{f'_c}$  MPa<sup>0.5</sup>) and that in the inelastic beam tensile reinforcement,  $\mu_Y$ , is  $0.5\mu_E$ . The residual bond strength,  $\mu_R$ , is selected from the CEB-FIP Model code (1990) as  $0.15\mu_E$ . The considered bond strength variation is illustrated in terms of the beam reinforcement stress in Figure 5.4.

The proposed model derives the fraction factor  $\alpha$  from the trilinear stress-strain model of the reinforcing steel as shown in Figure 5.5. Juxtaposing Equations (5.3), (5.5), and (5.9), the fraction factor  $\alpha$  is derived as follows:

$$A_s f_s - n \pi \phi_b \int_0^{l_h} \mu(f_s) dx = \alpha A_s f_s \left( 1 - 0.85 \frac{h_b}{H} \right) \Rightarrow \alpha = \frac{H}{H - 0.85 h_b} \left( 1 - \frac{4}{\phi_b} \frac{\int_0^{l_h} \mu(f_s) dx}{f_s} \right) \quad (5.11)$$

where  $A_s = n\pi\phi_b^2/4$  is used in Equation (5.11). The assumed breaking points of reinforcing steel stress ( $f_o, f_p,$  and  $f_r$ ) and intermediate values of fraction factor ( $\alpha_1$  and  $\alpha_2$ ) are derived below.

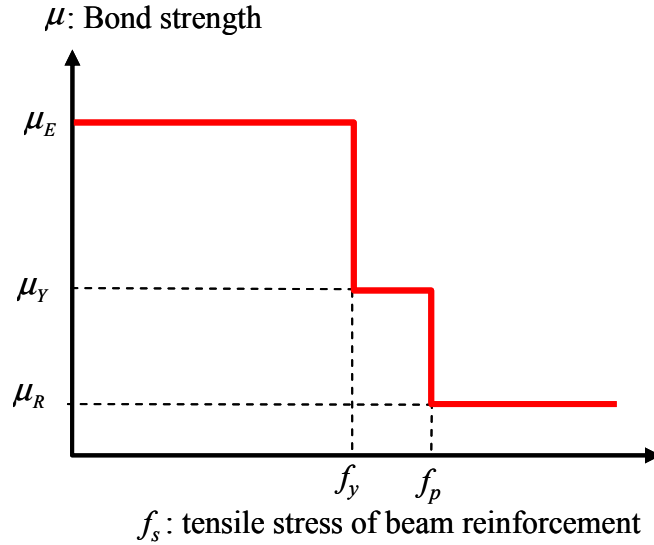


Fig. 5.4 Adopted bond strength model.

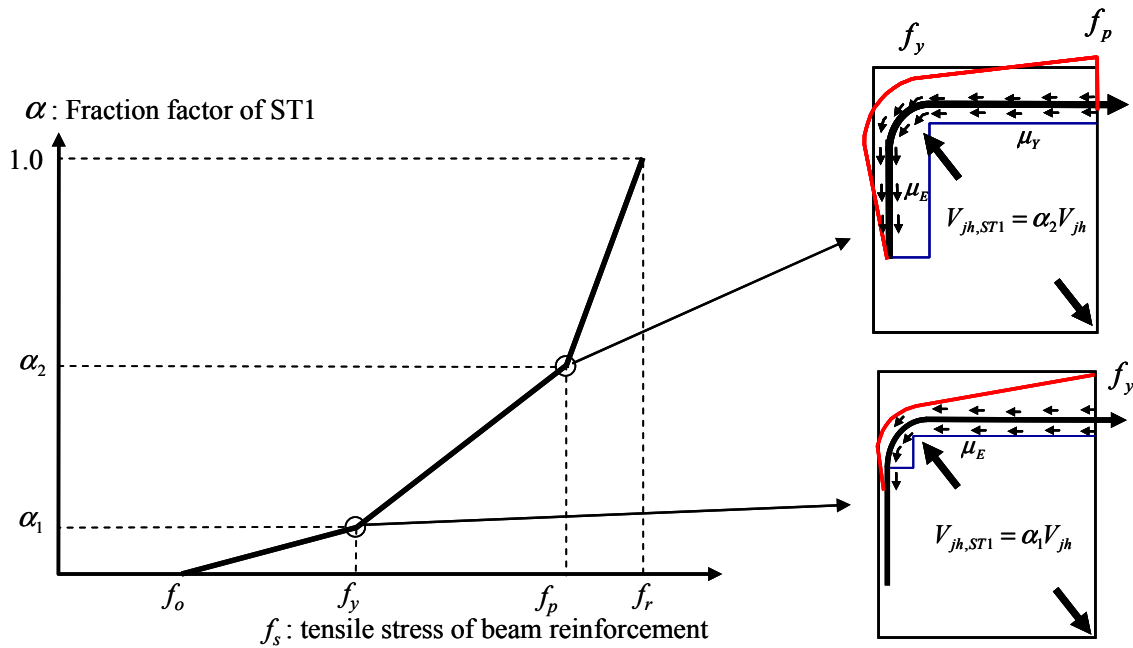


Fig. 5.5 Trilinear curve of fraction factor.

### *Derivation of $f_o$*

The contribution of ST1 is negligible as long as the bond strength of ST2 is able to resist all of the horizontal shear force. The tensile stress of beam reinforcement at this point,  $f_o$  in Figure 5.5, is given by

$$f_o = \frac{4}{\phi_b} \mu_E l_h \quad (5.12)$$

### *Derivation of $\alpha_1$*

The fraction factor  $\alpha_1$  corresponds to the onset of yielding of the beam reinforcement at the column face. Therefore,

$$\alpha_1 = \frac{H}{H - 0.85h_b} \left( 1 - \frac{4}{\phi_b} \frac{\mu_E}{f_y} l_h \right) \quad (5.13)$$

where  $f_y$  is the yield strength of the beam longitudinal reinforcement.

### *Derivation of $f_p$ and $f_r$*

The tensile stress  $f_p$  is defined when the beam reinforcement yielding propagates over the width of ST2. Therefore, the bond strength of concrete surrounding the beam reinforcement is equal to  $\mu_Y$  over the entire length  $l_h$ . Accordingly and referring to Figure 5.5, one obtains the following,

$$f_p = f_y + \frac{4}{\phi_b} \mu_Y l_h \quad (5.14)$$

The tensile stress  $f_r$  corresponding to  $\alpha = 1.0$  is expressed implicitly using Equation (5.11), since the bond distribution cannot be explicitly defined at  $\alpha = 1.0$ . It is to be noted that the tensile stress  $f_p$  can be equated to  $f_r$  if  $\alpha_2$  corresponding to  $f_p$  is equal to 1.0 (Fig. 5.5). Therefore, the tensile stress value of the beam reinforcement  $f_r$  by letting  $\alpha = 1.0$  in Equation 5.11 is expressed as follows:

$$f_r = \frac{4}{\phi_b} \frac{H}{0.85h_b} \int_0^{l_h} \mu(f_r) dx \geq f_p \quad (5.15)$$

### Derivation of $\alpha_2$

The fraction factor  $\alpha_2$  is defined when the tensile stress of the beam longitudinal reinforcement at the column face reaches  $f_p$ . Therefore,

$$\alpha_2 = \frac{H}{H - 0.85h_b} \left( 1 - \frac{4}{\phi_b} \frac{\mu_y}{f_y + \frac{4}{\phi_b} \mu_y l_h} l_h \right) \leq 1.0 \quad (5.16)$$

### 5.2.4 Definition of Joint Shear Failure

Beam-column joint shear strength is defined as the horizontal joint shear force at the maximum concrete strength of the C-C-T node in the diagonal strut ST1. Hence, it is predicted as follows:

$$V_{jh,ST1,max} = c \frac{b_j h_c \sqrt{f'_c} \cos \theta}{1.31 + 0.085 \left( \frac{h_b}{h_c} \right)}, \quad \theta = \tan^{-1} \left( \frac{h_b}{h_c} \right) \quad (5.17)$$

where  $c$  is a constant to be determined, and  $b_j = (b_c + b_b)/2$ . Note that  $b_c$  and  $b_b$  are the respective widths of the column and beam cross sections. The expression in Equation (5.17) makes use of the findings from Chapter 4 without consideration of the effect of the beam reinforcement. To predict the joint shear strength, the constant  $c$  is obtained for the case of the minimum joint shear strength at which the fraction factor can be set to 1.0. From Hakuto et al. (2000), the normalized horizontal joint shear stress  $\gamma b_j h_c \sqrt{f'_c}$  where  $\gamma = 4 \text{ psi}^{0.5}$  ( $0.33 \text{ MPa}^{0.5}$ ) is taken as the minimum joint shear strength to trigger the joint shear failure with a joint aspect ratio,  $h_b/h_c = 500/460 \approx 1.1$ , i.e.,  $\theta = 47.4^\circ$ . Applying this suggestion to define the constant  $c$ , one obtains

$$c \frac{\cos(0.83)}{1.31 + 0.085 \times 1.1} = \gamma \Rightarrow c = 2.07\gamma \quad (5.18)$$

Following the fraction factor function in Figure 5.5 and the determined value of  $c$  from Equation (5.18), the joint shear strength is calculated by an iterative procedure using the algorithm illustrated in Figure 5.6.

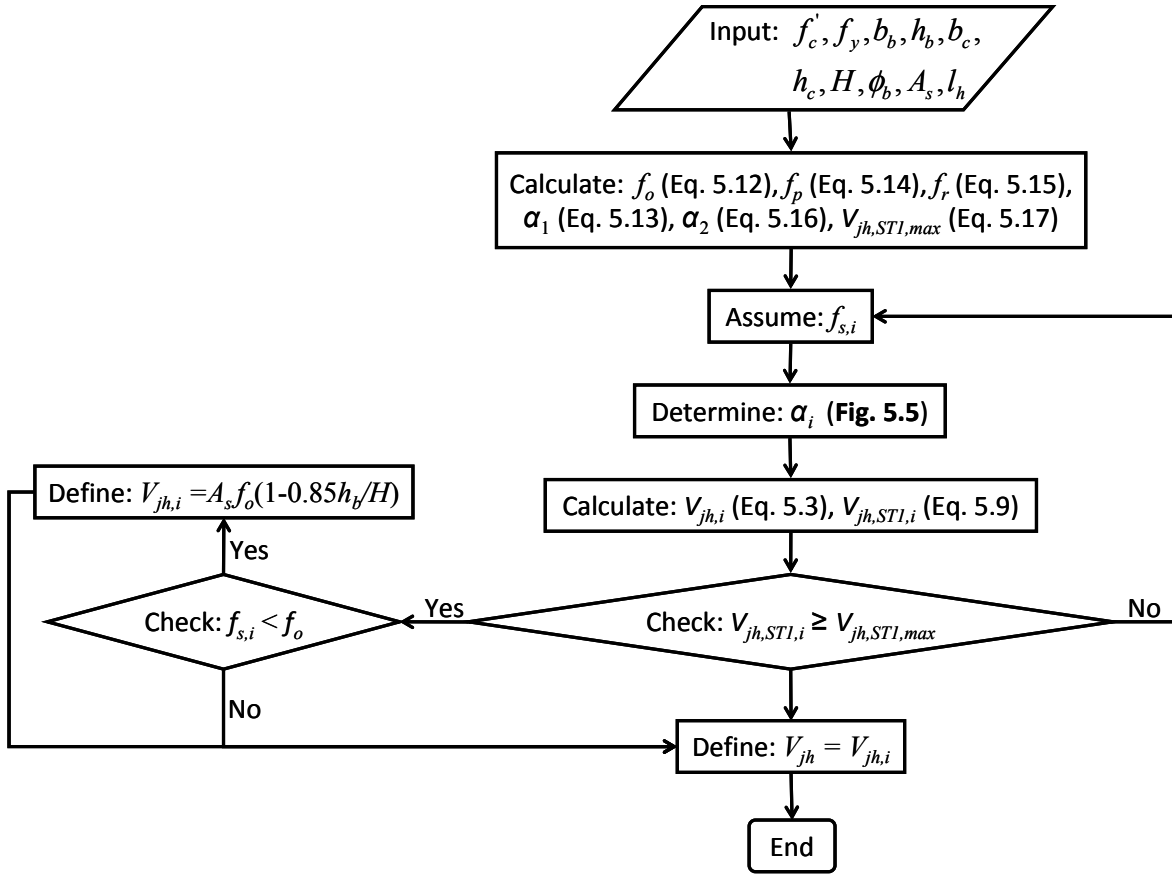
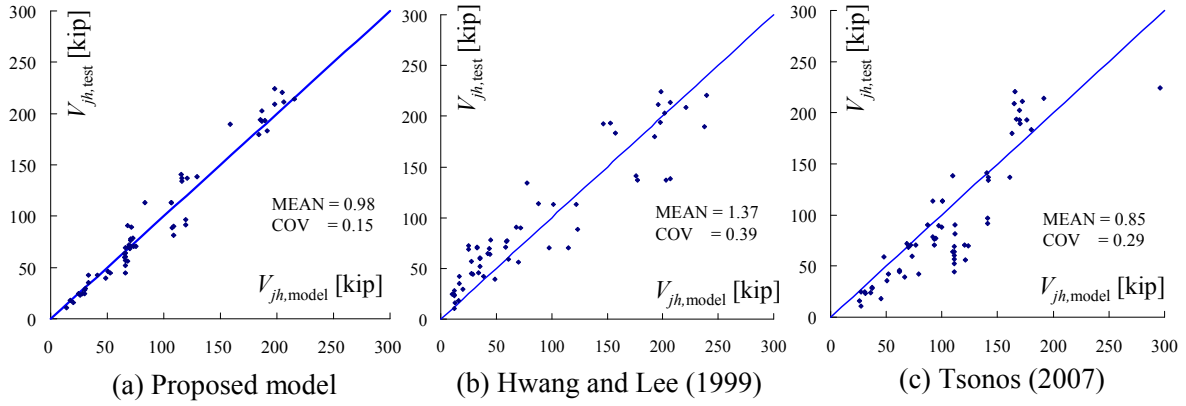


Fig. 5.6 Solution algorithm of proposed analytical joint shear strength model.

### 5.3 EVALUATION OF ANALYTICAL MODEL

#### 5.3.1 Evaluation of Test Data for Literature

The experimentally determined shear strengths of unreinforced exterior joints from the database are compared to the predicted shear strength from the proposed shear strength model in Table 5.1. These predications are based on  $l_h = 0.65h_c$ , which is obtained from Table 5.2, indicating that the analytical predictions are acceptable for the listed values of  $l_h$  and better correlated with the experimental results for  $l_h = 0.65h_c$ . The evaluation results using the proposed model are compared with those from two existing strength models proposed by Hwang and Lee (1999) and by Tsonos (2007) in Figure 5.7.



Note: Mean and COV = Coefficient of Variation for  $V_{jh,test}/V_{jh,model}$ , 1 kip = 4.45 kN

**Fig. 5.7 Comparison of evaluation results with existing analytical models.**

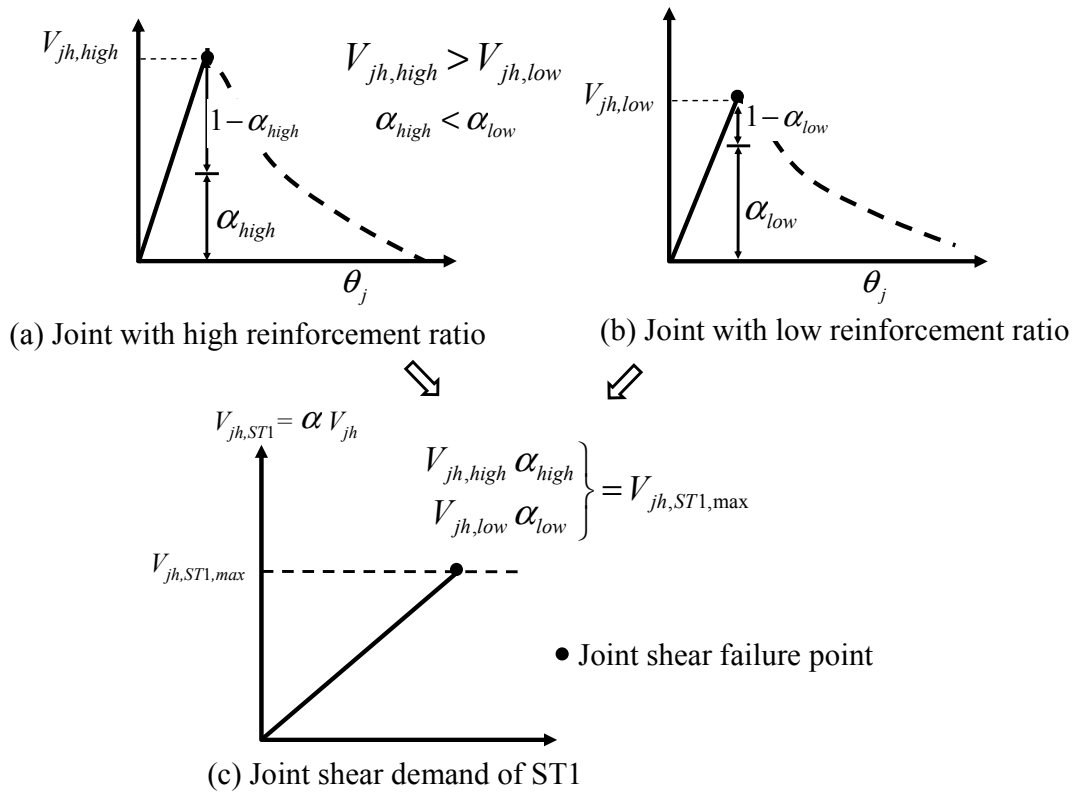


**Fig. 5.8 Illustration of two different shear strengths in same joint.**

**Table 5.1 Prediction of joint shear strength and tensile stress of beam reinforcement at joint shear failure.**

Reference	Specimen	$f'_c$ (ksi)	$f_{y,beam}$ (ksi)	$V_{jh,test}$ (kip)	$v_{jh,test} / \sqrt{f'_c}$ (psi <sup>0.5</sup> )	$f_{s,model}$ (ksi)	$V_{jh,model}$ (kip)	$v_{jh,model} / \sqrt{f'_c}$ (psi <sup>0.5</sup> )	Failure mode* <sub>2</sub>	$V_{jh,test} / V_{jh,model}$
Hanson and Connor (1967, 1972)	V	3.30	51.0	138.4	11.9	37.6	130.7	11.2	J	1.06
	7	5.70	51.0	189.7	12.4	46.1	160.1	10.5	BJ	1.19
Hwang et al. (2005)	0T0	9.76	63.1	224.1	9.4	73.5(Y* <sup>1</sup> )	199.3	8.4	BJ	1.12
Uzumeri (1977)	SP1	4.46	50.3	140.9	10.4	45.2	116.4	8.6	BJ	1.21
	SP2	4.51	50.6	136.9	10.1	45.5	117.1	8.6	BJ	1.17
	SP5	4.63	50.4	136.7	8.9	47.2	121.6	7.9	BJ	1.12
Wong (2005)	BS-L	4.48	75.4	70.9	8.1	56.7	71.1	8.2	J	1.00
	BS-U	4.50	75.4	76.7	8.8	56.7	71.2	8.2	J	1.08
	BS-L-LS	4.58	75.4	77.5	8.8	57.1	71.6	8.1	J	1.08
	BS-L-300	4.94	75.4	113.5	12.4	63.9	84.6	9.2	BJ	1.34
	BS-L-600	5.28	75.4	63.8	6.7	55.9	66.2	7.0	J	0.96
	BS-L-V2T20	4.73	75.4	89.7	10.0	57.7	72.4	8.1	J	1.24
	BS-L-V4T10	4.10	75.4	90.6	10.9	55.0	69.0	8.3	J	1.31
	JA-NN03	6.50	75.4	56.0	5.3	80.9(Y)	68.9	6.6	BJ	0.81
	JA-NN15	6.67	75.4	69.9	6.6	81.5(Y)	69.4	6.5	BJ	1.00
JB-NN03	6.87	75.4	70.4	6.5	86.4(Y)	76.2	7.1	BJ	0.92	
Pantelides et al. (2002)	01	4.79	66.5	193.2	10.9	53.7	191.5	10.8	J	1.01
	02	4.38	66.5	179.6	10.6	52.0	185.6	11.0	J	0.97
	03	4.93	66.5	183.4	10.2	54.2	193.5	10.8	J	0.95
	04	4.58	66.5	202.7	11.7	52.8	188.5	10.9	J	1.08
	05	4.60	66.5	192.6	11.1	52.9	188.7	10.9	J	1.02
	06	4.50	66.5	193.9	11.3	52.5	187.3	10.9	J	1.04
Clyde et al. (2000)	02	6.70	65.9	213.9	12.1	61.8	217.2	12.3	J	0.98
	06	5.94	65.9	211.4	12.7	59.1	207.7	12.5	J	1.02
	04	5.37	65.9	208.9	13.2	56.9	200.1	12.6	J	1.04
	05	5.82	65.9	220.8	13.4	58.7	206.2	12.5	J	1.07
Ortiz (1993)	BCJ1	4.93	104.4	68.8	10.5	68.9	70.9	10.9	J	0.97
	BCJ3	4.79	104.4	72.4	11.3	68.2	70.2	10.9	J	1.03
	BCJ5	5.51	104.4	70.6	10.2	71.7	73.8	10.7	J	0.96
	BCJ6	5.08	104.4	70.8	10.7	69.6	71.7	10.8	J	0.99

**Table 5.1—continued.**

Scott and Hamil (1998)	C4ALN0	6.15	75.7	24.8	10.5	44.7	24.8	10.5	P	1.00	
	C4ALH0	15.08	75.7	42.3	11.4	61.0	33.8	9.1	P	1.25	
	C6LN0	7.40	75.7	23.4	9.0	47.6	26.4	10.2	J	0.89	
	C6LH0	14.65	75.7	35.4	9.7	60.3	33.5	9.2	J	1.06	
Paker and Bullman (1997)	4a	5.66	82.7	43.0	4.5	55.7	66.7	6.9	CF	0.67	
	4b	5.66	82.7	50.3	5.2	55.1	65.9	6.9	J	0.78	
	4c	5.66	82.7	62.0	6.4	55.1	65.9	6.9	J	0.96	
	4d	5.66	82.7	54.7	5.7	55.1	65.9	6.9	J	0.85	
	4e	5.66	82.7	58.4	6.1	55.1	65.9	6.9	J	0.91	
	4f	5.66	82.7	66.7	6.9	55.1	65.9	6.9	J	1.04	
Kananda (1984)	U40L	3.52	56.1	57.7	7.5	47.9	66.0	8.5	J	0.91	
	U20L	3.87	56.1	42.4	5.2	60.6(Y)	41.7	5.2	A	1.02	
	B101	4.63	56.8	78.3	8.8	53.1	73.3	8.3	J	1.07	
Gohbarah and Said (2001)	T-1	4.47	61.6	124.5	12.0	63.1(Y)	107.7	10.4	BJ	1.05	
	T-2	4.47	61.6	117.0	11.3	63.1(Y)	107.7	10.4	BJ	1.05	
Sarsam and Phipps (1985)	EX-2	7.61	75.4	39.6	7.0	67.3	49.2	8.7	BJ	0.81	
Woo (2003)	Model 5	3.84	55.8	16.8	6.3	54.9	19.9	8.2	BJ	0.81	
Liu (2006)	RC-1	2.81	46.9	29.3	7.2	54.9(Y)	30.8	7.6	BJ	0.95	
Engindeniz (2008)	SP1-NS	3.74	45.7	81.4	7.3	48.2(Y)	109.4	9.8	J	0.74	
	SP1-EW	3.74	45.7	90.4	8.1	48.2 (Y)	109.4	9.8	J	0.83	
	SP2-NS	5.02	45.7	91.7	7.1	53.0(Y)	120.3	9.3	J	0.76	
	SP2-EW	5.02	45.7	96.9	7.5	53.0(Y)	120.3	9.3	J	0.81	
Karayannis et al. (2008)	A0	4.58	84.1	18.2	4.3	95.6(Y)	17.5	4.2	BJ	1.05	
	B0	4.58	84.1	44.4	7.1	97.3(Y)	53.3	8.5	BJ	0.83	
	C0	4.58	84.1	45.9	7.3	87.9(Y)	51.2	8.1	BJ	0.90	
Gencoğlu & Eren (2002)	RCNH1	4.35	76.1	10.9	4.3	78.6(Y)	14.2	5.6	BF	0.77	
El-Amoury & Ghobara (2002)	T0	4.44	61.6	91.3	8.8	63.0(Y)	108.1	10.5	BJ	0.82	
Antonopoulos & Triantafillou (2003)	C-1	2.83	84.8	24.4	7.4	49.1	28.3	8.6	J	0.86	
	C-2	3.44	84.8	24.2	6.7	52.4	30.1	8.3	J	0.80	
	T-C	3.57	84.8	28.1	7.6	53.0	30.5	8.2	J	0.92	
Sagbas (2007)	ED1	4.51	50.6	134.1	9.9	45.5	117.1	8.6	BJ	1.15	
Note: 1 ksi = 6.90 MPa; 1 kip = 4.45 kN; $12.0 \sqrt{f'_c}$ psi = $1.0 \sqrt{f'_c}$ MPa; 1 in. = 25.38 mm										Mean	0.98
*1 Y = beam reinforcement yielding										Coefficient of Variation	0.15
*2 J = joint shear failure without beam reinforcement yielding, BJ = joint shear failure with beam reinforcement yielding, BF = beam flexural failure, CF = column flexural failure, P = pull-out failure, A = anchorage failure											

**Table 5.2 Statistics of evaluation results for investigated values of  $l_h$ .**

	$l_h = 0.6h_c$	$l_h = 0.65h_c$	$l_h = 0.7h_c$	$l_h = 0.75h_c$
Mean	1.016	0.985	0.955	0.927
COV	0.149	0.149	0.150	0.147

### 5.3.2 Prediction of Joint Shear Failure Modes

The proposed model can predict the joint shear strength for both types of beam-column joint shear failure modes, i.e., with and without yielding of beam reinforcement. The concept is illustrated in Figure 5.8 to explain how to obtain different joint shear strengths in two identical unreinforced exterior joints except for the beam longitudinal reinforcement ratio. The one having a high reinforcement ratio will show high joint shear strength with a small fraction factor in Figure 5.8(a), while the other having low reinforcement ratio will show low joint shear strength with a large fraction factor in Figure 5.8(b). In both cases, joint shear failures take place when the shear demand of ST1 reaches its capacity (Fig. 5.8(c)).

From the evaluation results of the test data and failure modes for unreinforced exterior beam-column joints, the proposed analytical model is verified to possess high accuracy. It is indispensable to assure the prediction of beam reinforcement yielding in this model to justify the fraction factor. The accuracy of this model for predicting the beam reinforcement yielding is clearly shown in Table 5.1. Therefore, the proposed model is capable of predicting the joint failure mode without using modification of the diagonal strut width and without the need for the estimation of a ductility factor.

## 5.4 SIMULATION OF LITERATURE TESTS USING ANALYTICAL MODEL

There have been several attempts to simulate RC frames including the deformation of beam-column joints. Due to the inherent complex behavior of RC beam-column joints, rotational spring elements have usually been used to simply represent the combination of the shear deformation of a joint panel and the rotation due to bar slippage. The proposed analytical model predicts the joint shear strength from the tensile stress of the beam longitudinal reinforcement under the assumption that the principal tensile strain is predefined by the joint aspect ratio. Therefore, the proposed model can provide the envelope of the joint shear stress-strain

relationship that can be transformed into the moment-rotation relationship of the rotational spring. From Equations (2.3) and (5.2), the horizontal shear strain and stress are given by

$$\gamma_{xy} = \sqrt{4\left(\varepsilon_1 - \frac{\varepsilon_y}{2}\right)^2 - \varepsilon_y^2} \quad (5.19)$$

$$v_{jh} \approx \frac{A_s f_s}{b_j h_c} \left(1 - 0.85 \frac{h_b}{H}\right) \quad (5.20)$$

In the J failure mode, the joint shear stress-strain relationship is assumed to be linear before joint shear failure, while in the BJ failure mode, the joint shear stress-strain relationship is assumed to be bilinear, as shown in Figure 5.9(a). Knowing the frame and joint dimensions, the moment-rotation relationship of the rotational spring is obtained from the shear stress-strain relationship of the joint as follows:

$$M_j = v_{jh} b_j h_c / \lambda, \quad \lambda = \frac{2L}{(2L + h_c) j d_b} - \frac{1}{H} \quad (5.21)$$

$$\theta_j = \gamma_{xy} + \Delta_{slip} / j d_b \quad (5.22)$$

where  $M_j$  is the moment of the joint panel at the center of the panel,  $L$  is the length from the beam inflection point to the column face,  $j d_b$  is the effective depth of the beam cross section,  $\theta_j$  is the joint rotation, and  $\Delta_{slip}$  is the relative movement of beam reinforcement with respect to the perimeter of the joint panel. The denominator  $\lambda$  in Equation (5.21) makes use of the global equilibrium equation from Chapter 4. The total rotation of the joint spring is defined as the sum of the joint shear strain and slip rotation (Fig. 5.9).

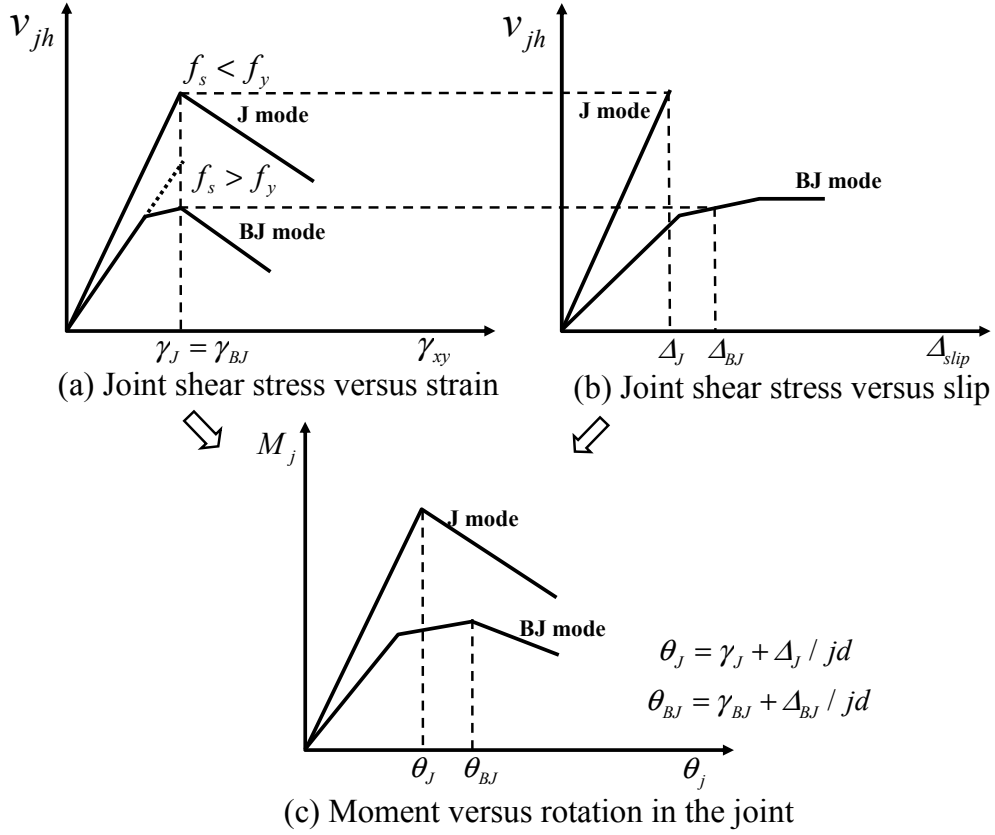


**Fig. 5.9 Relationship of moment versus joint rotation.**

The bar stress-slip relationship is defined as follows:

$$\text{for } f_s < f_y : \Delta_{slip} = \int_0^{l_s} \frac{\mu_E}{E} \frac{4}{\phi_b} x dx = \frac{\mu_E}{E} \frac{2}{\phi_b} l_s^2 \quad (5.23a)$$

$$\begin{aligned} \text{for } f_s \geq f_y : \Delta_{slip} &= \int_0^{l_E} \frac{\mu_E}{E} \frac{4}{\phi_b} x dx + \int_{l_E}^{l_Y+l_E} \left\{ \frac{f_y}{E} + \frac{\mu_Y}{E_h} \frac{4}{\phi_b} (x - l_E) \right\} dx \\ &= \frac{\mu_E}{E} \frac{2}{\phi_b} l_E^2 + \frac{f_y}{E} l_Y + \frac{\mu_Y}{E_h} \frac{2}{\phi_b} l_Y^2 \end{aligned} \quad (5.23b)$$

where  $E$  and  $E_h$  are the elastic and hardening moduli of the beam reinforcement, respectively,

$l_s = \frac{f_s \phi_b}{\mu_E} \frac{\phi_b}{4}$ ,  $l_E = \frac{f_y \phi_b}{\mu_E} \frac{\phi_b}{4}$ , and  $l_Y = \frac{f_s - f_y}{\mu_Y} \frac{\phi_b}{4}$ , see Figure 5.10. It is assumed that the elastic anchorage length  $l_E$  can be extended to the tail of the hook, based on the tensile strain distribution of hooked bars in the exterior beam-column joints (Scott 1996).

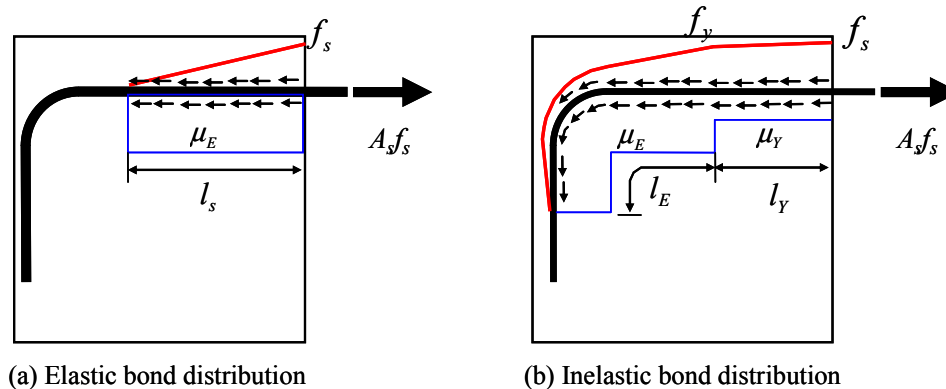


**Fig. 5.10 Bond distribution along hooked bar (Lowe and Altoontash 2003).**

The analyses of two tests from (Wong 2005) are performed in OpenSees (Mazzoni et al. 2007) by replacing the joint region with the rotational spring element obtained from Equations (5.21) and (5.22) using the proposed model to compare the analytical results to the experimental ones. A zero length rotational spring is used to simulate the joint rotation, and the joint offset option is used to rigidly link the center of the joint with the column and beam faces (Fig. 5.11(a)). The conventional analysis is also performed without considering the joint rotation or geometry (Fig. 5.11(b)). The “Hysteretic Material” in OpenSees (Mazzoni et al. 2007) is used for defining a multi-linear response of the rotational spring. The comparison of J failure mode due to a large amount of beam reinforcement is shown in Figure 5.12(a), and that of the BJ failure mode due to a relatively small amount of beam reinforcement is shown in Figure 5.12(b). These comparisons illustrate that the proposed model accurately predicts the strength and deformation at joint shear failure in both types, i.e., the J and BJ failure modes. It is noted that both specimens are symmetrical with respect to positive and negative loading directions. The lower initial stiffness in the simulation results from the simplified linear and bilinear joint shear stress-strain relationships for the J and BJ modes, respectively. In recent studies by Kim and LaFave (2007), and Anderson et al. (2008), high stiffness is assigned in the joint shear stress-strain relationship up to the initiation of diagonal cracking, and reduced linear stiffness follows up to the next critical point. In this regard, the initial stiffness of the joint shear stress-strain relationships assumed in this study underestimates the real initial stiffness, which is more significant in the J failure mode. Finally, it is noted that the post-failure behavior of the joint, which is not part of this study, is qualitatively represented by dotted lines in Figure 5.12. The initial stiffness and post-failure behavior will be investigated as a future extension of this study.

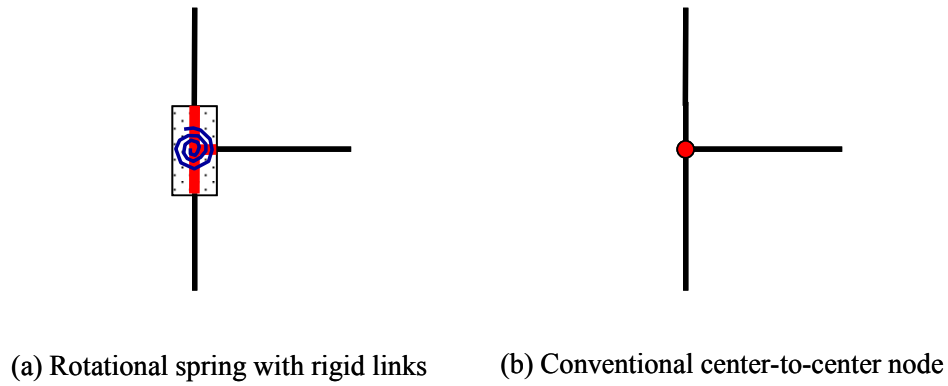
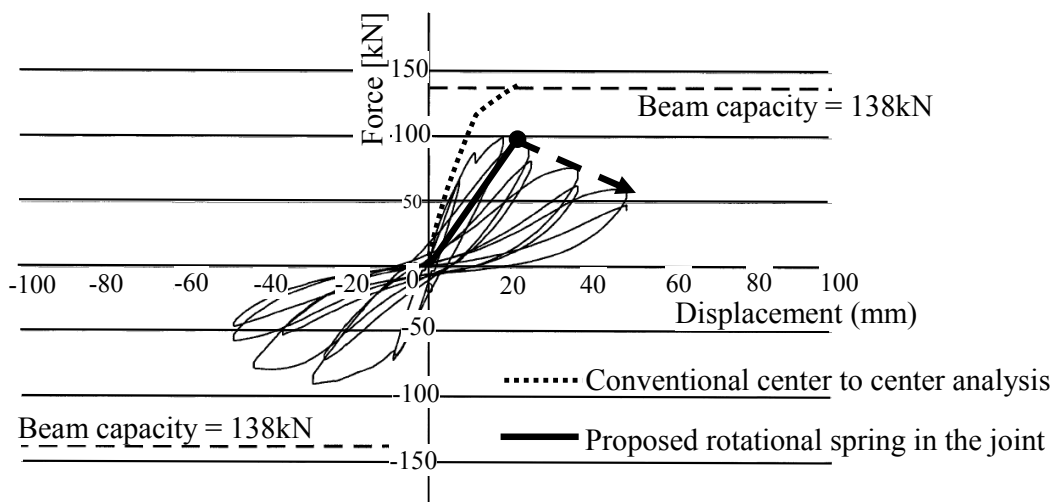
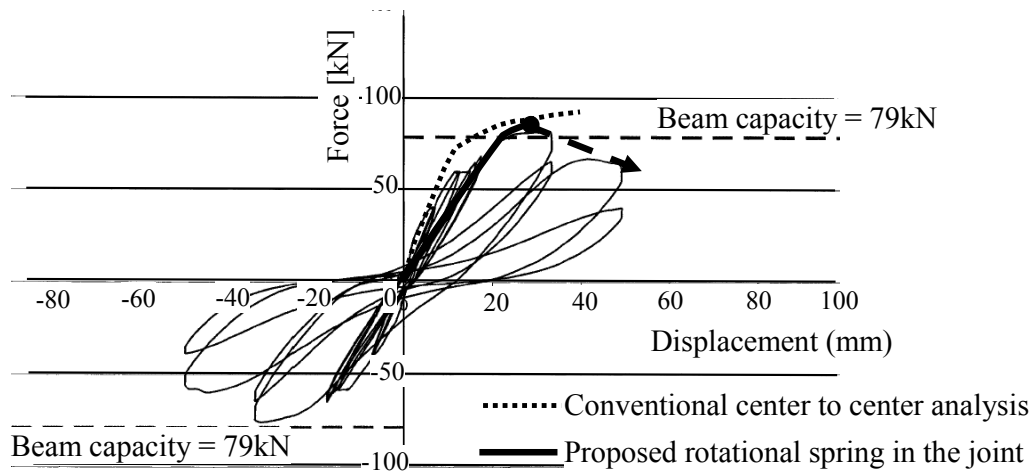


**Fig. 5.11 Modeling of beam-column joint.**



(a) J failure (BS-L)



(b) BJ failure (JA-NN03)

**Fig. 5.12 Simulated results by proposed model.**

## 6 Summary and Concluding Remarks

From the extensive database of unreinforced exterior beam-column joint tests, parametric studies are performed. The variables needed to introduce the influencing parameters of the proposed shear strength equation are derived using a consistent mechanistic approach. The main concluding remarks from this study are as follows:

1. The high joint aspect ratio reduces the shear strength of unreinforced exterior beam-column joints. The first reason is that the steeper diagonal strut is less effective to equilibrate the horizontal joint shear force, and the second reason is that the concrete strength of a diagonal strut is smaller for higher aspect ratios due to an increase of the principal tensile strain.
2. The shear strength of unreinforced exterior beam-column joints is controlled by the beam reinforcement index, which is the joint shear demand, if the beam reinforcement index is between the values corresponding to the maximum and minimum joint shear strengths.
3. The column axial load has little influence on the joint shear strength of unreinforced beam-column joints given that the positive effects are canceled by the negative ones. This is verified by the observation from a large experimental database.
4. Two variables for the better prediction of the shear strength are derived as  $\frac{\cos \theta}{1.31 + 0.085 (h_b/h_c)}$  and  $\frac{A_s f_y}{b_j h_c \sqrt{f'_c}} \left(1 - 0.85 \frac{h_b}{H}\right)$  to include the influences of the joint aspect ratio and the beam reinforcement index, respectively.
5. A semi-empirical equation is proposed to predict the shear strength of unreinforced exterior beam-column joints. The evaluation of existing experimental data using the proposed equation shows high accuracy, which is superior to several existing models from literature.

The proposed semi-empirical model assumes that joint shear strength is governed by joint shear demand if the joint shear demand is located between some values, based on the observation from

the database. In other words, the unreinforced exterior beam-column joint having the same concrete strength and geometry fail in shear at different levels of horizontal joint shear stress with changing beam reinforcement ratio. A reasonable failure mechanism of the unreinforced exterior beam-column joints is needed to explain this multiple joint shear strength. In addition to the strength model, it is also necessary to estimate joint deformation including joint shear distortion and beam reinforcement slip for simulation of structural frames.

A new analytical model to meet these requirements is developed to predict the shear strength of unreinforced exterior beam-column joints. The proposed model is developed considering the realistic behavior of unreinforced exterior beam-column joints. Two inclined struts are assumed to resist the horizontal joint shear in a parallel system and the fraction of each strut contribution is formulated using a bond deterioration mechanism. The proposed model is validated by the evaluation of a large database of unreinforced exterior beam-column joint tests from published literature. Furthermore, the analyses of tests from literature are performed using a rotational spring element of the joint panel based on the proposed model. From the validation and simulations using the proposed model, the following is concluded:

1. The proposed analytical model accurately predicts the shear strength of unreinforced exterior beam-column joints.
2. The yielding of beam longitudinal reinforcement is predicted with high accuracy by the proposed analytical model and thus two different types of joint shear failure, i.e., with and without beam longitudinal reinforcement yielding, are captured without the need for the complexity of ductility consideration.
3. The relationship of moment versus rotation in the joint region is derived from the proposed analytical model. Two published tests, which were designed to show different types of failure, are analyzed using a rotational spring to represent the joint behavior. The force versus displacement relationships accurately simulated the response compared with the less accurate predictions using the conventional center-to-center analysis.

## REFERENCES

- AASHTO, "Standard Specifications for Highway Bridges," 16th Edition, *American Association State and Highway Transportation Officials*, Washington DC, 1996.
- ACI Committee 318, "Building Code Requirements for Structural Concrete (ACI 318-1995) and Commentary (318R-1995)," *American Concrete Institute*, Farmington Hills, Mich., 1995.
- ACI Committee 318, "Building Code Requirements for Structural Concrete (ACI 318-08) and Commentary (318R-08)," *American Concrete Institute*, Farmington Hills, Mich., 2008.
- Alath S, and Kunnath, S.K., "Modeling Inelastic Shear Deformation in RC Beam-Column Joints," *Engineering Mechanics: Proceedings of Tenth Conference*, University of Colorado at Boulder, ASCE, Vol.2, pp822-825
- Alire, D. A., "Seismic Evaluation of Existing Unconfined RC Beam-Column Joints," *MSCE thesis*, University of Washington, 2002.
- Altoontash, A., and Deierlein, G.G., "A Versatile Model for Beam-Column Joints," *ASCE Structures Congress Proceedings*, Seattle, Washington, 2003.
- Anderson, M., Lehman, D., and Stanton, J., "A Cyclic Shear Stress-Strain Model for Joints without Transverse Reinforcement," *Engineering Structures*, No. 30, 2008, pp. 941-954.
- Antonopoulos, C. P. and Triantafillou, T. C., "Experimental Investigation of FRP-Strengthened RC Beam-Column Joints," *ACSE Journal of Composites for Construction*, V. 7, No. 1, Feb. 2003, pp 39-49.
- Bakir, P. G., and Bodurođlu, H. M., "A New Design Equation for Predicting the Joint Shear Strength of Monotonically Loaded Exterior Beam-Column Joints," *Engineering Structures*, V. 24, 2002, pp. 1105-1117.
- Bažant, Z. P., and Yu, Q., "Designing Against Size Effect on Shear Strength of RC Beams without Stirrups: II. Verification and Calibration," *ACSE Journal of Structural Engineering*, V. 131, No. 12, December 2005, pp. 1886-1897.
- Belarbi, A., and Hsu, T.T.C., "Constitutive Laws of Softened Concrete in Biaxial Tension-Compression," *ACI Structural Journal*, V. 92, No. 5, Sep.-Oct. 1995, pp. 562-573.
- Beres, A., White, R. N., and Gergely, P., "Seismic Performance of Interior and Exterior Beam-to-Column Joints Related to Lightly RC Frame Buildings: Detailed Experimental Results," *Structural Engineering Report 92-7*, School of Civil and Environmental Engineering, Cornell University, Ithaca, New York, November 1992.
- Biddah, A., and Ghobarah, A., "Modelling of Shear Deformation and Bond Slip in Reinforced Concrete Joints," *Structural Engineering and Mechanics*, V.7, No. 4, 1999, pp. 413-432
- Booth, E., and Fenwick, R., "Concrete Structures in Earthquake Regions: Design and Analysis," *Longman Scientific and Technical*, 1994.
- BSI: "CP 110: 1972 The Structural Use of Concrete. Part I: Design, Materials and Workmanship," British Standards Institution, London, 1972.
- Canadian Standard Association, "Design of Concrete Structures (CAN3-A23.3M94)," *Structural Design*, Roxdale, 1994.
- Celik, O.C., and Ellingwood, B.R., "Modeling beam-column joints in fragility assessment of gravity load designed reinforced concrete frames," *Journal of Earthquake Engineering*, V.12, No. 3, 2008, pp. 357-381
- Clyde, C., Pantelides, C. P., and Reaveley, L. d., "Performance-Based Evaluation of Exterior RC Building Joints for Seismic Excitation," *PEER Report 2000/05*, July 2000.

- Collins, M. P. and Mitchell, D., "A Rational Approach to Shear Design - The 1984 Canadian Code Provisions," *ACI Structural Journal*, V. 83, No. 6, Nov.-Dec. 1986, pp. 925-933.
- Collins, M. P., Mitchell, D., Adebar, P., and Vecchio, F. J., "A General Shear Design Method," *ACI Structural Journal*, V. 93, No. 1, Jan.-Feb. 1996, pp. 36-45.
- Comité Euro-International du Béton, "Bulletin d'Information No. 213/214 CEB-FIP Model Code 1990," London: Thomas Telford, 1993.
- El-Amoury, T. and Ghobarah, A., "Seismic Rehabilitation of Beam-Column Joints Using GFRP Sheets," *Engineering Structures*, No. 24, 2002, pp. 1397-1407.
- Engindeniz, M., "Repair and Strengthening of Pre-1970 RC Corner Beam-Column Joints Using CFRP Composites," *PhD thesis*, Georgia Institute of Technology, 2008.
- Eurocode 2, "Design of Concrete Structures, Part 1: General Rules and Rules for Buildings (DD ENV 1992-1-1: 1992)," *Commission of the European Communities*, 1992.
- FEMA Publication 273, "NEHRP Guidelines for the Seismic Rehabilitation of Buildings," *Federal Emergency Management Agency*, Washington, 1997.
- Gencoğlu, M. and Eren I., "An Experimental Study on the Effect of Steel Fiber RC on the Behavior of the Exterior Beam-Column Joints Subjected to Reversal Cyclic Loading," *Turkish Journal of Engineering & Environmental Science*, V. 26, 2002, pp 493-502.
- Ghobarah, A. and Said, A., " Seismic Rehabilitation of Beam-Column Joints using FRP laminates," *Journal of Earthquake Engineering*, V. 5, No. 1, 2001, pp 113-129.
- Hanson, N. W., and Conner, H. W., "Seismic Resistance of RC Beam-Column Joints," *ACSE Journal of Structural Division*, V. 93, No. ST5, Oct. 1967, pp 533-560.
- Hanson, N. W., and Conner, H. W., "Tests of RC Beam-Column Joints under Simulated Seismic Loading," *Portland Cement Association Research and Development Bulletin*, 1972.
- Hakuto, S., Park, R. and Tanaka, H., "Seismic Load Tests on Interior and Exterior Beam-Column Joints with Substandard Reinforcing Details," *ACI Structural Journal*, V. 97, No. 1, January 2000, pp. 11-25.
- Hegger, J., Sherif, A., and Roeser, W., "Nonseismic Design of Beam-Column Joints," *ACI Structural Journal*, V. 100, No. 5, Sept.-Oct. 2003, pp. 654-664.
- Hertanto, E., "Seismic Assessments of Pre-1970s Reinforced Concrete Structure," *MSCE thesis*, University of Canterbury, 2005.
- Hsu, T.T.C., "Softened truss model theory for shear and torsion," *ACI Structural Journal*, V. 85, No. 6, Nov.-Dec. 1988, pp. 624-634.
- Hwang, S. J. and Lee, H. J., "Analytical Model for Predicting Shear Strength of Exterior RC Beam-Column Joints for Seismic Resistance," *ACI Structural Journal*, V. 96, No. 5, Sept.-Oct. 1999, pp. 846-857.
- Hwang, S. J., Wang, K. C., and Lee, H. J., "Designing and Retrofitting Strategy of RC Beam-Column Joints," *Proceedings of SINO-UK Joint Workshop on Deep Excavations and Earthquake Resistance Design of Structures*, Lin, H.D., ed., Taiwan 2001.
- Hwang, S. J. and Lee, H. J., "Strength Prediction for Discontinuity Regions by Softened Strut-and-Tie Model," *ACSE Journal of Structural Engineering*, V. 128, No. 12, December 2002, pp. 1519-1526.
- Hwang, S. J., Lee, H. J., Liao, T. F., Wang, K. C., and Tsai, H.H., "Role of Hoops on Shear Strength of RC Beam-Column Joints," *ACI Structural Journal*, V. 102, No. 3, May-June 2005, pp. 445-453.

- Jirsa, J. O., Breen, J. E., Bergmeister, K., Barton, D., Anderson, R. and Bouadi, H., "Experimental Studies of Nodes in Strut-And-Tie models," *Report of the IABSE Colloquium on Structural Concrete*, Stuttgart, Germany, 1991, pp. 525-532.
- Joint ACI-ASCE Committee 352, "Recommendations for Design of Beam-Column Joints in Monolithic RC Structures (352R-02)," *American Concrete Institute*, Farmington Hills, Mich., 2002.
- Kanada, K., Kondon, G., Fujii, S., and Morita, S., "Relation Between Beam Bar Anchorage and Shear Resistance at Exterior Beam-Column Joints," *Transaction of the Japan Concrete Institute*, V. 6, 1984, pp. 433-440.
- Karayannis, C. G., Chalioris, C. E., and Sirkelis, G. M., "Local Retrofit of Exterior RC Beam-Column Joints Using Thin RC Jackets- An Experimental Study," *Earthquake Engineering and Structural Dynamics*, V. 37, 2008, pp. 727-746.
- Kim, J. and LaFave, J. M., "Key Influence Parameters for the Joint Shear Behavior of RC (RC) Beam-Column Connections," *Engineering Structures*, No. 29, 2007, pp. 2523-2539.
- Kurose, Y., "Recent Studies on RC Beam-Column Joints in Japan," *PMFSEL Report No. 87-8*, University of Texas at Austin, Dec. 1987.
- Kurose, Y., Guimaraes, G., Liu, Z., Kreger, M., and Jirsa, J. O., "Study of Reinforced Concrete Beam-Column Joints Under Uniaxial and Biaxial Loading," *PMFSEL Report No. 88-2*, University of Texas at Austin, Dec. 1988.
- Lehman, D.E., and Moehle, J.P., "Seismic Performance of Well-Confined Concrete Bridge Columns," *PEER Report 1998/01*, University of California, Berkeley, Dec. 2000.
- Liu, C., "Seismic Behavior of Beam-Column Joint Assemblies Reinforced with Steel Fibers," *MSCE thesis*, University of Canterbury, 2006.
- Lowes, L.N., and Altoontash, A., "Modeling Reinforced-Concrete Beam-Column Joints Subjected to Cyclic Loading," *ACSE Journal of Structural Engineering*, V. 129, No. 12, December 2003, pp. 1686-1697.
- Lowes, L.N., Mitra, N., and Altoontash, A., "A Beam-Column Joint Model for Simulating the Earthquake Response of Reinforced Concrete Frames," *PEER Report 2003/10*, 2004.
- MacGregor, J. G., "RC Mechanics and Design," Englewood Cliffs, NJ: *Prentice-Hall*, 1988.
- Mander, J.B., Priestley, M.J.N., and Park, R., "Theoretical Stress-Strain Model for Confined Concrete," *ACSE Journal of Structural Engineering*, V. 114, No. 8, August 1988, pp. 1804-1826.
- Meinheit, D.F., and Jirsa, J.O., "The Shear Strength of Reinforced Concrete Beam-Column Joints," *CESRL Report No. 77-1*, University of Texas at Austin, Jan. 1977.
- Minami, K. and Nishimura, Y., "Anchorage Strength of Bent Bar in Exterior Joints," *2nd U.S.-N.Z.-Japan Seminar*, Tokyo, May 1985.
- Mitra, N., and Lowes, L.N., "Evaluation, Calibration, and Verification of a Reinforced Concrete Beam-Column Joint Model," *ACSE Journal of Structural Engineering*, V. 133, No. 1, January 2007, pp. 105-120.
- Moehle, J.P., Private communication, 2008.
- NZS 3101:1995, "Concrete Structures Standard, NZS 3101," *Standard Association of New Zealand*, Wellington, 1995.
- Ohwada, Y., "A Study on Effect of Lateral Beams on RC Beam-Column Joints (1)," *Transaction of AIJ*, Extra, No. 2510, Oct. 1976.
- Ohwada, Y., "A Study on Effect of Lateral Beams on RC Beam-Column Joints (2)," *Conference of AIJ*, No. 61, 1977.

- Ortiz, I. R., "Strut-and-Tie Modeling of Reinforce Concrete Short Beams and Beam-Column Joints," *PhD thesis*, University of Westminster, 1993.
- Pampanin, S., Magenes, G., and Carr, A., "Modeling of Shear Hinge Mechanism in Poorly Detailed RC Beam Column Joints," FIB Symposium, *Concrete Structures in Seismic Regions*, Athens, 2003.
- Pantazopoulou, S., and Bonacci, J., "Consideration of Questions about beam-column joints," *ACI Structural Journal*, V. 89, No. 1, Jan.-Feb. 1992, pp. 27-37.
- Pantelides, C. P., Hansen, J., Nadauld, J., and Reaveley, L. d., "Assessment of RC Building Exterior Joints with Substandard Details," *PEER Report 2002/18*, May 2002.
- Park, R., "A Static Force-Based Procedure for the Seismic Assessment of Existing Reinforced Concrete Moment Resisting Frames," *Bulletin of the New Zealand National Society for Earthquake Engineering*, V. 30, No. 3, 1997, pp. 213-226.
- Parker, D. E. and Bullman, P. J. M., "Shear Strength within RC Beam-Column Joints," *The Structural Engineer*, V. 75, No. 4, Feb. 1997, pp. 53-57.
- Paulay, T., Park, R. and Priestley M. J. N., "RC Beam Column Joints under Seismic Actions," *ACI Structural Journal*, V. 75, No. 11, November 1978, pp. 585-593.
- Priestley, M.J.N., "Displacement-Based Seismic Assessment of Reinforced Concrete Buildings," *Journal of Earthquake Engineering*, V. 1, No. 1, Jan. 1997, pp. 157-192.
- Sagbas, G., "Nonlinear Finite Element Analysis of Beam-Column Subassemblies," *Master of Applied Science thesis*, University of Toronto, 2007.
- Sarsam, K.F. and Phipps, M.E., "The Shear Design of In-situ Reinforced Beam-Column Joints Subjected to Monotonic Loading," *Magazine of Concrete Research*, V. 37, No. 130, March 1985, pp. 16-28.
- Schlaich, J. and Schäfer, K., "Design and Detailing of Structural Concrete Using Strut-And-Tie Models," *The Structural Engineer*, V. 69, No. 6, 1991, pp. 113-125.
- Schlaich, J., Schäfer, K., and Jennewein, M., "Toward a Consistent Design of Structural Concrete," *PCI Journal*, V. 32, No. 3, 1987, pp. 74-150.
- Scott, B.D., Park, R., and Priestley, M.J.N., "Stress-Strain Behavior of Concrete Confined by Overlapping Hoops at Low and High Strain Rates," *ACI Journal Proceedings*, V. 79, No. 1, Jan.-Feb. 1982, pp. 13-27.
- Scott, R.H., "The Effects of Detailing on RC Beam Column Connection Behavior," *The Structural Engineer*, V. 70, No. 18, Sep. 1997, pp. 318-324.
- Scott, R.H., Feltham, I., and Whittle, R. T., "Reinforced Beam-Column Connections and BS 8110," *The Structural Engineer*, V. 72, No. 4, Feb. 1994, pp. 55-60.
- Scott, R.H., and Hamil, S.J., "Connection Zone Strain in the Reinforced Concrete Beam Column Connections," *Proceedings of the 11<sup>th</sup> International Conference on Experimental Mechanics*, Oxford, UK, 1998, pp. 65-69.
- Taylor, H.P.J., "The Behavior of In-situ Concrete Beam-Column Joints," *Technical Report 42.492*, Cement and Concrete Association, Wexham Springs, UK, 1974.
- Theiss, A.G., "Modeling the Earthquake Response of Older Reinforced Concrete Beam-Column Building Joints," *MSCE thesis*, University of Washington, 2005.
- Tsonos, A.G., "Cyclic Load Behavior of RC Beam-Column Subassemblages of Modern Structures," *ACI Structural Journal*, V. 104, No. 4, July-August 2007, pp. 468-478.
- Uzumeri, S.M., "Strength and Ductility of Cast-In-Place Beam-Column Joints," *ACI Structural Journal*, SP53, 1977, pp. 293-350.

- Vecchio, F.J., and Collins, M.P., "The Modified Compression-Field Theory of Reinforced Concrete Elements Subjected to Shear," *ACI Structural Journal*, V. 83, No. 2, Mar.-Apr. 1986, pp. 219-231.
- Vollum, R.L., "Design and Analysis of Exterior Beam Column Connections," *PhD thesis*, Imperial College of Science Technology and Medicine-University of London, 1998.
- Vollum, R. L. and Newman, J.B., "Strut and Tie Models for Analysis/Design of External Beam-Column Joints," *Magazine of Concrete Research*, V. 51, No. 6, Dec. 1999, pp.415-425.
- Walker, S.G., "Seismic Performance of Existing RC Beam-Column Joints," *MSCE thesis*, University of Washington, 2001.
- Wilson, I.D., "SIFCON Joints in Pre-Cast Concrete Structures," *Proceedings of the 8<sup>th</sup> BCA Annual Conference on Higher Education and the Concrete Industry*, Southampton, 1998, pp. 227-239.
- Wong, H.F., "Shear Strength and Seismic Performance of Non-Seismically Designed RC Beam-Column Joints," *PhD thesis*, Hong Kong University of Science and Technology, 2005.
- Woo, S.W., "Seismic Performance of RC Frames in a Low to Moderate Seismicity Region," *PhD thesis*, Korea University, 2003.
- Youssef, M., and Ghobarah, A., "Modelling of RC Beam-Column Joints and Structural Walls," *Journal of Earthquake Engineering*, V.5, No. 1, 2001, pp. 93-111.
- Zhang, L., and Jirsa, J.O., "A Study of Shear Behavior of RC Beam-Column Joints," *PMFSEL Report No. 82-1*, University of Texas at Austin, Feb. 1982.

## PEER REPORTS

PEER reports are available individually or by yearly subscription. PEER reports can be ordered at [http://peer.berkeley.edu/publications/peer\\_reports.html](http://peer.berkeley.edu/publications/peer_reports.html) or by contacting the Pacific Earthquake Engineering Research Center, 1301 South 46<sup>th</sup> Street, Richmond, CA 94804-4698. Tel.: (510) 665-3448; Fax: (510) 665-3456; Email: [peer\\_editor@berkeley.edu](mailto:peer_editor@berkeley.edu)

- PEER 2009/02** *Improving Earthquake Mitigation through Innovations and Applications in Seismic Science, Engineering, Communication, and Response. Proceedings of a U.S.-Iran Seismic Workshop.* October 2009.
- PEER 2009/01** *Evaluation of Ground Motion Selection and Modification Methods: Predicting Median Interstory Drift Response of Buildings.* Curt B. Haselton, Ed. June 2009.
- PEER 2008/10** *Technical Manual for Strata.* Albert R. Kottke and Ellen M. Rathje. February 2009.
- PEER 2008/09** *NGA Model for Average Horizontal Component of Peak Ground Motion and Response Spectra.* Brian S.-J. Chiou and Robert R. Youngs. November 2008.
- PEER 2008/08** *Toward Earthquake-Resistant Design of Concentrically Braced Steel Structures.* Patxi Uriz and Stephen A. Mahin. November 2008.
- PEER 2008/07** *Using OpenSees for Performance-Based Evaluation of Bridges on Liquefiable Soils.* Stephen L. Kramer, Pedro Arduino, and HyungSuk Shin. November 2008.
- PEER 2008/06** *Shaking Table Tests and Numerical Investigation of Self-Centering Reinforced Concrete Bridge Columns.* Hyung IL Jeong, Junichi Sakai, and Stephen A. Mahin. September 2008.
- PEER 2008/05** *Performance-Based Earthquake Engineering Design Evaluation Procedure for Bridge Foundations Undergoing Liquefaction-Induced Lateral Ground Displacement.* Christian A. Ledezma and Jonathan D. Bray. August 2008.
- PEER 2008/04** *Benchmarking of Nonlinear Geotechnical Ground Response Analysis Procedures.* Jonathan P. Stewart, Annie On-Lei Kwok, Youssef M. A. Hashash, Neven Matasovic, Robert Pyke, Zhiliang Wang, and Zhaohui Yang. August 2008.
- PEER 2008/03** *Guidelines for Nonlinear Analysis of Bridge Structures in California.* Ady Aviram, Kevin R. Mackie, and Božidar Stojadinović. August 2008.
- PEER 2008/02** *Treatment of Uncertainties in Seismic-Risk Analysis of Transportation Systems.* Evangelos Stergiou and Anne S. Kiremidjian. July 2008.
- PEER 2008/01** *Seismic Performance Objectives for Tall Buildings.* William T. Holmes, Charles Kircher, William Petak, and Nabih Youssef. August 2008.
- PEER 2007/12** *An Assessment to Benchmark the Seismic Performance of a Code-Conforming Reinforced Concrete Moment-Frame Building.* Curt Haselton, Christine A. Goulet, Judith Mitrani-Reiser, James L. Beck, Gregory G. Deierlein, Keith A. Porter, Jonathan P. Stewart, and Ertugrul Taciroglu. August 2008.
- PEER 2007/11** *Bar Buckling in Reinforced Concrete Bridge Columns.* Wayne A. Brown, Dawn E. Lehman, and John F. Stanton. February 2008.
- PEER 2007/10** *Computational Modeling of Progressive Collapse in Reinforced Concrete Frame Structures.* Mohamed M. Talaat and Khalid M. Mosalam. May 2008.
- PEER 2007/09** *Integrated Probabilistic Performance-Based Evaluation of Benchmark Reinforced Concrete Bridges.* Kevin R. Mackie, John-Michael Wong, and Božidar Stojadinović. January 2008.
- PEER 2007/08** *Assessing Seismic Collapse Safety of Modern Reinforced Concrete Moment-Frame Buildings.* Curt B. Haselton and Gregory G. Deierlein. February 2008.
- PEER 2007/07** *Performance Modeling Strategies for Modern Reinforced Concrete Bridge Columns.* Michael P. Berry and Marc O. Eberhard. April 2008.
- PEER 2007/06** *Development of Improved Procedures for Seismic Design of Buried and Partially Buried Structures.* Linda Al Atik and Nicholas Sitar. June 2007.
- PEER 2007/05** *Uncertainty and Correlation in Seismic Risk Assessment of Transportation Systems.* Renee G. Lee and Anne S. Kiremidjian. July 2007.
- PEER 2007/04** *Numerical Models for Analysis and Performance-Based Design of Shallow Foundations Subjected to Seismic Loading.* Sivapalan Gajan, Tara C. Hutchinson, Bruce L. Kutter, Prishati Raychowdhury, José A. Ugalde, and Jonathan P. Stewart. May 2008.
- PEER 2007/03** *Beam-Column Element Model Calibrated for Predicting Flexural Response Leading to Global Collapse of RC Frame Buildings.* Curt B. Haselton, Abbie B. Liel, Sarah Taylor Lange, and Gregory G. Deierlein. May 2008.

- PEER 2007/02** *Campbell-Bozorgnia NGA Ground Motion Relations for the Geometric Mean Horizontal Component of Peak and Spectral Ground Motion Parameters.* Kenneth W. Campbell and Yousef Bozorgnia. May 2007.
- PEER 2007/01** *Boore-Atkinson NGA Ground Motion Relations for the Geometric Mean Horizontal Component of Peak and Spectral Ground Motion Parameters.* David M. Boore and Gail M. Atkinson. May. May 2007.
- PEER 2006/12** *Societal Implications of Performance-Based Earthquake Engineering.* Peter J. May. May 2007.
- PEER 2006/11** *Probabilistic Seismic Demand Analysis Using Advanced Ground Motion Intensity Measures, Attenuation Relationships, and Near-Fault Effects.* Polsak Tothong and C. Allin Cornell. March 2007.
- PEER 2006/10** *Application of the PEER PBEE Methodology to the I-880 Viaduct.* Sashi Kunnath. February 2007.
- PEER 2006/09** *Quantifying Economic Losses from Travel Forgone Following a Large Metropolitan Earthquake.* James Moore, Sungbin Cho, Yue Yue Fan, and Stuart Werner. November 2006.
- PEER 2006/08** *Vector-Valued Ground Motion Intensity Measures for Probabilistic Seismic Demand Analysis.* Jack W. Baker and C. Allin Cornell. October 2006.
- PEER 2006/07** *Analytical Modeling of Reinforced Concrete Walls for Predicting Flexural and Coupled-Shear-Flexural Responses.* Kutay Orakcal, Leonardo M. Massone, and John W. Wallace. October 2006.
- PEER 2006/06** *Nonlinear Analysis of a Soil-Drilled Pier System under Static and Dynamic Axial Loading.* Gang Wang and Nicholas Sitar. November 2006.
- PEER 2006/05** *Advanced Seismic Assessment Guidelines.* Paolo Bazzurro, C. Allin Cornell, Charles Menun, Maziar Motahari, and Nicolas Luco. September 2006.
- PEER 2006/04** *Probabilistic Seismic Evaluation of Reinforced Concrete Structural Components and Systems.* Tae Hyung Lee and Khalid M. Mosalam. August 2006.
- PEER 2006/03** *Performance of Lifelines Subjected to Lateral Spreading.* Scott A. Ashford and Teerawat Juirnarongrit. July 2006.
- PEER 2006/02** *Pacific Earthquake Engineering Research Center Highway Demonstration Project.* Anne Kiremidjian, James Moore, Yue Yue Fan, Nesrin Basoz, Ozgur Yazali, and Meredith Williams. April 2006.
- PEER 2006/01** *Bracing Berkeley. A Guide to Seismic Safety on the UC Berkeley Campus.* Mary C. Comerio, Stephen Tobriner, and Ariane Fehrenkamp. January 2006.
- PEER 2005/16** *Seismic Response and Reliability of Electrical Substation Equipment and Systems.* Junho Song, Armen Der Kiureghian, and Jerome L. Sackman. April 2006.
- PEER 2005/15** *CPT-Based Probabilistic Assessment of Seismic Soil Liquefaction Initiation.* R. E. S. Moss, R. B. Seed, R. E. Kayen, J. P. Stewart, and A. Der Kiureghian. April 2006.
- PEER 2005/14** *Workshop on Modeling of Nonlinear Cyclic Load-Deformation Behavior of Shallow Foundations.* Bruce L. Kutter, Geoffrey Martin, Tara Hutchinson, Chad Harden, Sivapalan Gajan, and Justin Phalen. March 2006.
- PEER 2005/13** *Stochastic Characterization and Decision Bases under Time-Dependent Aftershock Risk in Performance-Based Earthquake Engineering.* Gee Liek Yeo and C. Allin Cornell. July 2005.
- PEER 2005/12** *PEER Testbed Study on a Laboratory Building: Exercising Seismic Performance Assessment.* Mary C. Comerio, editor. November 2005.
- PEER 2005/11** *Van Nuys Hotel Building Testbed Report: Exercising Seismic Performance Assessment.* Helmut Krawinkler, editor. October 2005.
- PEER 2005/10** *First NEES/E-Defense Workshop on Collapse Simulation of Reinforced Concrete Building Structures.* September 2005.
- PEER 2005/09** *Test Applications of Advanced Seismic Assessment Guidelines.* Joe Maffei, Karl Telleen, Danya Mohr, William Holmes, and Yuki Nakayama. August 2006.
- PEER 2005/08** *Damage Accumulation in Lightly Confined Reinforced Concrete Bridge Columns.* R. Tyler Ranf, Jared M. Nelson, Zach Price, Marc O. Eberhard, and John F. Stanton. April 2006.
- PEER 2005/07** *Experimental and Analytical Studies on the Seismic Response of Freestanding and Anchored Laboratory Equipment.* Dimitrios Konstantinidis and Nicos Makris. January 2005.
- PEER 2005/06** *Global Collapse of Frame Structures under Seismic Excitations.* Luis F. Ibarra and Helmut Krawinkler. September 2005.
- PEER 2005/05** *Performance Characterization of Bench- and Shelf-Mounted Equipment.* Samit Ray Chaudhuri and Tara C. Hutchinson. May 2006.

- PEER 2005/04** *Numerical Modeling of the Nonlinear Cyclic Response of Shallow Foundations.* Chad Harden, Tara Hutchinson, Geoffrey R. Martin, and Bruce L. Kutter. August 2005.
- PEER 2005/03** *A Taxonomy of Building Components for Performance-Based Earthquake Engineering.* Keith A. Porter. September 2005.
- PEER 2005/02** *Fragility Basis for California Highway Overpass Bridge Seismic Decision Making.* Kevin R. Mackie and Božidar Stojadinović. June 2005.
- PEER 2005/01** *Empirical Characterization of Site Conditions on Strong Ground Motion.* Jonathan P. Stewart, Yoojoong Choi, and Robert W. Graves. June 2005.
- PEER 2004/09** *Electrical Substation Equipment Interaction: Experimental Rigid Conductor Studies.* Christopher Stearns and André Filiatrault. February 2005.
- PEER 2004/08** *Seismic Qualification and Fragility Testing of Line Break 550-kV Disconnect Switches.* Shakhzod M. Takhirov, Gregory L. Fenves, and Eric Fujisaki. January 2005.
- PEER 2004/07** *Ground Motions for Earthquake Simulator Qualification of Electrical Substation Equipment.* Shakhzod M. Takhirov, Gregory L. Fenves, Eric Fujisaki, and Don Clyde. January 2005.
- PEER 2004/06** *Performance-Based Regulation and Regulatory Regimes.* Peter J. May and Chris Koski. September 2004.
- PEER 2004/05** *Performance-Based Seismic Design Concepts and Implementation: Proceedings of an International Workshop.* Peter Fajfar and Helmut Krawinkler, editors. September 2004.
- PEER 2004/04** *Seismic Performance of an Instrumented Tilt-up Wall Building.* James C. Anderson and Vitelmo V. Bertero. July 2004.
- PEER 2004/03** *Evaluation and Application of Concrete Tilt-up Assessment Methodologies.* Timothy Graf and James O. Malley. October 2004.
- PEER 2004/02** *Analytical Investigations of New Methods for Reducing Residual Displacements of Reinforced Concrete Bridge Columns.* Junichi Sakai and Stephen A. Mahin. August 2004.
- PEER 2004/01** *Seismic Performance of Masonry Buildings and Design Implications.* Kerri Anne Taeko Tokoro, James C. Anderson, and Vitelmo V. Bertero. February 2004.
- PEER 2003/18** *Performance Models for Flexural Damage in Reinforced Concrete Columns.* Michael Berry and Marc Eberhard. August 2003.
- PEER 2003/17** *Predicting Earthquake Damage in Older Reinforced Concrete Beam-Column Joints.* Catherine Pagni and Laura Lowes. October 2004.
- PEER 2003/16** *Seismic Demands for Performance-Based Design of Bridges.* Kevin Mackie and Božidar Stojadinović. August 2003.
- PEER 2003/15** *Seismic Demands for Nondeteriorating Frame Structures and Their Dependence on Ground Motions.* Ricardo Antonio Medina and Helmut Krawinkler. May 2004.
- PEER 2003/14** *Finite Element Reliability and Sensitivity Methods for Performance-Based Earthquake Engineering.* Terje Haukaas and Armen Der Kiureghian. April 2004.
- PEER 2003/13** *Effects of Connection Hysteretic Degradation on the Seismic Behavior of Steel Moment-Resisting Frames.* Janise E. Rodgers and Stephen A. Mahin. March 2004.
- PEER 2003/12** *Implementation Manual for the Seismic Protection of Laboratory Contents: Format and Case Studies.* William T. Holmes and Mary C. Comerio. October 2003.
- PEER 2003/11** *Fifth U.S.-Japan Workshop on Performance-Based Earthquake Engineering Methodology for Reinforced Concrete Building Structures.* February 2004.
- PEER 2003/10** *A Beam-Column Joint Model for Simulating the Earthquake Response of Reinforced Concrete Frames.* Laura N. Lowes, Nilanjan Mitra, and Arash Altoontash. February 2004.
- PEER 2003/09** *Sequencing Repairs after an Earthquake: An Economic Approach.* Marco Casari and Simon J. Wilkie. April 2004.
- PEER 2003/08** *A Technical Framework for Probability-Based Demand and Capacity Factor Design (DCFD) Seismic Formats.* Fatemeh Jalayer and C. Allin Cornell. November 2003.
- PEER 2003/07** *Uncertainty Specification and Propagation for Loss Estimation Using FOSM Methods.* Jack W. Baker and C. Allin Cornell. September 2003.
- PEER 2003/06** *Performance of Circular Reinforced Concrete Bridge Columns under Bidirectional Earthquake Loading.* Mahmoud M. Hachem, Stephen A. Mahin, and Jack P. Moehle. February 2003.

- PEER 2003/05** *Response Assessment for Building-Specific Loss Estimation.* Eduardo Miranda and Shahram Taghavi. September 2003.
- PEER 2003/04** *Experimental Assessment of Columns with Short Lap Splices Subjected to Cyclic Loads.* Murat Melek, John W. Wallace, and Joel Conte. April 2003.
- PEER 2003/03** *Probabilistic Response Assessment for Building-Specific Loss Estimation.* Eduardo Miranda and Hesameddin Aslani. September 2003.
- PEER 2003/02** *Software Framework for Collaborative Development of Nonlinear Dynamic Analysis Program.* Jun Peng and Kincho H. Law. September 2003.
- PEER 2003/01** *Shake Table Tests and Analytical Studies on the Gravity Load Collapse of Reinforced Concrete Frames.* Kenneth John Elwood and Jack P. Moehle. November 2003.
- PEER 2002/24** *Performance of Beam to Column Bridge Joints Subjected to a Large Velocity Pulse.* Natalie Gibson, André Filiatrault, and Scott A. Ashford. April 2002.
- PEER 2002/23** *Effects of Large Velocity Pulses on Reinforced Concrete Bridge Columns.* Greg L. Orozco and Scott A. Ashford. April 2002.
- PEER 2002/22** *Characterization of Large Velocity Pulses for Laboratory Testing.* Kenneth E. Cox and Scott A. Ashford. April 2002.
- PEER 2002/21** *Fourth U.S.-Japan Workshop on Performance-Based Earthquake Engineering Methodology for Reinforced Concrete Building Structures.* December 2002.
- PEER 2002/20** *Barriers to Adoption and Implementation of PBEE Innovations.* Peter J. May. August 2002.
- PEER 2002/19** *Economic-Engineered Integrated Models for Earthquakes: Socioeconomic Impacts.* Peter Gordon, James E. Moore II, and Harry W. Richardson. July 2002.
- PEER 2002/18** *Assessment of Reinforced Concrete Building Exterior Joints with Substandard Details.* Chris P. Pantelides, Jon Hansen, Justin Nadauld, and Lawrence D. Reaveley. May 2002.
- PEER 2002/17** *Structural Characterization and Seismic Response Analysis of a Highway Overcrossing Equipped with Elastomeric Bearings and Fluid Dampers: A Case Study.* Nicos Makris and Jian Zhang. November 2002.
- PEER 2002/16** *Estimation of Uncertainty in Geotechnical Properties for Performance-Based Earthquake Engineering.* Allen L. Jones, Steven L. Kramer, and Pedro Arduino. December 2002.
- PEER 2002/15** *Seismic Behavior of Bridge Columns Subjected to Various Loading Patterns.* Asadollah Esmaeily-Gh. and Yan Xiao. December 2002.
- PEER 2002/14** *Inelastic Seismic Response of Extended Pile Shaft Supported Bridge Structures.* T.C. Hutchinson, R.W. Boulanger, Y.H. Chai, and I.M. Idriss. December 2002.
- PEER 2002/13** *Probabilistic Models and Fragility Estimates for Bridge Components and Systems.* Paolo Gardoni, Armen Der Kiureghian, and Khalid M. Mosalam. June 2002.
- PEER 2002/12** *Effects of Fault Dip and Slip Rake on Near-Source Ground Motions: Why Chi-Chi Was a Relatively Mild M7.6 Earthquake.* Brad T. Aagaard, John F. Hall, and Thomas H. Heaton. December 2002.
- PEER 2002/11** *Analytical and Experimental Study of Fiber-Reinforced Strip Isolators.* James M. Kelly and Shakhzod M. Takhirov. September 2002.
- PEER 2002/10** *Centrifuge Modeling of Settlement and Lateral Spreading with Comparisons to Numerical Analyses.* Sivapalan Gajan and Bruce L. Kutter. January 2003.
- PEER 2002/09** *Documentation and Analysis of Field Case Histories of Seismic Compression during the 1994 Northridge, California, Earthquake.* Jonathan P. Stewart, Patrick M. Smith, Daniel H. Whang, and Jonathan D. Bray. October 2002.
- PEER 2002/08** *Component Testing, Stability Analysis and Characterization of Buckling-Restrained Unbonded Braces<sup>TM</sup>.* Cameron Black, Nicos Makris, and Ian Aiken. September 2002.
- PEER 2002/07** *Seismic Performance of Pile-Wharf Connections.* Charles W. Roeder, Robert Graff, Jennifer Soderstrom, and Jun Han Yoo. December 2001.
- PEER 2002/06** *The Use of Benefit-Cost Analysis for Evaluation of Performance-Based Earthquake Engineering Decisions.* Richard O. Zerbe and Anthony Falit-Baiamonte. September 2001.
- PEER 2002/05** *Guidelines, Specifications, and Seismic Performance Characterization of Nonstructural Building Components and Equipment.* André Filiatrault, Constantin Christopoulos, and Christopher Stearns. September 2001.

- PEER 2002/04** *Consortium of Organizations for Strong-Motion Observation Systems and the Pacific Earthquake Engineering Research Center Lifelines Program: Invited Workshop on Archiving and Web Dissemination of Geotechnical Data, 4–5 October 2001.* September 2002.
- PEER 2002/03** *Investigation of Sensitivity of Building Loss Estimates to Major Uncertain Variables for the Van Nuys Testbed.* Keith A. Porter, James L. Beck, and Rustem V. Shaikhutdinov. August 2002.
- PEER 2002/02** *The Third U.S.-Japan Workshop on Performance-Based Earthquake Engineering Methodology for Reinforced Concrete Building Structures.* July 2002.
- PEER 2002/01** *Nonstructural Loss Estimation: The UC Berkeley Case Study.* Mary C. Comerio and John C. Stallmeyer. December 2001.
- PEER 2001/16** *Statistics of SDF-System Estimate of Roof Displacement for Pushover Analysis of Buildings.* Anil K. Chopra, Rakesh K. Goel, and Chatpan Chintanapakdee. December 2001.
- PEER 2001/15** *Damage to Bridges during the 2001 Nisqually Earthquake.* R. Tyler Ranf, Marc O. Eberhard, and Michael P. Berry. November 2001.
- PEER 2001/14** *Rocking Response of Equipment Anchored to a Base Foundation.* Nicos Makris and Cameron J. Black. September 2001.
- PEER 2001/13** *Modeling Soil Liquefaction Hazards for Performance-Based Earthquake Engineering.* Steven L. Kramer and Ahmed-W. Elgamal. February 2001.
- PEER 2001/12** *Development of Geotechnical Capabilities in OpenSees.* Boris Jeremi . September 2001.
- PEER 2001/11** *Analytical and Experimental Study of Fiber-Reinforced Elastomeric Isolators.* James M. Kelly and Shakhzod M. Takhirov. September 2001.
- PEER 2001/10** *Amplification Factors for Spectral Acceleration in Active Regions.* Jonathan P. Stewart, Andrew H. Liu, Yoojoong Choi, and Mehmet B. Baturay. December 2001.
- PEER 2001/09** *Ground Motion Evaluation Procedures for Performance-Based Design.* Jonathan P. Stewart, Shyh-Jeng Chiou, Jonathan D. Bray, Robert W. Graves, Paul G. Somerville, and Norman A. Abrahamson. September 2001.
- PEER 2001/08** *Experimental and Computational Evaluation of Reinforced Concrete Bridge Beam-Column Connections for Seismic Performance.* Clay J. Naito, Jack P. Moehle, and Khalid M. Mosalam. November 2001.
- PEER 2001/07** *The Rocking Spectrum and the Shortcomings of Design Guidelines.* Nicos Makris and Dimitrios Konstantinidis. August 2001.
- PEER 2001/06** *Development of an Electrical Substation Equipment Performance Database for Evaluation of Equipment Fragilities.* Thalia Agnanos. April 1999.
- PEER 2001/05** *Stiffness Analysis of Fiber-Reinforced Elastomeric Isolators.* Hsiang-Chuan Tsai and James M. Kelly. May 2001.
- PEER 2001/04** *Organizational and Societal Considerations for Performance-Based Earthquake Engineering.* Peter J. May. April 2001.
- PEER 2001/03** *A Modal Pushover Analysis Procedure to Estimate Seismic Demands for Buildings: Theory and Preliminary Evaluation.* Anil K. Chopra and Rakesh K. Goel. January 2001.
- PEER 2001/02** *Seismic Response Analysis of Highway Overcrossings Including Soil-Structure Interaction.* Jian Zhang and Nicos Makris. March 2001.
- PEER 2001/01** *Experimental Study of Large Seismic Steel Beam-to-Column Connections.* Egor P. Popov and Shakhzod M. Takhirov. November 2000.
- PEER 2000/10** *The Second U.S.-Japan Workshop on Performance-Based Earthquake Engineering Methodology for Reinforced Concrete Building Structures.* March 2000.
- PEER 2000/09** *Structural Engineering Reconnaissance of the August 17, 1999 Earthquake: Kocaeli (Izmit), Turkey.* Halil Sezen, Kenneth J. Elwood, Andrew S. Whittaker, Khalid Mosalam, John J. Wallace, and John F. Stanton. December 2000.
- PEER 2000/08** *Behavior of Reinforced Concrete Bridge Columns Having Varying Aspect Ratios and Varying Lengths of Confinement.* Anthony J. Calderone, Dawn E. Lehman, and Jack P. Moehle. January 2001.
- PEER 2000/07** *Cover-Plate and Flange-Plate Reinforced Steel Moment-Resisting Connections.* Taejin Kim, Andrew S. Whittaker, Amir S. Gilani, Vitelmo V. Bertero, and Shakhzod M. Takhirov. September 2000.
- PEER 2000/06** *Seismic Evaluation and Analysis of 230-kV Disconnect Switches.* Amir S. J. Gilani, Andrew S. Whittaker, Gregory L. Fenves, Chun-Hao Chen, Henry Ho, and Eric Fujisaki. July 2000.

- PEER 2000/05** *Performance-Based Evaluation of Exterior Reinforced Concrete Building Joints for Seismic Excitation.* Chandra Clyde, Chris P. Pantelides, and Lawrence D. Reaveley. July 2000.
- PEER 2000/04** *An Evaluation of Seismic Energy Demand: An Attenuation Approach.* Chung-Che Chou and Chia-Ming Uang. July 1999.
- PEER 2000/03** *Framing Earthquake Retrofitting Decisions: The Case of Hillside Homes in Los Angeles.* Detlof von Winterfeldt, Nels Roselund, and Alicia Kitsuse. March 2000.
- PEER 2000/02** *U.S.-Japan Workshop on the Effects of Near-Field Earthquake Shaking.* Andrew Whittaker, ed. July 2000.
- PEER 2000/01** *Further Studies on Seismic Interaction in Interconnected Electrical Substation Equipment.* Armen Der Kiureghian, Kee-Jeung Hong, and Jerome L. Sackman. November 1999.
- PEER 1999/14** *Seismic Evaluation and Retrofit of 230-kV Porcelain Transformer Bushings.* Amir S. Gilani, Andrew S. Whittaker, Gregory L. Fenves, and Eric Fujisaki. December 1999.
- PEER 1999/13** *Building Vulnerability Studies: Modeling and Evaluation of Tilt-up and Steel Reinforced Concrete Buildings.* John W. Wallace, Jonathan P. Stewart, and Andrew S. Whittaker, editors. December 1999.
- PEER 1999/12** *Rehabilitation of Nonductile RC Frame Building Using Encasement Plates and Energy-Dissipating Devices.* Mehrdad Sasani, Vitelmo V. Bertero, James C. Anderson. December 1999.
- PEER 1999/11** *Performance Evaluation Database for Concrete Bridge Components and Systems under Simulated Seismic Loads.* Yael D. Hose and Frieder Seible. November 1999.
- PEER 1999/10** *U.S.-Japan Workshop on Performance-Based Earthquake Engineering Methodology for Reinforced Concrete Building Structures.* December 1999.
- PEER 1999/09** *Performance Improvement of Long Period Building Structures Subjected to Severe Pulse-Type Ground Motions.* James C. Anderson, Vitelmo V. Bertero, and Raul Bertero. October 1999.
- PEER 1999/08** *Envelopes for Seismic Response Vectors.* Charles Menun and Armen Der Kiureghian. July 1999.
- PEER 1999/07** *Documentation of Strengths and Weaknesses of Current Computer Analysis Methods for Seismic Performance of Reinforced Concrete Members.* William F. Cofer. November 1999.
- PEER 1999/06** *Rocking Response and Overturning of Anchored Equipment under Seismic Excitations.* Nicos Makris and Jian Zhang. November 1999.
- PEER 1999/05** *Seismic Evaluation of 550 kV Porcelain Transformer Bushings.* Amir S. Gilani, Andrew S. Whittaker, Gregory L. Fenves, and Eric Fujisaki. October 1999.
- PEER 1999/04** *Adoption and Enforcement of Earthquake Risk-Reduction Measures.* Peter J. May, Raymond J. Burby, T. Jens Feeley, and Robert Wood.
- PEER 1999/03** *Task 3 Characterization of Site Response General Site Categories.* Adrian Rodriguez-Marek, Jonathan D. Bray, and Norman Abrahamson. February 1999.
- PEER 1999/02** *Capacity-Demand-Diagram Methods for Estimating Seismic Deformation of Inelastic Structures: SDF Systems.* Anil K. Chopra and Rakesh Goel. April 1999.
- PEER 1999/01** *Interaction in Interconnected Electrical Substation Equipment Subjected to Earthquake Ground Motions.* Armen Der Kiureghian, Jerome L. Sackman, and Kee-Jeung Hong. February 1999.
- PEER 1998/08** *Behavior and Failure Analysis of a Multiple-Frame Highway Bridge in the 1994 Northridge Earthquake.* Gregory L. Fenves and Michael Ellery. December 1998.
- PEER 1998/07** *Empirical Evaluation of Inertial Soil-Structure Interaction Effects.* Jonathan P. Stewart, Raymond B. Seed, and Gregory L. Fenves. November 1998.
- PEER 1998/06** *Effect of Damping Mechanisms on the Response of Seismic Isolated Structures.* Nicos Makris and Shih-Po Chang. November 1998.
- PEER 1998/05** *Rocking Response and Overturning of Equipment under Horizontal Pulse-Type Motions.* Nicos Makris and Yiannis Roussos. October 1998.
- PEER 1998/04** *Pacific Earthquake Engineering Research Invitational Workshop Proceedings, May 14-15, 1998: Defining the Links between Planning, Policy Analysis, Economics and Earthquake Engineering.* Mary Comerio and Peter Gordon. September 1998.
- PEER 1998/03** *Repair/Upgrade Procedures for Welded Beam to Column Connections.* James C. Anderson and Xiaojing Duan. May 1998.
- PEER 1998/02** *Seismic Evaluation of 196 kV Porcelain Transformer Bushings.* Amir S. Gilani, Juan W. Chavez, Gregory L. Fenves, and Andrew S. Whittaker. May 1998.

**PEER 1998/01** *Seismic Performance of Well-Confined Concrete Bridge Columns.* Dawn E. Lehman and Jack P. Moehle.  
December 2000.

## ONLINE REPORTS

The following PEER reports are available by Internet only at [http://peer.berkeley.edu/publications/peer\\_reports.html](http://peer.berkeley.edu/publications/peer_reports.html)

- PEER 2009/106** *Shear Strength Models of Exterior Beam-Column Joints without Transverse Reinforcement.* Sangjoon Park and Khalid M. Mosalam. November 2009.
- PEER 2009/105** *Reduced Uncertainty of Ground Motion Prediction Equations through Bayesian Variance Analysis.* Robb Eric S. Moss. November 2009.
- PEER 2009/104** *Advanced Implementation of Hybrid Simulation.* Andreas H. Schellenberg, Stephen A. Mahin, Gregory L. Fenves. November 2009.
- PEER 2009/103** *Performance Evaluation of Innovative Steel Braced Frames.* T. Y. Yang, Jack P. Moehle, and Božidar Stojadinović. August 2009.
- PEER 2009/102** *Reinvestigation of Liquefaction and Nonliquefaction Case Histories from the 1976 Tangshan Earthquake.* Robb Eric Moss, Robert E. Kayen, Liyuan Tong, Songyu Liu, Guojun Cai, and Jiaer Wu. August 2009.
- PEER 2009/101** *Report of the First Joint Planning Meeting for the Second Phase of NEES/E-Defense Collaborative Research on Earthquake Engineering.* Stephen A. Mahin et al. July 2009.
- PEER 2008/104** *Experimental and Analytical Study of the Seismic Performance of Retaining Structures.* Linda Al Atik and Nicholas Sitar. January 2009.
- PEER 2008/103** *Experimental and Computational Evaluation of Current and Innovative In-Span Hinge Details in Reinforced Concrete Box-Girder Bridges. Part 1: Experimental Findings and Pre-Test Analysis.* Matias A. Hube and Khalid M. Mosalam. January 2009.
- PEER 2008/102** *Modeling of Unreinforced Masonry Infill Walls Considering In-Plane and Out-of-Plane Interaction.* Stephen Kadysiewski and Khalid M. Mosalam. January 2009.
- PEER 2008/101** *Seismic Performance Objectives for Tall Buildings.* William T. Holmes, Charles Kircher, William Petak, and Nabih Youssef. August 2008.
- PEER 2007/101** *Generalized Hybrid Simulation Framework for Structural Systems Subjected to Seismic Loading.* Tarek Elkhoraibi and Khalid M. Mosalam. July 2007.
- PEER 2007/100** *Seismic Evaluation of Reinforced Concrete Buildings Including Effects of Masonry Infill Walls.* Alidad Hashemi and Khalid M. Mosalam. July 2007.